DOKUZ EYLÜL UNIVERSITY

GRADUATE SCHOOL OF NATURAL AND APPLIED SCIENCES

ANALYSIS AND DESIGN OF SYNCHRONOUS/ASYNCHRONOUS COOPERATIVE COMMUNICATION SYSTEMS

by

Mümtaz YILMAZ

December, 2009

İZMİR

ANALYSIS AND DESIGN OF SYNCHRONOUS/ASYNCHRONOUS COOPERATIVE COMMUNICATION SYSTEMS

A Thesis Submitted to the
Graduate School of Natural and Applied Sciences of Dokuz Eylül University
In Partial Fulfillment of the Requirements for the Degree of Doctor of Philosophy in
Electrical & Electronics Engineering, Electrical & Electronics Engineering Program

by
Mümtaz YILMAZ

December, 2009
İZMİR

Ph.D. THESIS EXAMINATION RESULT FORM

We have read the thesis entitled **"ANALYSIS AND DESIGN OF SYNCHRONOUS/ASYNCHRONOUSCOOPERATIVE COMMUNICATION SYSTEMS"** completed by **MÜMTAZ YILMAZ** under supervision of **ASST.PROF.DR. REYAT YILMAZ** and we certify that in our opinion it is fully adequate, in scope and in quality, as a thesis for the degree of Doctor of Philosophy.

Asst.Prof.Dr. Reyat YILMAZ

Supervisor

Prof.Dr. R. Alp KUT	Asst.Prof.Dr. Olcay AKAY
Thesis Committee Member	Thesis Committee Member
Prof.Dr. Mete SEVERCAN	Prof.Dr. Mustafa GÜNDÜZALP
Examining Committee Member	Examining Committee Member

Prof.Dr. Cahit HELVACI
Director
Graduate School of Natural and Applied Sciences

ACKNOWLEDGEMENTS

I would like express my thanks to many people who made this thesis possible. First, I would like to express my gratitude to my advisor, Dr. Reyat Yılmaz, not only for his insights in research, but also for his understanding, open-mindedness and kindness with people. From the beginning of my M.Sc. study till the end of my Ph.D. study now, his guidance and never ending enthusiasm helped me to overcome the problems I faced.

I would also like to express my gratitude to members of my thesis progress committee: Dr. Olcay Akay and Dr. R. Alp Kut. Their generous contributions of time, valuable insights and suggestions made an important impact on my thesis. Also I would like to thank Dr. Tolga Duman for his kind support during my stay at the wireless communications laboratory at ASU. He helped me with his deep scientific knowledge and his advices.

I would also like to thank my colleagues, Dr. Özgür Tamer, Dr. Tolga Sürgevil, Uğur Torun, Dr. Barış Bozkurt, Dr. Metehan Makinacı, Adem Çelebi and Dr. Selçuk Kılınç for their support and friendship.

I would like to extend my deepest appreciation to my family. My father's never ending belief in me and my mother's unconditional love and support continued throughout my study. Also it was my sister's encouragement that made me to progress whenever I'm depressed.

Mümtaz Yılmaz

ANALYSIS AND DESIGN OF SYNCHRONOUS/ASYNCHRONOUS COOPERATIVE COMMUNICATION SYSTEMS

ABSTRACT

The main objective of this thesis is to analyze and develop practical cooperative communication schemes considering the synchronization issue as well. The initial research is on distributed application of turbo and multilevel codes via user cooperation. For distributed turbo coded cooperative scheme, an upper bound on bit error rate is expressed for fading channels incorporating the erroneous inter-user transmission in the analysis. For multilevel coded cooperative scheme, orthogonal signaling is employed in order to embed the data of both users in single symbol and detect independently at the destination. The multilevel coded cooperative system is shown to attain the performance of non-cooperative multilevel coded counterpart employing two transmit antennas.

The second research direction is on low density parity check coded cooperative communication over wireless relay channel. The performance of decode-and-forward (DF) protocol is compared with both detect-and-forward (DetF) and amplify-and-forward (AF) protocols for fading channels. The DF protocol has better performance than other two for fast fading channel as long as the relay decodes the source codeword with small probability of error. However, the DetF protocol is shown to be more appropriate for quasi-static fading channel. Finally, asynchronism is introduced on relay channel by assuming a time delay and phase offset between source and relay transmission. Information theoretical analysis is realized initially and afterwards, a receiver, employing maximum a posteriori probability (MAP) type detector, is proposed. The asynchronous system employing the proposed receiver is shown to even outperform synchronous system for additive white Gaussian noise channel. However a small performance loss, which even vanishes for small relative delay values, is observed for fading channel. As an alternative to complex MAP type detector, a reduced complexity minimum mean square error type of detector is proposed.

Keywords : cooperative communication, channel coding, relay channel, fading channel.

İŞBİRLİKLİ SENKRON/ASENKRON İLETİŞİM SİSTEMLERİNİN ANALİZ VE TASARIMI

ÖZ

Bu tezdeki temel amaç, pratik işbirlikli iletişim şemalarının eşzamanlılık ta dikkate alınarak incelenip geliştirilmesidir. İlk araştırma turbo ve çok düzeyli kodların kullanıcı işbirliği yoluyla dağıtık uygulanmaları üzerinedir. Dağıtık turbo kodlanmış işbirlikli sistem için kullanıcılar arası hatalı iletim analize katılarak sönümlemeli kanallardaki bit hata oranı için bir üst sınır gösterilmiştir. Çok düzeyli kodlanmış işbirlikli sistemde ise her iki kullanıcının bilgisini tek bir sembole birleştirebilmek ve hedefte bağımsız olarak sezebilmek için dikgen sinyal kullanılmıştır. Çok düzeyli kodlanmış işbirlikli sistemin iki iletim anteni kullanan işbirliksiz çok düzeyli kodlanmış sistemin performansına ulaştığı gösterilmiştir.

İkinci araştırma alanı kablosuz röle kanal üzerinden düşük yoğunluklu eşlik denetim kodlanmış işbirlikli iletişimdir. Sönümlemeli kanallar için çöz-ilet protokolünün performansı sez-ilet ve yükselt-ilet protokolleri ile karşılaştırılmıştır. Hızlı sönümlemeli kanal için, röle düşük hata olasılığı ile kaynak kodunu çözdüğü sürece çöz-ilet protokolü diğer iki protokolden daha üstün başarıma sahiptir. Durağan sönümlemeli kanalda ise sez-ilet protokolünün daha uygun olduğu gösterilmiştir. Son olarak, röle kanalda kaynak ve röle iletimleri arasında zaman gecikmesi ve faz kayması varsayılarak eşzamansızlık tanımlanmıştır. İlk olarak bilgi kuramsal analiz gerçekleştirilmiş ve sonrasında maksimum sonsal olasılık türünde sezici tasarlanmıştır. Toplamsal beyaz Gauss gürültülü kanalda, tasarlanan alıcıyı uygulayan eşzamansız sistem eşzamanlı sistemden daha iyi bir başarım göstermiştir. Ancak sönümlemeli kanalda, düşük zaman gecikmeleri için azalan küçük bir performans düşüşü gözlenmiştir. Karmaşık maksimum sonsal olasılık sezicisine alternatif olarak, düşük karmaşıklıkta minimum ortalama karesel hata türünde bir sezici tasarlanmıştır.

Anahtar sözcükler: İşbirlikli iletişim, kanal kodlama, röle kanal, sönümlemeli kanal.

CONTENTS

Page

CHAPTER ONE
INTRODUCTION

1.1 Background and Contributions

The main objective of a communication system is to transmit and receive information reliably and efficiently from transmitter to the receiver through an imperfect channel. The main examples of the communication channels are additive white Gaussian noise (AWGN), fading, inter-symbol interference (ISI), multiple-input multiple-output (MIMO) and relay channels. Shannon (1948) proved that by using a random coding approach, arbitrarily low error probability can be achieved over these noisy channels provided that the transmission rate is lower than the channel capacity. For this reason the performance of a practical coding scheme is quantified by its margin to the channel capacity. The capacities of AWGN, fading and ISI channels are evaluated and are known but there are still more complicated channel models and problems. For example single letter capacity for relay channel still cannot be defined and only upper/lower limits are given.

Shannon's result is one of the most important milestones in the history of communication theory. Although Shannon defined the necessity of coding in order to approach the capacity, he did not define the coding technique explicitly. Initiated with his work, many practical coding schemes have been proposed in the literature, trying to approach the channel capacity. Almost 50 years after the work of Shannon, the discovery of turbo codes (Berrou, Glavieux, & Thitimajshima, 1993) and rediscovery of low-density parity-check (LDPC) codes (Mackay, 1999) enabled to approach to the Shannon limit very closely. It is shown in numerous works that both types of codes give excellent capacity-approaching performance under different types of channels. LDPC codes are shown to achieve within 0.04dB of the Shannon capacity of the channel at a bit error rate (BER) level of 10^{-6} in AWGN channel (Chung, Forney, Richardson, & Urbanke, 2001). The performance of 1/2 rated turbo code under AWGN channel is shown to be at 0.7dB from Shannon limit at a BER level of 10^{-5} (Berrou et. al. ,1993). Moreover,

by employing iterative decoding algorithms, they have reasonable implementation complexity and can be easily incorporated into practical systems.

Since channel coding introduces extra parity bits to be transmitted, the duration of each binary symbol decreases as a result of which the required bandwidth increases. In order to obtain coding gain without bandwidth expansion, trellis coded modulation (TCM) is proposed (Ungerboeck, 1982). TCM uses a signal set with more elements than the required for uncoded transmission. Multilevel codes, originally designed for AWGN channels (Imai & Hirakawa, 1977), are shown to be an alternative to TCM for fading channels (Zhang & Vucetic, 1995). The outputs of multiple component codes are demultiplexed and modulated in the same symbol. The performance of the system increases for higher levels, so it is important to apply more powerful codes in lower levels. Convolutional codes are used generally as component codes in multilevel coding but the use of turbo codes is shown to increase the performance (Wachsmann, 1995).

In a fading environment, the received signal can be highly attenuated as a result of the multipath between the transmitter and the receiver. Providing the receiver with independent faded versions of information signal is an efficient way to mitigate the detrimental effects of wireless fading channels. This technique is named as diversity and is a powerful tool to obtain better spectral and power efficiencies. The early diversity techniques, time and frequency diversity, were widely applied in communication systems. As an alternative, spatial diversity is introduced by locating multiple antennas far enough to ensure the independence between their channels (Tarokh, Seshadri, & Calderbank, 1998). By transmitting independently faded copies of a signal using multiple antennas, transmit diversity techniques can greatly enhance the reliability of the information without sacrificing bandwidth (Alamouti, 1998). Spatial diversity can be applied at the receiver side by the use of multiple antennas.

Recently, cooperative diversity (Sendonaris, Erkip, & Aazhang, 2003) has been proposed to exploit spatial diversity for wireless nodes in a distributed manner similar to the idea of MIMO transmission. In this new scheme, diversity gain is

achieved via users acting as a relay for their partners and cooperation is implemented in a code division multiple access (CDMA) system. It is shown that significant gain can be achieved via cooperation. Initiated with this work, various cooperative communication schemes are proposed in the literature. The relay channel is the basic type of channel under which cooperation can be applied. Analogous to collocated antenna arrays, the distributed spatial diversity can greatly increase the channel capacity, reduce the power cost and enhance the system reliability. The relays can be integrated into both military and commercial applications such as sensor networks, cellular systems and ad-hoc networks. The research on relay systems focuses on both information theoretical analysis under specific channel conditions and the design of practical cooperative schemes with appropriate signaling techniques. One of the first efforts that investigates the capacity of relay channel is realized by Cover and El Gamal (1979). In this work, they derive exact capacity expressions under certain conditions, and evaluate lower and upper bounds on achievable rates for Gaussian channels. The information theoretical analysis of relay channel has also been studied for ergodic fading channels (Host-Madsen & Zhang, 2005; Kramer, Gastpar & Gupta, 2005) and non-ergodic fading channels (Host-Madsen & Zhang, 2005; Nabar, Bölcskei & Kneubühler, 2004). The use of multiple antennas at the relays (Wang, Zhang & A. Host-Madsen, 2005; Bölcskei, Nabar, Oyman & Paulraj, 2006) and the use of multiple relays have also been proposed (Reznik, Kulkarni & Verdu, 2004).

The main motivation behind the research on cooperative communication is the promise of achieving the capabilities of multi-input multi-output systems even when the terminals can only support a single antenna. As a result, a natural extension for cooperative communication is to adapt space-time codes in cooperation (Nabar et. al., 2004). There are many different construction methods for space-time coded cooperation. For example, in (Janani et. al. 2004) and (Nabar et. al., 2004), all the users form a virtual antenna array. Or, as presented in (Laneman, & Wornell, 2003), all the relays that can successfully decode the source signal constitute space-time block codes based on orthogonal designs. Different types of space-time codes are exploited for cooperation. In two-user case, since bits are transmitted through two antennas, the simple and effective

Alamouti scheme is incorporated (Laneman & Wornell, 2003). Space-time trellis codes are also employed distributively (Dohler, Rassool, & Aghvami, 2003).

In cooperative communication, various types of forwarding protocols are applied at the cooperating users or relays. The simplest types of these protocols are amplify-and-forward (AF) and decode-and-forward (DF) (Cover & El Gamal, 1979). As the names imply, the received signal is only amplified without any processing or decoded before re-encoded and forwarded. As variations of AF and DF protocols, selection and incremental relaying are applied in a multi-user wireless network (Laneman, Tse, & Wornell, 2004). It was shown that except from fixed decode and forward protocol, each of the cooperative protocols achieve full diversity. In addition to AF and DF protocols, detect-and-forward (DetF) (Benjillali & Szczecinski, 2009) and compress-and-forward (CF) (Cover & El Gamal, 1979) (also named as "quantize-and-forward" and "estimate-and-forward (EF)") techniques have also been proposed. As an extension to DF protocol, the authors proposed a new scheme in (Janani, Hedayat, Hunter, & Nosratinia, 2004) under the cooperative communication framework called "coded cooperation". Fundamentally, it is based on transmitting different portions of the source codeword over independent fading paths with the assist of other users or relays in order to introduce diversity. Both rate compatible punctured convolutional codes (RCPCC) and turbo codes are used as component codes. Extension to space time coded cooperation is also realized. The basic assumption in this work is that whenever the cooperating users detect erroneous information from their partners, controlled by control redundancy check (CRC) codes, they resign cooperative mode and transmit information of their own. Simulations results (Janani et. al. 2004) for two user scenario, also supported with theoretical bounds, demonstrate that both users benefit from cooperation even one of them has better channel to destination when RCPCC's are employed for fast fading channel. For the case of turbo codes, the user that has better channel loses some performance as a result of cooperation for fast fading channel. For slow fading channel, cooperative communication is shown to be beneficial for both users, independent from coding technique (Janani et. al. 2004).

There exists works in the literature that carries out theoretical performance analysis for turbo coded cooperative schemes that considers the erroneous inter-user channel. In (Li, Vucetic, Wong, & Dohler 2006), a distributed turbo coding scheme is proposed for relay channel, in which instead of decoding the source codeword, a soft estimate of source information is calculated and forwarded to destination. The presented performance analysis also includes the effect of source-relay channel. It is shown that the proposed scheme approaches the performance of error free source-relay channel for high signal to noise ratio (SNR) and achieves a higher throughput. In the other related work a distributed turbo coded scheme is proposed over half duplex relay channel (Roy & Duman, 2006). The BER analysis for AWGN channel is carried out in two steps: at first, the error probability of source-relay channel is defined and then the overall bound for BER is determined including the effect of source-relay error probability calculated at first step.

Our initial research direction in this thesis is on employing turbo coding distributively through user cooperation. Different from original coded cooperative scheme (Janani et. al. 2004), we assume that users do not employ error detection for the inter-user transmission and always operate in cooperation mode. We extend the theoretical performance analysis in (Roy & Duman, 2006) for fading channel considering the erroneous inter-user communication. We evaluate the theoretical bit error rate bounds for spesific inter-user channel SNR's and compare with simulation results under fast and quasi-static fading channel.

There exists several works that exploits the use of multilevel codes in a cooperative system. In (Ishii, Ishibashi, & Ochiai, 2009), using multilevel coded modulation cooperative diversity is achieved. The proposed system is extendable to any number of users and shown to outperform not only a time division cooperative diversity but also signal superposition diversity. In a similar work (Ishii, Ishibashi, & Ochiai, 2008), multilevel coded pulse amplitude modulation (PAM) is proposed under the framework of cooperative system with more than two cooperating nodes. This system also outperforms time division and signal

superposition cooperative transmissions. Additionally this system is shown to obtain a diversity gain *N*, where *N* is the number of cooperating nodes.

In the context of coded cooperative systems, we next consider the use of multilevel codes under user cooperative framework. We propose a multilevel coded cooperative system based on orthogonal signaling between the cooperating users. Orthogonal signaling for a cooperative framework is originally proposed in (Mahinthan & Mark, 2005) for an uncoded system. In that scheme, each transmitted signal from either cooperating user contains information of both users. Additionally, orthogonality is enabled by assigning in-phase and quadrature components of the modulated signal to individual users. This eliminates the need of individual channels for each cooperating user. We modify the set partitioning of multilevel scheme in the way that provides the orthogonality as well. We apply convolutional codes as component codes, but in order to supply additional protection, we also consider turbo codes for the first level of the multilevel code.

The increasing interest in relay assisted communication resulted with significant literature presenting practical schemes as well. As a natural extension, the use of channel coding techniques in practical schemes is exploited to approach the capacity limits. The incorporation of turbo codes in relay system is proposed in (Zhao & Valenti, 2003). The distributed application of turbo codes is followed by the work that exploits the channel state information in cooperative turbo coded system (Souryal & Vojcic, 2004). All of these works assume that the source and relay transmits over orthogonal channels. Although this assumption simplifies the receiver structure, it reduces spectral efficiency. To achieve the capacity promised by relay channel, Zhang and Duman proposed turbo coded cooperative schemes for full duplex (2005) and half duplex relay channel (2007) in both of which source and relay uses the same channel for transmission. These schemes are shown to approach the capacity limits of relay channel very closely (Zhang & Duman, 2005, 2007).

As an alternative to turbo codes, LDPC codes are also exploited for wireless relay channel and the research focuses on code design and optimization in general.

In (Baynast, Chakrabarti, Sabharwal & Aazhang, 2006), code optimization and threshold calculation is performed for a half duplex relay channel. The asymptotic performance of designed codes are shown to be 0.6 dB from the theoretical limit. In (Razaghi & Yu, 2007) bilayer LDPC codes are considered to implement binning in DF mode for the relay channel. Using bilayer density evolution, proper bilayer LDPC codes are designed that can approach theoretical DF rate. The generalized design in (Chakrabarti, Baynast, Sabharwal & Aazhang, 2007) brings four contributions for the field of LDPC code design for relay systems. First, side information from relay is conveyed through additional parity bits. Second is the reduction in complexity of encoding and decoding process, obtained via simplifications in system design. While the third contribution is the derivation of relationship between the multiple LDPC code profiles used for relay code design, final contribution is the reduction at complexity of density evolution obtained by adapting Gaussian approximation. Similar approximation is also proposed in (Li,, Yue, Khojastepour, Wang, & Madihian, 2008), and code optimization is realized via modified differential evolution procedure. The code design implemented in (Li, et. al., 2008) is based on factor graph decoupling and successive decoding. Other from code design, the work in (Bo, Lin, Peiliang, & Qinru, 2006) exploits LDPC codes in distributed space time cooperative system. The proposed system is shown to reduce transmission error and offer diversity gain. Following the framework in (Zang & Duman, 2005, 2007), Hu & Duman (2007) incorporates LDPC codes instead of turbo codes in wireless relay channel. With properly designed codes over fading channels, LDPC coded cooperative system is shown to outperform its turbo coded counterpart for both half and full duplex cases.

As a second research direction, we extend the LDPC coded cooperative system in (Hu & Duman, 2007) by applying several different types of forwarding protocols (AF, DF and DetF) at the relay. We set up individual signaling scheme for each protocol and compare the performances for specific type of fading channel. These protocols differ in the way that the relay processes the received signal and forwards to the destination. We apply iterative detection/decoding at the destination to obtain the best performance. Depending on the ability of relay to transmit and receive at the same time, full and half duplex modes are considered

at the relay and both ergodic and non-ergodic fading channels are assumed. The quality of inter-user channel arises as the basic factor that determines the overall performance. While DF protocol is appropriate for ergodic fading relay channel on condition that source-relay transmission is almost error free, DetF protocol appears to be a better choice for quasi-static fading channel.

A difficult problem in cooperative communication is the block and symbol synchronization among the cooperating users. Synchronization for cooperative communication is much more difficult than the case of collocated antennas. In some applications like wireless ad hoc networks, there is no central coordinator to ensure the synchronization of the whole system. And for some other scenarios including wireless sensor networks, it is not feasible to employ complicated synchronization algorithms. In addition to these general considerations, coded systems usually work at very low SNR, which makes the problem more difficult.

The amount of works considering the asynchronism issue for relay and cooperative systems is ever-increasing. In the former reference (Li, 2004), imperfect synchronization and channel dispersion are integrated and a time-reversed space-time block code is exploited. Timing and carrier frequency synchronization errors are shown to be tolerated and full transmission diversity is achieved. In another related work (Wei, Goeckel, & Valenti, 2006) asynchronism is handled with decision feedback equalizer applying the minimum mean-squared error criterion and cooperative diversity gain is shown to be achieved for asynchronous case by combining separate inputs from the multiple relay channels. Lie & Xia (2007) construct space-time trellis codes for binary phase shift keying (BPSK) modulation scheme using stack construction. Full diversity order is shown to be achieved using this type of space-time trellis codes, without the symbol synchronization requirement. It's also shown that when relative timing errors/differences are known at the destination and the optimum decoding method is used, the proposed space time trellis codes perform even better in asynchronous case. Orthogonal frequency division multiplexing (OFDM) technique is also considered in the system design for combatting asynchronization. In (Guo & Xia,

2008), a distributed space time coding scheme based on linear dispersion coding is presented and OFDM is employed as a solution for timing errors.

As a final research, we consider asynchronization problem for relay channel and focus on asynchronism in the coded relay system. We express the received signals mathematically when timing error and phase offset exist between the source and the relay nodes. We also present information theoretical analysis of asynchronous relay channel. We show that asynchronism may be handled with appropriate maximum a posteriori probability (MAP) type receiver. We also search for reduced complexity but sub-optimum detectors and propose a linear minimum mean square error (LMMSE) type of receiver. We use the measure of average mutual information in order to determine the convergence behavior of the system. We also evaluate actual performance via simulations and compare predicted convergence threshold with simulation results.

1.1. Outline of Thesis

The thesis is organized as follows: In Chapter 2 we review the concept of channel capacity together with several examples. Two capacity approaching codes (turbo codes and LDPC codes) are introduced and the iterative decoding methods of these codes are presented. Additionally we revisit convergence prediction via extrinsic information transfer (EXIT) charts. This tool is used as performance measurement tool in Chapter 5 later in the thesis.

In Chapter 3, we firstly summarize cooperative communication together with coded cooperation. We present signaling for the distributed turbo coding scheme formed with two cooperating user. After giving the theoretical BER analysis for fading channel, we present simulation results. Then we introduce multilevel coded cooperative system based on orthogonal signaling and present appropriate multilevel codes for this scheme. We propose an appropriate set partitioning rule and define the signaling. We apply both convolutional and turbo codes as component codes and evaluate the performance of the system for both fast and

quasi-static fading channels. The simulation results are compared with derived union upper bound on BER.

We review the relay channel and its information theoretical limits in Chapter 4. We set up LDPC coded cooperative communication system over relay channel and compare various forwarding protocols used at the relay. Specifically we apply DF, AF and DetF protocols and compare their performance obtained by Monte Carlo simulations.

We consider the impact of asynchronism on this cooperative communication system in Chapter 5. We propose a receiver employing optimum MAP type detector that can cope with asynchronism. The EXIT chart method is used to determine the convergence threshold of the system. Since MAP detector has increasing complexity with modulation level, we propose suboptimum LMMSE detector in order to reduce complexity. The simulation results are also presented in order to evaluate the system performance. Finally, we give a summary of the thesis and future research directions in Chapter 6.

CHAPTER TWO
CHANNEL CAPACITY AND CAPACITY APPROACHING CODES

In this chapter, we present the main results of channel capacity theorem and discuss existing information theoretical results for various channel models including AWGN channel and fading channel. In light of these results, we review two capacity approaching codes. The two types of coding technique that we revisit are the LDPC and turbo codes. We also deal with convergence analysis method which can be used to figure out the iterative decoder performance.

Initially, channel capacity concept is introduced and several existing results are presented in Section 2.1. We give an overview of LDPC and turbo codes together with iterative decoding algorithms in Section 2.2. Several convergence analysis tools are presented in Section 2.3 and the chapter is concluded in Section 2.4.

2.1 Channel Capacity

The channel capacity, introduced by Shannon in his seminal paper (Shannon, 1948), is defined as the highest transmission rate of the information that can be sent over a communication channel with arbitrarily low probability of error. In this initial work of information theory, Shannon proved the capacity of a communication channel perturbed by white Gaussian noise. Thereafter the capacity limits of different channel models have been exploited by researchers over the years. The capacity of a discrete-time memoryless channel (DMC) is defined as the maximal mutual information between the channel input and output, maximized over marginal probability mass function, i.e,

$$C = \max_{p(x)} I\left(X;Y\right), \tag{2.1}$$

where X and Y are the channel input and channel output, respectively. The mutual information between two random variables is defined as,

$$I(X;Y) = E\left[\log \frac{p(X,Y)}{p(X)\,p(Y)}\right], \tag{2.2}$$

where the expectation is over the joint density of X and Y.

Gaussian input distribution has been proven to achieve the capacity for many channels with AWGN. But this is not the case for many applications since the inputs are chosen from a finite alphabet, i.e. from a modulation constellation with a finite size such as phase shift keying (PSK) and quadrature amplitude modulation (QAM). Generally it is impossible to achieve the above capacity under such an input constraint. Therefore it is necessary to compute the constrained capacity and achievable information rates with specific input distributions.

AWGN channel is one of the simplest DMC whose input-output relation is given as,

$$Y = X + Z, \tag{2.3}$$

where Z is the noise component with zero mean and a variance of $N_0/2$ per dimension. Assuming Gaussian input, the capacity of this channel is given by

$$C_{AWGN} = \frac{1}{2}\log_2(1+2\rho). \tag{2.4}$$

bits per channel use, where $\rho = E_s / N_0$ is the SNR, and E_s is the input symbol energy. On the other hand, the achievable information rate for the AWGN channel with independent and uniformly distributed (i.u.d.) binary inputs can be computed as

$$I_b(\rho) = 1 - \int_{-\infty}^{\infty} \frac{e^{-\tau^2/2}}{\sqrt{2\pi}} \log_2\left(1 + e^{-2\tau\sqrt{2\rho}-4\rho}\right) d\tau. \tag{2.5}$$

For a MIMO flat fading channel, the output is given by,

$$Y = \sqrt{\rho / N_t} HX + Z \,, \tag{2.6}$$

where $X = \left[X_1, X_2, ..., X_{N_t} \right]^T$ is the transmitted signal vector with unit energy constraint and $Y = \left[Y_1, Y_2, ..., Y_{N_r} \right]^T$ is the received signal vector and H is the channel matrix whose elements are the channel coefficients between the N_t transmit antennas and N_r receive antennas. These coefficients are zero mean complex Gaussian random variables with unit variance for Rayleigh fading. Assuming ergodic fading, the capacity is computed as,

$$C_{MIMO} = E\left[\log_2 \left(\det \left(I_{N_r} + \frac{\rho}{N_t} HH^* \right) \right) \right], \tag{2.7}$$

where '*' is the Hermitian operation, I_{N_r} is the $N_r \times N_r$ identity matrix and $E[.]$ represents the expectation with respect to the statistics of the channel matrix H. Again this capacity can be achieved on condition that the input is complex Gaussian distributed with a covariance matrix of I_{N_t}. A special case of this channel model is the single input single output flat fading channel in which case the capacity is given by,

$$C_{SISO} = \int_0^\infty e^{-\gamma} \log_2 \left(1 + \gamma\rho \right) d\gamma \,, \tag{2.8}$$

and similar to the AWGN case, the achievable information rate with i.u.d. binary inputs can be computed as

$$I_b(\rho) = -\int_0^\infty 2\gamma e^{-\gamma^2} \int_{-\infty}^{\infty} \frac{e^{-\tau^2/2}}{\sqrt{2\pi}} \log_2 \left(\frac{1}{2} + \frac{1}{2} e^{-2\tau\gamma\sqrt{2\rho} - 4\gamma^2\rho} \right) d\tau d\gamma \,. \tag{2.9}$$

2.2 Capacity Approaching Codes

2.2.1 LDPC Codes

LDPC codes are a group of linear block codes with near capacity-achieving performance. The idea of constructing a linear block code using a parity check matrix with low density of 1's is first proposed by Gallager (1963) in his doctoral thesis but rarely applied for more than thirty years. The work of Tanner (1981) was another milestone in LDPC history. He generalized the LDPC codes and introduced a Tanner graph representation which greatly facilitated the decoding process. Afterwards, LDPC codes are rediscovered (Mackay, 1999) and aroused interest again after the invention of turbo codes (Berrou et. al., 1993). They have been successfully applied and analyzed in many different channels such as binary erasure channel (BEC) (Barak, & Feder, 2004), binary symmetric channel (BSC) (Gallager, 1963), AWGN channel (Mackay,1999), Rayleigh fading channel (Hou et. al., 2001), ISI channel (Kavcic, Ma, & Mitzenmacher, 2003), etc.

Compared to parallel concatenated convolutional (turbo) codes, LDPC codes have several advantages. Firstly, the use of message passing algorithm greatly reduces their decoding complexity. Also, there exist various decoding algorithms (Richardson & Urbanke, 2001), (e.g. bit flipping algorithm, belief propagation (BP) algorithm), which provide a good tradeoff between complexity and performance. In addition, for many LDPC codes, there is very low or even no error floor which is typical observation for turbo codes. The lack of error floor ensures a good decoding performance at high SNR's as reported in the literature. Moreover, most of the decoding errors are detectable. The occurrence rate of undetected errors is related to the distance properties of the code. Possibly the major drawback of LDPC codes is their high encoding complexity when compared with other codes. The generator matrix is not generally dense and has a high dimension. However, several successful ways have appeared to deal with this problem (Richardson & Urbanke, 2000).

As previously mentioned, LDPC codes are a class of linear block codes. Although they can be generalized to GF(q), q ≥ 2, we deal with the binary case, i.e. GF(2). Like any linear block code, an (*n,k*) LDPC code can be represented using an $(n-k)\times n$ parity check matrix H_c. The main property of this code is that H_c has very low density of 1's. Generally, we consider two kinds of LDPC codes: Regular LDPC codes and irregular LDPC codes. For regular codes, H_c has exactly d_v 1's in each column and exactly d_c 1's in each row, where d_v, $d_c \ll (n-k)$. If H_c is full rank, we know that $d_c = d_v n/(n-k)$ and the code rate is equal to $R_c = k/n = 1 - d_v/d_c$. For irregular LDPC codes, d_v and d_c are not constant for each column and each row. Usually, the degree distribution polynomials are used for defining LDPC codes (Luby, Mitzenmacher, Shokrollahi, & Spielman, 2001).

A Tanner graph can be used to represent LDPC codes. This representation not only provides an easier way to characterize the code but also facilitates the implementation of the decoding algorithm. As an example, let us consider a very simple (10,5) LDPC code with a parity check matrix

$$H_c = \begin{bmatrix} 1 & 0 & 0 & 1 & 1 & 1 & 0 & 0 & 1 & 0 \\ 1 & 1 & 0 & 1 & 0 & 0 & 1 & 0 & 1 & 0 \\ 0 & 0 & 1 & 0 & 1 & 1 & 0 & 1 & 0 & 1 \\ 0 & 1 & 1 & 0 & 0 & 0 & 1 & 1 & 0 & 1 \\ 1 & 0 & 1 & 1 & 0 & 1 & 0 & 0 & 1 & 0 \end{bmatrix}. \tag{2.10}$$

The Tanner graph of this code is depicted in Fig. 2.1. The bipartite graph has two kinds of nodes: Variable nodes (represented by the circles) and check nodes (represented by the squares). The edges connecting these two types of nodes are defined according to the matrix H_c, i.e. the check node i is connected to variable node j if h_{ij} (the element in the ith row and jth column of H_c) equals to 1.

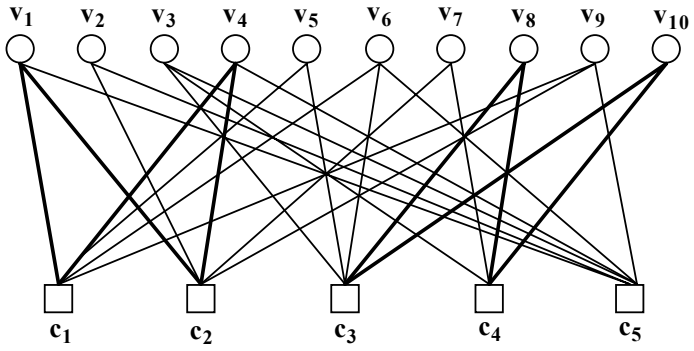

Figure 2.1 Tanner graph representation of the code example.

In the graph, we observe that, there exist cycles. A cycle is a path that starts from one node and comes back to the same node after passing through several edges. The cycle length is defined as the number of edges it goes through and the girth of a graph is defined to be the minimum cycle length. For example, in this graph, there exist several length-4 cycles which are depicted using the bold lines. The existence of cycles, especially short cycles, degrades the iterative decoding performance. Therefore, they should be avoided as much as possible. Based on the Tanner graph representation, we can express the irregular LDPC codes using the degree distribution polynomials (edge perspective), which are defined as

$$\lambda(x) = \sum_{i=1}^{D_v} \lambda_i x^{d_v^i}, \tag{2.11}$$

$$\rho(x) = \sum_{i=1}^{D_c} \rho_i x^{d_c^i}, \tag{2.12}$$

where $\lambda_i(\rho_i)$ denotes the fraction of all edges that are connected to the variable (check) node with degree $d_v^i(d_c^i)$, $D_v(D_c)$ is the number of different variable (check) node degrees. They can also be represented using a different degree distribution polynomials (node perspective),

$$\lambda'(x) = \sum_{i=1}^{D_v} \lambda_i' x^{d_v^i}, \tag{2.13}$$

$$\rho'(x) = \sum_{i=1}^{D_c} \rho_i' x^{d_c^i}, \tag{2.14}$$

where $\lambda_i' = \frac{\lambda_i / d_v^i}{\sum \lambda_i / d_v^i}$ and $\rho_i' = \frac{\rho_i / d_v^i}{\sum \rho_i / d_v^i}$ are the fraction of nodes that are connected to the variable and check nodes with degree d_v^i and d_c^i, respectively.

2.2.1.1 Message Passing Algorithm

For LDPC codes, there exists an iterative decoding algorithm which computes the probability distributions of the variables iteratively over a graph-based model. It has been developed under different application scenarios and has different names, such as the belief propagation algorithm, the message passing algorithm and the sum-product algorithm (Richardson & Urbanke, 2001). The algorithm tries to calculate the a posteriori probability (APP) for each variable iteratively similar to the turbo decoding algorithm.

The decoding algorithm is based on the bipartite graph introduced in Fig. 2.1. Log likelihood messages are exchanged between variable nodes and check nodes and decisions are made after a predefined number of iterations. At each iteration, there are two steps, corresponding to two directions of information flow. In the first half iteration, each variable node collects all the messages from the channel and its neighbors (the check nodes that are connected to it), and passes the extrinsic information to its neighbors. In the next half iteration, each check node computes the extrinsic information for its neighboring variable nodes. After a predetermined number of iterations or after a certain stopping criterion is satisfied, whichever occurs first, the decoder outputs the soft log likelihood ratio (LLR) information or hard decision on each bit.

As an example, consider the code in Fig. 2.2. We use $a_{ij}^{(k)}$ to denote the message passed from variable node i to check node j, and $b_{ij}^{(k)}$ to denote the message from check node i to variable node j at the kth iteration, respectively. The

message flow representing the process to compute the extrinsic information from variable node v_9 to check node c_2 is depicted in Fig. 2.2. Node v_9 collects the channel message y_9 and messages from all the neighboring check nodes (c_1 and c_5) except node c_2, updates the soft information and sends it to c_2. The reason of excluding c_2 is the same as the one in the turbo decoding case, i.e. to reduce the correlation of the messages passed over different iterations. The second half of the iteration is similar. An example is also given in Fig. 2.2., where we consider the message flow from c_3 to v_3. Node c_3 exploits the information from all the neighboring nodes except v_3 and generates the extrinsic information for v_3.

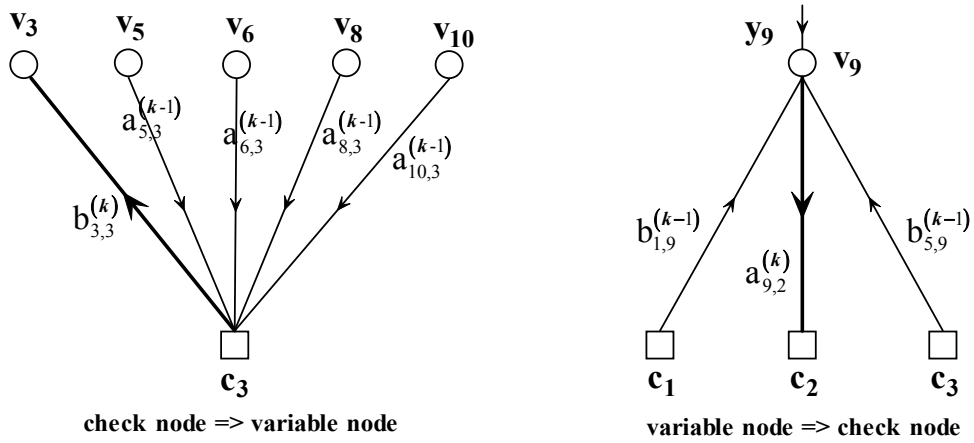

Figure 2.2 Example of the message passing algorithm.

The messages exchanged during the decoding process are assumed to be statistically independent. This assumption is achieved if the Tanner graph has no cycles and the decoding algorithm is optimal. For other graphs with girth κ, this assumption is true only up to $\kappa/2$ iterations. But it can be stated that the decoding algorithm is still effective as long as the cycles that have a length of four are avoided.

The earliest LDPC codes are regular codes. In the consideration of code design, one issue is the choice of variable node degree d_v. If we employ optimal maximum a posteriori probability/maximum likelihood (ML) decoder, the performance increases with variable nodes of high degree. However, for the suboptimal BP decoder, the sum-product algorithm does not work well for

relatively dense graphs and the decoder performance is degraded. For this reason the performance of regular codes is inversely proportional with variable node degree d_v. Regular LDPC codes have a simple structure and a good distance property. But considering the capacity approaching capability, another group of LDPC codes called irregular LDPC codes (Richardson, Shokrollahi, & Urbanke, 2001) are more powerful. By allowing irregularity in the code construction and optimizing the degree distribution, they can outperform the regular codes and approach the capacity limits more closely. We illustrate their performance over an AWGN channel in Fig. 2.3. With the increasing block length, the performance differences with the Shannon limit are decreased significantly, similar to the case of turbo codes. At a BER of 10^{-5}, irregular codes with information block length 10000 can achieve a coding gain of 8.7 dB over uncoded system. Regular codes with the same block length are 0.7 dB worse. As the the block length increases, the gain of irregular codes over regular codes increases as well, since the degree distribution is usually optimized under the assumption of infinite block length.

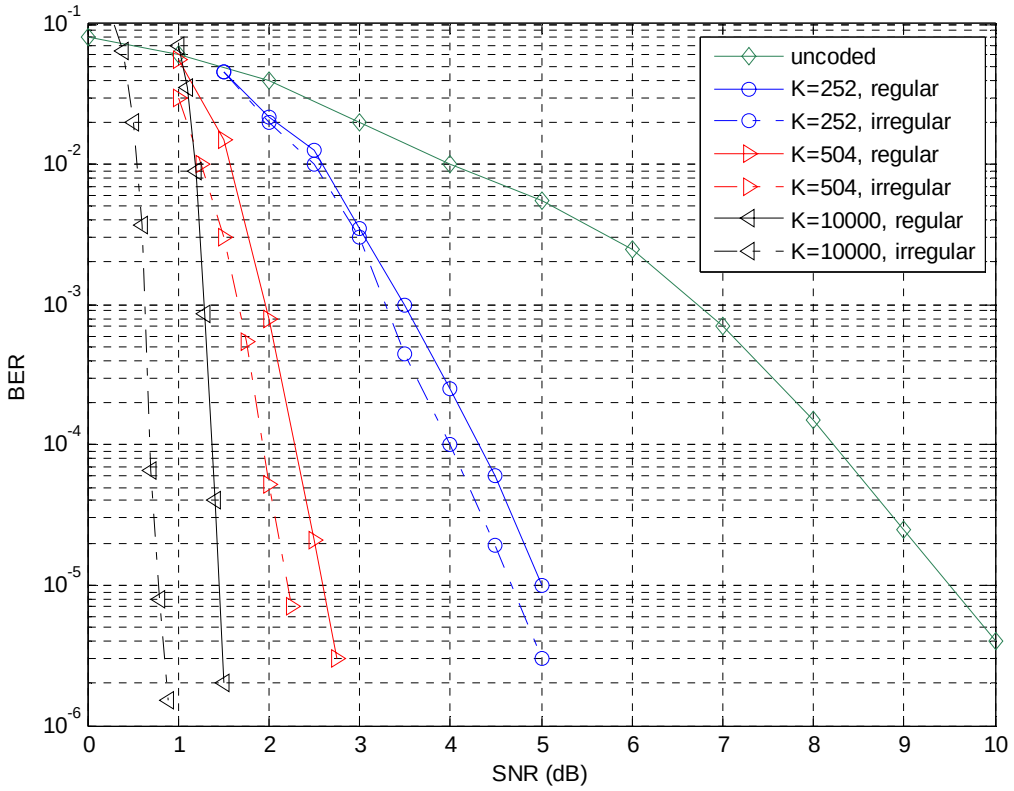

Figure 2.3 Performance of regular and irregular LDPC codes over AWGN channel.

Next, we show some performance results over ergodic Rayleigh fading channels in Fig. 2.4. For irregular codes, we use a degree distributions optimized for Rayleigh fading channels (Hou et. al. 2001). In this case, irregular codes are still superior to the regular ones.

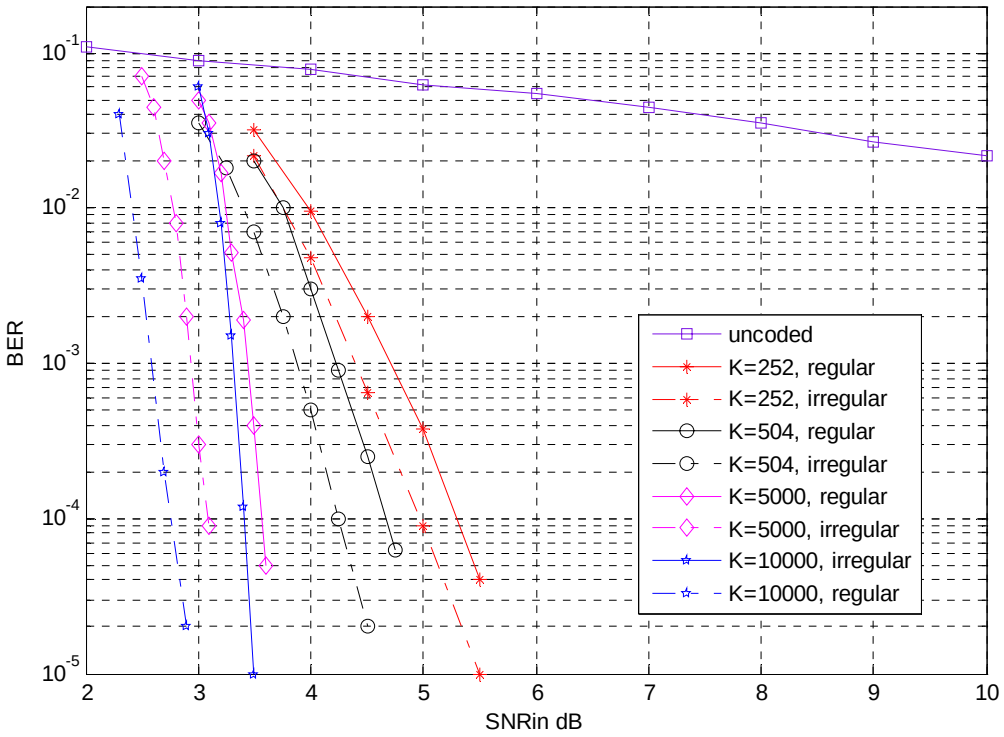

Figure 2.4 Performance of LDPC codes over ergodic fading channel.

2.2.2 Turbo Codes

Turbo codes are a class of very powerful error correcting codes introduced by a group of French researchers in 1993 (Berrou et al.,1993). They lead an important improvement in coding theory due to their capability to approach the Shannon limit. Over the past decade, many researchers have exploited the potential of turbo codes and progressed significantly in this area. Turbo codes have been proposed for many applications such as deep space and satellite communications, as well as standards like digital video broadcasting terrestrial (DVB-T) and third-generation cellular systems (UMTS and CDMA2000).

A simple turbo encoder can be formed by concatenation of two recursive systematic convolutional (RSC) codes separated by a random interleaver, as shown in Fig. 2.5. The information bit sequence X is first sent into RSC 1 encoder and a set of parity bits P1 is generated. X is interleaved and sent into RSC 2 encoder (it may be different from RSC 1) and another set of parity bits P2 is also generated. After passing through an optional puncturing step, the parity bits are sent over the channel together with the systematic bits. Here, the role of puncturing mechanism is to increase the code rate by periodically deleting bits according to a puncturing pattern. Different code rates can be achieved by using different puncturing patterns. Unlike the classical interleaver which rearranges the bits in some predetermined manner, the random interleaver reorders the bits in a way not suiting any apparent order before being encoded by the second component code. The interleaver size also has a significant effect on BER performance. The design of the interleaver can be reviewed in (Duman, 2002).

The code concatenation can also be implemented in serial form as in Fig. 2.6. For the serially concatenated structures, the information bits are first encoded by an outer encoder, then the coded bits are fed into the inner encoder after going through an interleaver. The choice of appropriate encoders also plays a crucial role in the design of turbo codes. In (Benedetto, Garello, & Montorsi, 1998), tables of the "optimal" RSC encoders are presented for various rates. The combination of code concatenation, recursive encoding, random interleaving and iterative decoding greatly enhances the error rate performance of such systems at very low SNR's.

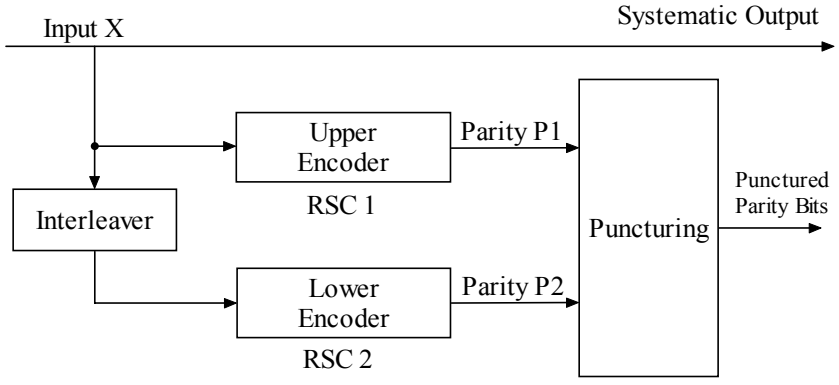

Figure 2.5 Diagram of a standard turbo encoder, parallel concatenation.

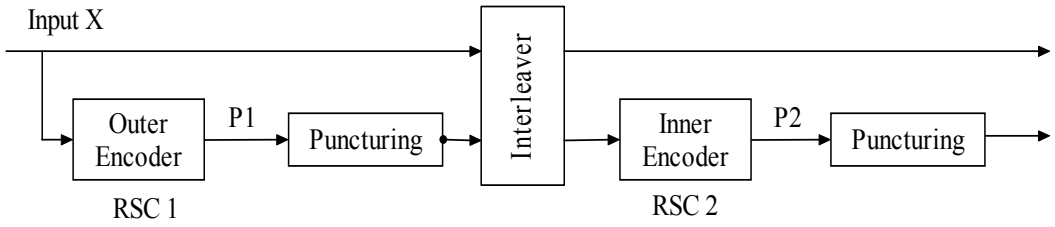

Figure 2.6 Diagram of a standard serial concatenated code.

Since turbo codes are linear, their error probability is directly related to their weight distribution. To ensure a good performance, the encoder should avoid low-weight codewords, or at least reduce their numbers. For input sequences with weights 3 or more, the probability of generating low-weight sequences from both the original sequence and the interleaved one is small. Hence, the major concern is the weight-1 and weight-2 input sequences. One very distinct aspect of turbo encoder is that it chooses the RSC code as a component code.

For a non-recursive encoder, a finite-weight input always produces a finite-weight output. However, for an RSC encoder, it produces a finite-weight output only when the input polynomial is divisible by the feedback polynomial. Thus, for a weight-1 input sequence, the encoder always produces an infinite-weight output. Therefore, the main contribution to the error probability is from the weight-2 sequences. Due to the scrambling operation of the interleaver, even if some low-weight codewords are possible at the output of the first encoder, the possibility of another low-weight codeword at the output of the second encoder is greatly reduced. Therefore, the combination of the RSC encoder and the long interleaver minimizes the occurrence of low-weight outputs, thus providing a good basis for better BER performance at low SNR's.

2.2.3.1 Turbo Decoding Algorithm

A standard turbo decoder structure is shown in Fig. 2.7. Y^s, Y^{p1} and Y^{p2} are the AWGN channel outputs corresponding to the systematic bit sequence X, and parity bit sequences P1 and P2, respectively, as shown in Fig. 2.4. The overall

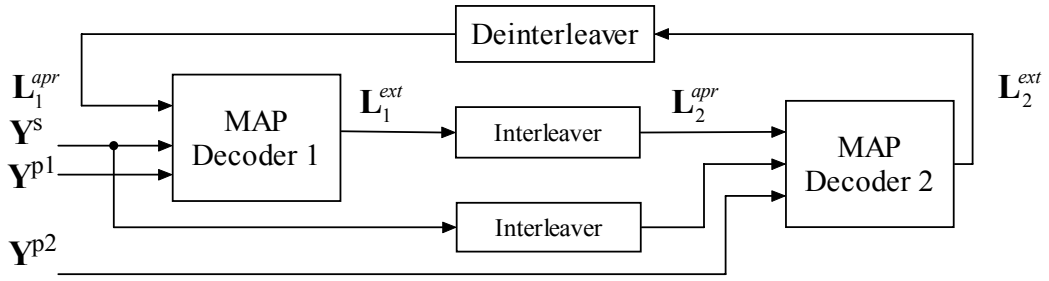

Figure 2.7 Diagram of an iterative turbo decoder.

decoder is a suboptimal iterative decoder. The basic idea is to pass the soft extrinsic information from the output of one decoder to the input of the other one, and use it as the a priori information. There exist two MAP decoding modules for each of the component codes. One of the decoders takes Y^s, Y^{p1} and the a priori information L_1^{apr} (deinterleaved extrinsic information from decoder 2) as the input, while the other one takes the interleaved version of Y^s, Y^{p2} and the a priori information L_2^{apr} (interleaved extrinsic information from decoder 1) as the input. This information exchange is continued several times to produce more reliable decisions.

For each MAP decoding module, the soft output can be computed using the Bahl-Cocke-Jelinek-Raviv (BCJR) algorithm (Bahl, Cocke, Jelinek, & Raviv, 1974). If we define $Y_k = \left[Y_k^s \; Y_k^{p1} \right]$ and $Y_1^K = \left[Y_1, Y_2, ..., Y_K \right]$, where K is the interleaver size, the BCJR algorithm computes the LLR of the kth bit as,

$$L_1\left(X_k\right) + \log \frac{P\left(X_k = 1 \middle| Y_1^K\right)}{P\left(X_k = 0 \middle| Y_1^K\right)}. \tag{2.15}$$

The output extrinsic information is computed as

$$L_1^{ext}\left(X_k\right) = L_1\left(X_k\right) - L_1^{apr}\left(X_k\right) - 4Y_k^s / N_0. \tag{2.16}$$

The overall LLR information is composed of three parts: extrinsic information for decoder 2, a priori information from decoder 2 and the systematic information.

The second MAP decoder operates in a similar way and an information flow takes place between two decoders as shown in Fig. 2.7. As an example, we consider the turbo coding scheme with component RSC encoders $(21/37)_{octal}$, code rate R_c = 1/2 and interleaver length K = 10000. At the receiver side, 10 iterations are performed within the turbo decoder and the simulation results over an AWGN channel is illustrated in Fig. 2.8.

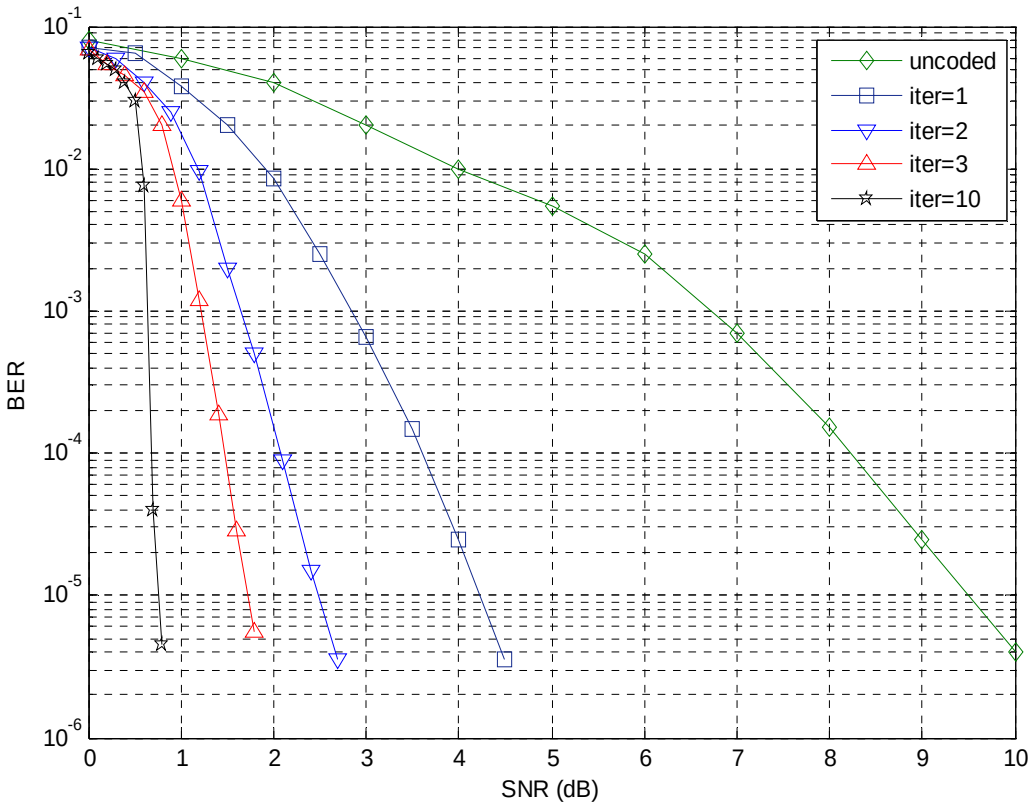

Figure 2.8 Performance of a turbo coded system, different iterations.

As we can observe from Fig. 2.8, the turbo coding scheme can achieve a much better BER performance compared to the uncoded scheme. When the number of iterations increases, the performance gain is increased. But after a certain number of iterations (in this example, after 10), the gain is limited, so there is no need to iterate any further. To achieve a BER of 10^{-5} an SNR of 0.75 dB is required for the turbo coded system, i.e. a coding gain of approximately 8.7 dB over uncoded system is achieved. The capacity and information rate results show that, minimum E_b/N_0 needed over AWGN channel is 0 dB for Gaussian inputs and 0.2 dB for i.u.d. binary inputs, at 1/2 bits per channel use. Therefore, the turbo coded

scheme is only 0.75 dB away from the Shannon capacity limit, and 0.55 dB away from the constrained capacity limit, respectively.

One of the most important factors affecting the turbo coding performance is the interleaver size. In Fig. 2.9, the error rate curves of the same turbo code is shown for various interleaver sizes. We observe that, as the interleaver size, *K*, increases,

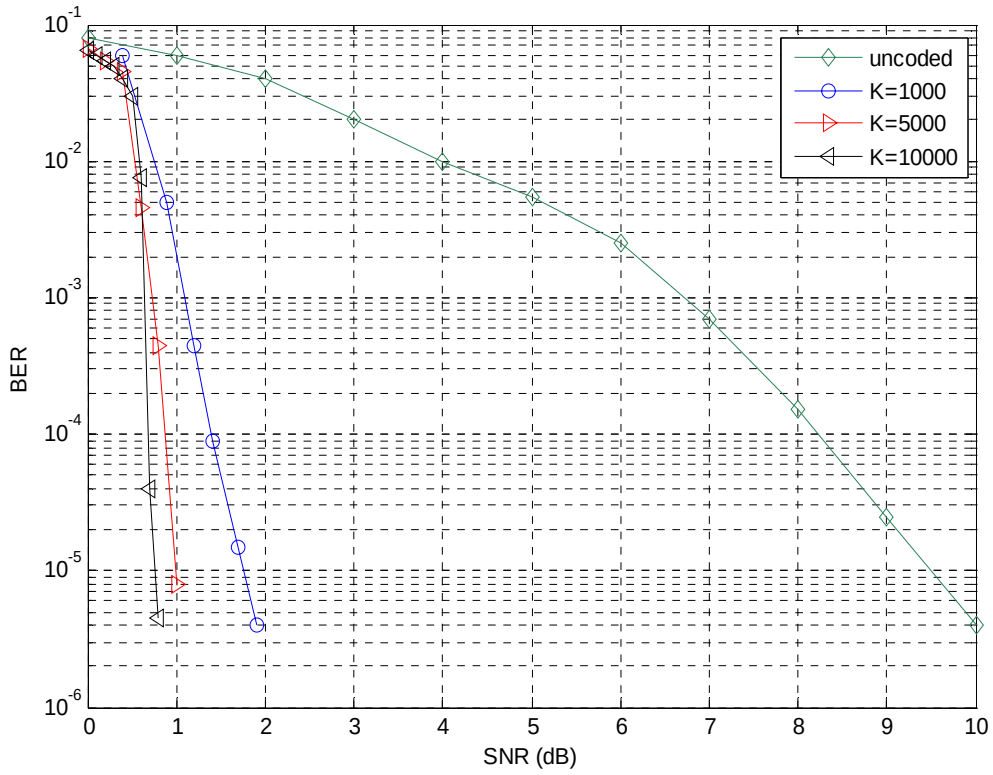

Figure 2.9 Performance of a turbo coded system, different interleaver sizes.

the BER performance improves significantly. However, there exists a trade-off between the interleaver size and the decoder latency. As the interleaver size increases, the decoder process time will be longer. For certain applications, this kind of delay may be undesirable.

2.3 Iterative Detection Techniques

In the previous section, we have discussed the basic algorithms to decode turbo and LDPC codes. It can be easily noticed that these two algorithms have similar aspects. They both separate the decoder into two parts and exchange information between these two modules. During the iterative process, they both use the notion of a priori information and extrinsic information. Actually, all these ideas can be separately or jointly extended to other applications. For example, we can form a closed loop between the detection process and the decoding process. By feeding back the soft information at the output of the decoder, we can further correct the detection results and improve the overall system performance. Similar ideas can be employed between estimation and decoding, or between equalization and decoding, and so on (Tuchler, Koetter, & Singer, 2002). This concept is usually called “turbo processing”, as illustrated in Fig. 2.10.

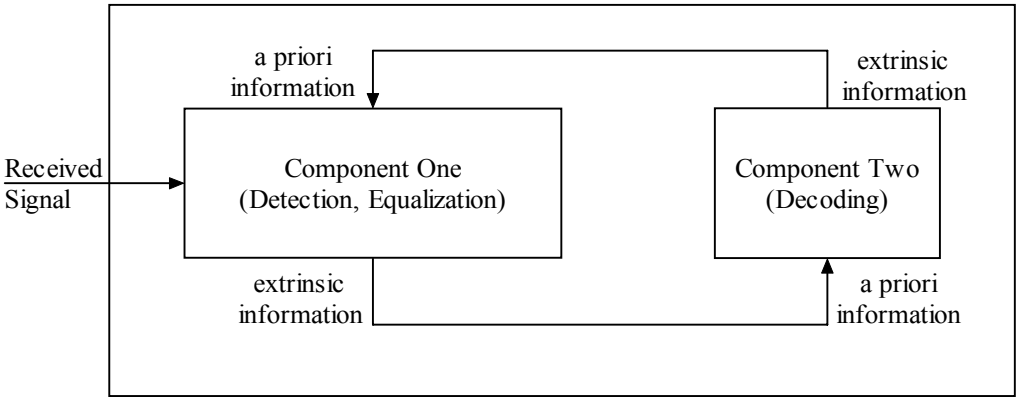

Figure 2.10 A general block diagram of turbo processing.

2.4 Convergence Analysis

For iterative decoding schemes, the BER curve usually can be divided into three regions: The low bit error rate region with negligible improvement with further iterations, the waterfall region and the error floor region. A large amount of research has been carried out to provide tools for analyzing and designing the codes. The bounding techniques in (Duman & Salehi, 1998) provide very useful

analytical results for medium to high SNR region. However, due to their limitations, they are not suitable for analysis in the waterfall region which is the major interest for many applications. For this reason the asymptotic (large block length) performance of iterative decoding at SNR's close to capacity is determined by figuring out a convergence threshold that characterizes their asymptotic performance. If the channel SNR is below this certain threshold, under iterative decoding, the decoder often converges to a fixed point (an incorrect solution) which in general results in large BER. Asymptotically, the smallest channel SNR under iterative decoding for which the probability of error goes to zero as the number of iterations becomes large is known as the convergence threshold for a particular code. Convergence thresholds can be determined by visualizing the input-output relationship of a constituent soft input soft output (SISO) decoder. There exist two main methods that describe this relationship between the input of the decoder (a-priori information) and the output of the decoder (extrinsic information).

2.4.1 Density Evolution

Density evolution is applied by tracking the probability density function of extrinsic information for both turbo (Divsalar, Dolinar, & Pollara, 2001) and LDPC codes (Richardson & Urbanke, 2001). For LDPC codes, it is implemented by tracking the probability densities of all the variable and check nodes under a certain message passing algorithm. By choosing the degree distribution with the lowest convergence threshold, we can use density evolution to design good codes over a specific channel. An example of irregular LDPC code design over AWGN channels is presented in (Richardson et. al., 2001). For Rayleigh fading channels, a similar density evolution technique is employed in (Hou et. al., 2001).

2.4.2 Extrinsic Information Transfer Charts

For large number of iterations, tracking the probability density function becomes computationally demanding. As a simplified alternative to density evolution, EXIT chart method uses the mutual information to estimate the

convergence threshold. It was originally designed for turbo codes (Ten Brink, 2001) but succesfully applied for LDPC codes as well (Ten Brink, et. al., 2004) This technique relates the mutual information between an information bit and the a priori input (I_a) to the mutual information between the same information bit and the corresponding a posteriori extrinsic estimate (I_e). Assuming that information bits are i.i.d. and antipodal signaling is applied, the average mutual information between a specific bit and its corresponding LLR value L is given by

$$I(X;L)=\frac{1}{2}\sum_{x=\pm 1}\int_{-\infty}^{\infty} p_L(\zeta|X=x).\log_2\frac{2p_L(\zeta|X=x)}{p_L(\zeta|X=-1)+p_L(\zeta|X=1)}d\zeta\,. \tag{2.17}$$

If L is approximated as a Gaussian random variable with variance σ_L^2 the mutual information is defined in a simpler form as,

$$J(\sigma_L)=1-\int_{-\infty}^{\infty}\frac{e^{-\left((\zeta-\sigma_L^2)/2\sigma_L^2\right)}}{\sqrt{2\pi}\sigma_L}\log_2\left(1+e^{-\zeta}\right)d\zeta\,. \tag{2.18}$$

Specifically, if we consider the turbo scheme, the a priori information at the input of the decoders can be assumed as independent and identically distributed (i.i.d.) Gaussian random variables since there exists random interleaver between the two decoders. As a result, a priori information is given by

$$L_a(b_i)=\frac{\sigma_a^2}{2}(2b_i-1)+n_a\,, \tag{2.19}$$

where $\sigma_a=J^{-1}(I_a)$, b_i is the ith systematic bit, and n_a is a Gaussian random variable with zero mean and a variance of σ_a^2. The Gaussian assumption is not valid for extrinsic information L_e, thus I_e is computed using histogram measurements and Eq. 2.17. Viewing I_e as a function of I_a and SNR, the extrinsic information transfer characteristic of a decoder is defined as

$$I_e = g\left(I_a, SNR\right). \tag{2.20}$$

Now we describe how the transfer characteristics of the constituent decoders can be used to determine the convergence threshold of a turbo code. The EXIT chart for a particular SNR can be formed by plotting the transfer characteristics of SISO decoder for two constituent encoders on a reverse set of axes (one on the x-y axis, the other on the y-x axis). The chart can then be used to trace the trajectory of iterative decoding as follows. For a given SNR, initially I_a = 0 corresponding to the first iteration of decoder 1, we determine the resulting I_e (vertically) using the transfer characteristics for decoder 1. Since the *a posteriori* extrinsic estimate of decoder 1 becomes the *a priori* value of decoder 2, the value of I_e from decoder 1 becomes I_a for the first iteration of decoder 2, and the resulting l_e for decoder 2 is determined (horizontally) using the transfer characteristics for decoder 2. This procedure is repeated to trace the trajectory of iterative decoding. If a *tunnel* exists between the two transfer characteristics, iterative decoding converges. If no tunnel exists, i.e. the two transfer characteristics touch or cross each other, iterative decoding does not converge. The output mutual information approaches one as the decoder converges, and probability of error approaches zero.

Fig. 2.11 shows a transfer characteristics of iterative decoding of turbo code (G=(31,33), memory 4) , E_b/N_0 at -0.5 dB, 0 dB and 0.5 dB. For E_b/N_0 = -0.5 dB the trajectory gets stuck after three iterations since both decoder characteristics intersect. For E_b/N_0 = 0 dB the trajectory has just managed to pass through the bottleneck. At E_b/N_0 = 0.5 dB, the extrinsic information reaches a value of 1 after four iterations and the decoder guarantees to converge.

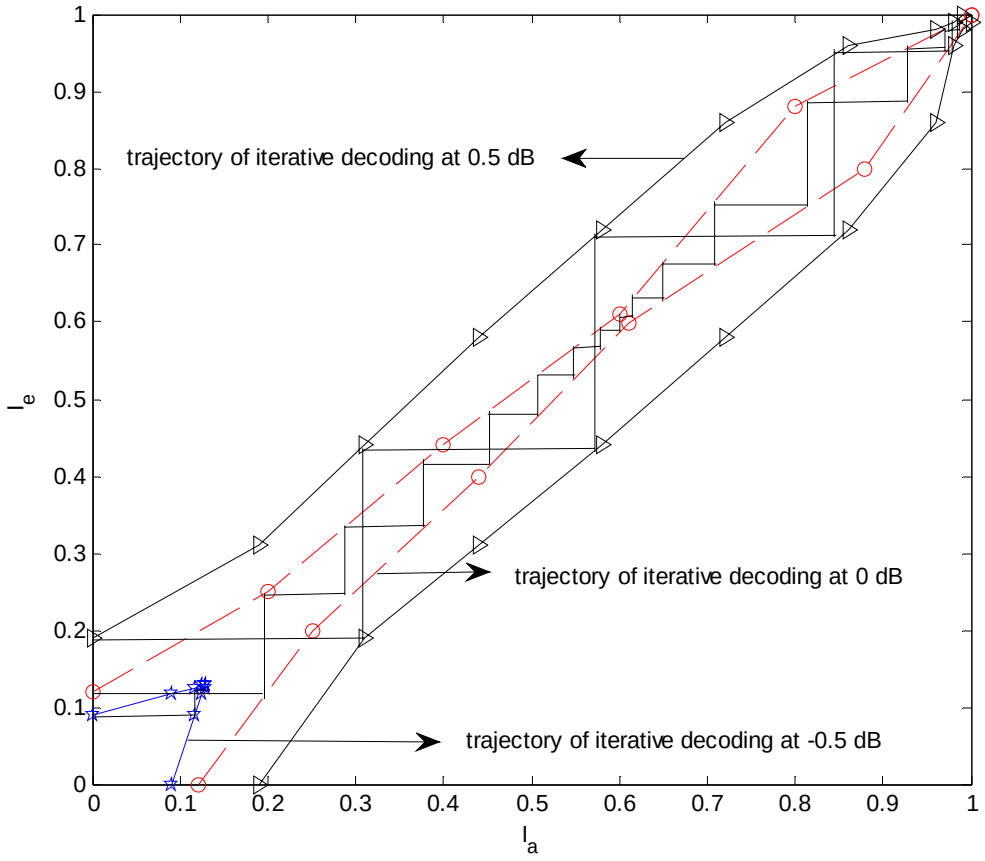

Figure 2.11 Simulated trajectories of iterative decoding.

2.5 Chapter Summary

In this chapter we introduced the channel capacity concept and revisited several known capacity results for AWGN, fading and ISI channels. These results will guide the information theoretical analysis in the following chapters. We discussed two powerful coding techniques (LDPC and turbo codes) and discussed their encoding/decoding methods. We also presented their performance via simulation results. The simulation results have shown that irregular LDPC codes have superior performance than regular LDPC codes. Also the performances of both types of LDPC codes increase with the increasing block length. Similar dependence holds for turbo codes as well. Both irregular LDPC codes and turbo codes are shown to approach Shannon limit very closely for AWGN channel. Finally, we described the EXIT chart tool to determine the convergence behaviour of the iterative decoding/detection process. This tool will also be used in the following chapters.

CHAPTER THREE
DISTRIBUTED TURBO AND MULTILEVEL CODED COOPERATIVE COMMUNICATION

In this chapter, we firstly review cooperative communication and its implementation issues. Next, we consider application of turbo codes distributively in a two user cooperative communication system. We analyze bit error rate of the system involving the re-encoded symbols in error and express an upper bound for overall BER of a single user. Afterwards, we summarize general framework of multilevel coding and then exploit multilevel codes under the cooperative communication framework. The performance of the proposed multilevel coded cooperative (MCC) scheme, obtained by simulations, is evaluated together with the derived upper bounds.

The chapter is organized as follows: The cooperative communication framework is introduced in Section 3.1 and relevant work is summarized therein. In Section 3.2, distributed turbo coding system realized via user cooperation is presented. Incorporating the erroneous inter-user transmission into the analysis, the derivation of upper bound on BER for this system is given. Multilevel coding technique is covered in Section 3.3 and the encoding and decoding methods are presented together with an analysis on the upper bound for probability of error. The proposed MCC system, its channel model and a pairwise error probability derivation are given in Section 3.4. After the simulation results given in the same section, the chapter is concluded in Section 3.5.

3.1 Overview of Cooperative Communication

The main design objective of the wireless communications is to achieve better spectral efficiency, power efficiency and data reliability. In this context, the use of various diversity techniques greatly facilities constructing efficient systems. By transmitting independently faded copies of a signal using multiple antennas, spatial diversity enables higher reliability of information without sacrificing

bandwidth. It can be applied together with temporal and frequency diversity and also is an effective candidate to them whenever the latter two cannot be applied. MIMO systems exploit spatial diversity and apply space time coding or spatial multiplexing techniques in the framework.

Recently, cooperative diversity has been proposed to exploit spatial diversity for wireless nodes in a distributed manner. In user cooperative communication (Sendoranis et. al. 2003), multiple users not only transmit their information but also assist the transmission of their partners. There is no separate relay node whose function is to enhance the source-destination transmission as proposed in the original relay channel. The main purpose of the user cooperative communication is to share the multiple users' antennas and gain transmit diversity through a virtual antenna array. Information theoretical analysis showed that the achievable rate region can be significantly enlarged by cooperation. Also the cell coverage is shown to be increased via cooperative communication.

Cooperative communication enables different signaling and user configurations. Except from the single relay channel, other possible channel models are illustrated in Fig. 3.1. In (a), there are multiple sources with information to send to the same destination. In addition to the source-destination links, there is cooperation between the sources and there is no separate relay. In (b), one transmitter broadcasts information to multiple receivers. In (c), there is only one source and one destination, but multiple relays try to help the transmission from the source to relay. The receivers exchange messages through collaboration (Li, Wong, & Shea, 2008) to obtain more reliable estimate of the message. Possibly the situation described in (d) is the most complex one. Multiple sources and multiple receivers communicate not only by cooperation at the transmitters, but also by collaboration at the receivers. Considering the applications of these models, the uplink and downlink of a cellular system may follow the configuration (a) and (b), respectively, while in a wireless ad-hoc network, communication between users resemble (c) and (d).

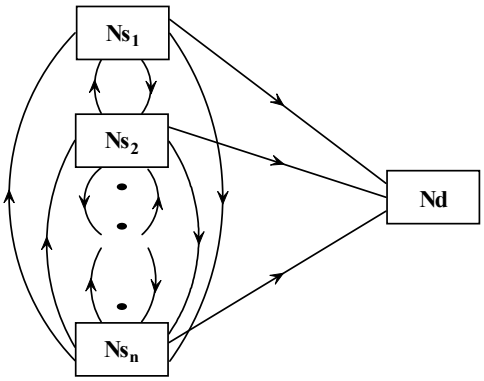

(a) multiple-access channel with cooperation

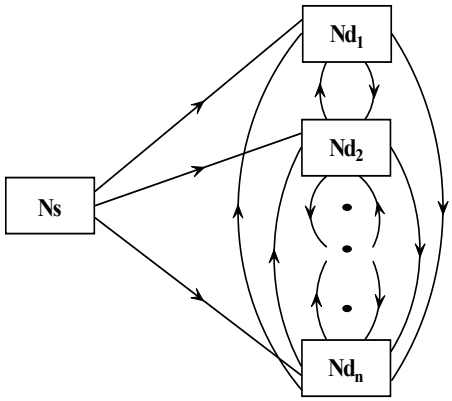

(b) broadcast channel with cooperation

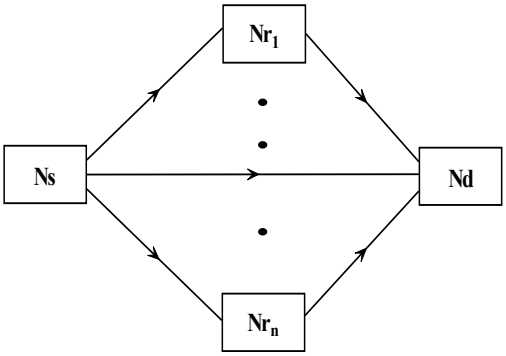

(c) parallel relaying channel

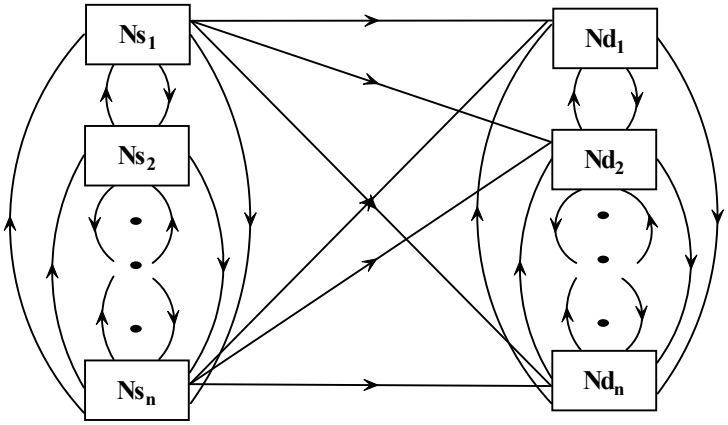

(d) interference channel with cooperation

Figure 3.1 Examples of cooperative communication.

3.1.1 Signaling Strategies

The main difference between the relaying protocols (AF, DetF, EF, DF and CF) is how the relay works. In the AF/DetF/EF mode, the relay simply receives/detects/estimates the source signal and transmits the signal to the destination obeying its power constraints. In the DF mode, the relay decodes, re-encodes and forwards the source information. As the name implies, the relays compress the received signal before forwarding to destination in the CF mode.

These fixed protocols can be adapted according to the channel conditions and overall performance can be improved. Several examples consist of selecting the relay based on the channel conditions, exploiting limited feedback from the destination, and employing a mixed mode relay, etc.

3.1.2 Coded Cooperation

Coded cooperation is an extension of DF method. It can be applied for both user cooperation and relay channels. Since simple AF or DF schemes are similar to repetition coding, they are not very effective at low SNRs. On the other hand, coded cooperation outperforms them by integrating the forward error correction (FEC) techniques into the system. The term ‘coded cooperation’, introduced in (Janani et. al., 2004), implies partitioning and distributive transmission of the codewords between the cooperating users or with the assist of relays. In multiple user scenario, each user tries to transmit incremental redundancy for his partner by sending different portions of the other user’s codeword via independent fading paths. In this way, cooperation is integrated into channel coding. The role of the partner can be fulfilled with relays as well. Various kinds of channel coding schemes are employed under coded cooperation framework.

In (Janani, et. al., 2004), RCPCC codes, turbo codes and space time turbo codes are applied distributively for two user case. The requirement for a user to operate in cooperative mode is to decode partner’s data without error. The error check is executed via CRC codes. Otherwise whenever an erroneous transmission

occurs, the user automatically turns to non-cooperative mode and transmits its own information. Consequently, the system is assumed to operate in one of the four cases, in which both users cooperate, one of users cooperates while other does not or the non-cooperative case, respectively. Therefore, the bit and block error analysis is dependent on the cooperation status of the system. When compared to the simple AF/DF schemes, coded cooperation generally performs better due to its coding gain. However, the RCPCC's used in (Janani et. al, 2004) are not optimal. In (Stefanov & Erkip, 2004), based on block fading channel model, design criteria for cooperative convolutional codes are derived.

The coded cooperative system in (Janani, et. al., 2004) is subjected to error free transmission between the users, so the path between the users is excluded from BER analysis therein. However the distributed turbo coding over relay channel scheme, proposed in (Li, et. al., 2006), assumes that the relays forward soft estimates of the symbols instead of making decisions and hence named as distributed turbo coding with soft information relaying (DTC-SIR). The DTC-SIR system always operates in cooperative mode as opposed to (Janani, et. al., 2004). Hence, the union bound for BER is calculated treating the path from source to destination over the relay as a serial two hop fading path. The performance of DTC-SIR system is compared with DTC system in which error-free transmission is ensured with automatic repeat request (ARQ) from the relay. It is shown that, due to imperfect decoding at the relay, the DTC-SIR has a performance loss compared with perfect DTC with ARQ, but performs better than DTC system without ARQ.

In (Roy & Duman, 2006), the authors propose a distributed turbo coding system over half duplex relay channel assuming that the relay decodes and forwards the source signal without an error check. The source and relay transmits in the same frequency band in the second time slot to improve spectral efficiency. The source transmits a portion of the codeword in the first time slot and transmits the remaining in the second slot. The relay constitutes turbo coding with the information it receives from the source during the first time slot. The union bound on BER over AWGN channel is computed considering the effect of erroneous

codeword transmitted by the relay. The simulation results show that for large SNR's and interleaver sizes the calculated bound is close to actual performance.

3.2 Distributed Turbo Coded Cooperative (DTCC) System

Since turbo codes are formed by demultiplexing the outputs of two parallel concatenated encoders, the individual outputs of two encoders can be transmitted by two cooperating nodes respectively in order to construct a distributive turbo coded system. Explicitly in our scenario, as also proposed in (Janani, et. al., 2004), while the output of first encoder is transmitted by the source itself, the codeword produced by encoding the interleaved message bits is transmitted by the cooperating user. Different from (Janani, et. al., 2004), we assume that users always operate in cooperative mode, i.e. no error check is applied for decoded information of partner.

3.2.1 Transmission Model

We consider a system consisting of two cooperating users, denoted as user1 and user2, with the aim of realizing turbo codes distributively via cooperation. It is assumed that users transmit through orthogonal channels to the destination, so that destination can individually detect users' data without additional complexity. We denote the systematic bits, parity bits of first RSC and parity bits of second RSC of the turbo code of *kth* user as b_{k1}, b_{k2}, b_{k3}, respectively. The rate of both RSC's is 1/2. The block diagram of the system and the transmission scheme is given in Fig 3.2. In this scheme, both users send their systematic bits and the parity bits of the first encoder to their partners and also to destination during the first signaling interval. After decoding the data received from the partner, users construct the second parity bits of their partners and forward to the destination in the second time slot. The users employ Viterbi algorithm to decode the received coded information of their partner. On the other hand, the destination uses iterative turbo decoding technique after it receives data of both users in two time slots.

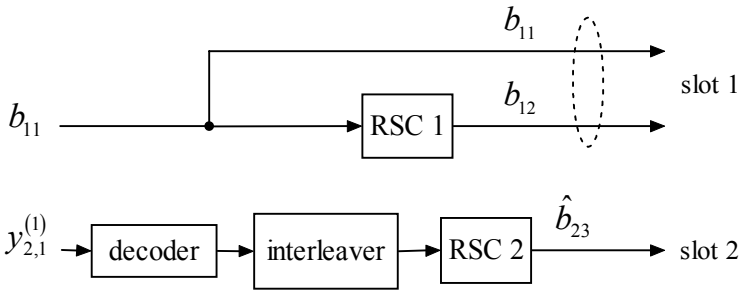

a) block diagram

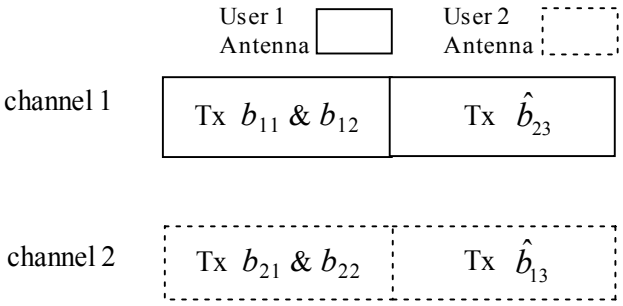

b) transmission model

Figure 3.2 Distributed turbo coded cooperation

Assuming BPSK modulation, we denote the signal transmitted by user $i \in \{1,2\}$ at time *n* and received at user $j \in \{0,1,2\}$ ($j \neq i$, $j = 0$ denotes the destination) as,

$$y_{i,j}^{(t)}(n) = h_{i,j}^{(t)}(n)\sqrt{E_{x,i}}x_i^{(t)}(n) + z_j^{(t)}(n), \tag{3.1}$$

where $x_i^{(t)}$ is the transmitted BPSK symbol from user *i* at time slot $t \in \{1,2\}$, z_j denotes the zero mean AWGN with variance N_j , and *h* is the Rayleigh distributed fading coefficient. The instantaneous received SNR for channel between users *i* and *j* is

$$\gamma_{i,j}(n) = \frac{\left(h_{i,j}^{(t)}(n)\right)^2 E_{x,i}}{N_j}. \tag{3.2}$$

3.2.2 Union Bound on Bit Error Probability of Turbo Coded Cooperation

In this section, taking into account the erroneous transmission between the cooperating users, an upper bound for BER of distributed turbo coded scheme from single user aspect is derived following the analysis in (Roy & Duman, 2006). First, quasi-static fading environment is assumed. Then, the analysis is extended to fast fading case. The error analysis is presented for user1 but it is also valid for user2. For quasi-static fading, the fading coefficients are constant over the codeword, i.e. $\gamma_{i,j}(n) = \gamma_{i,j}$. The average number of source codewords of user1 with information weight *i*, parity weight d' ($d_1 = i + d'$), which can be obtained using parity weight enumerating function (Divsalar, Dolinar, McEliece, & Pollara, 1995), is denoted by $t_{u1}(i, d')$. Assuming that all zero codeword is transmitted and the channel is quasi-static, the probability that user2 makes an error in i_e bits at the end of slot 1 can be upper bounded as,

$$p(i_e) \le \sum_{d'} t_{u1}(i_e, d') E_{\gamma_{1,2}} \left\{ Q\left(\sqrt{2(i_e + d') R_c \gamma_{1,2}} \right) \right\}, \tag{3.3}$$

where $E\{.\}$ denotes the expectation operator. Consequently, the probability that user2 transmits a codeword with d_e errors after re-encoding i_e erroneous bits is upper bounded by,

$$p_e(d_e) \le \sum_{i_e} \frac{t_{u2}(i_e, d_e)}{\binom{N/2}{i_e}} p(i_e), \tag{3.4}$$

where *N* is the length of the codeword transmitted by user1 in time slot 1. If $p_{ub}(d_e)$ denotes the union bound on overall error probability assuming that user2 caused d_e errors, then the upper bound on the average error probability can be found by averaging $p_{ub}(d_e)$ over probability mass function of d_e as,

$$p_e \le \sum_{d_e} p_e(d_e)\, p_{ub}(d_e). \tag{3.5}$$

We define the distributed turbo codeword as

$$\mathbf{c} = \left[c_{u1}(d_1) \;\; c_{u2}(d_2) \right], \tag{3.6}$$

where $c_{u1}(d_1)$ is the user1 component of weight d_1 transmitted during slot 1 and $c_{u2}(d_2)$ is the user2 component of weight d_2 transmitted during slot 2. Remembering our assumption that all zero codeword is transmitted by the user1 in slot 1 and user2 makes an error in d_e coded bits after decoding. we denote the codeword with erroneous user2 component as $\mathbf{c}^{(1)} = \left[c_{u1}^{(1)}(0) \;\; c_{u2}^{(1)}(d_e) \right]$. The decoder at the destination will make an error if the received signal falls into the decision region of another codeword $\mathbf{c}^{(2)} = \left[c_{u1}^{(2)}(d_1) \;\; c_{u2}^{(2)}(d_2) \right]$. Therefore, the error probability conditioned on the fact that $c^{(1)}$ is transmitted will depend upon the distance of $c^{(1)}$ with the decision boundary of the true codeword and $c^{(2)}$. In order to compute $p_{ub}(d_e)$ we need to compute the pairwise error probability (PEP) between $\mathbf{c}^{(1)}$ and $\mathbf{c}^{(2)}$. This probability depends on the number of bit positions where $c_{u2}^{(1)}(d_e)$ and $c_{u2}^{(2)}(d_2)$ overlap as illustrated in Fig. 3.3.

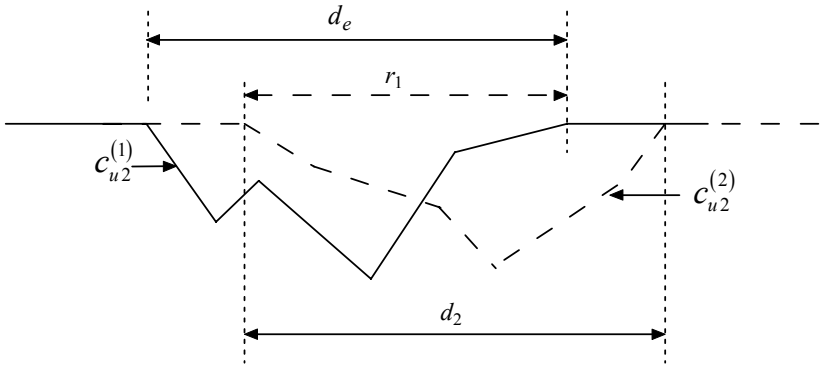

Figure 3.3 Illustration of r_1.

Let the number of overlapping positions be r_1. The probability mass function (PMF) of R_1 given d_e can be expressed as,

$$p_{R_1}(r_1) = \frac{\binom{d_e}{r_1}\binom{N-d_e}{d_2-r_1}}{\binom{N}{d_2}}. \tag{3.7}$$

If the error sequence for the user2 codeword component is defined as,

$$\begin{aligned} e &= c_{u2}^{(2)}(d_2) - c_{u2}^{(1)}(d_R), \\ &= [e_1, ..., e_N] \end{aligned} \tag{3.8}$$

then using the error definition above and the system model we can write the PEP as,

$$PEP\left(c^{(1)} \to c^{(2)} \middle| \gamma_{1,0}, \gamma_{2,0}\right) = Q\left(\sqrt{2R_c\gamma_{1,0}.d_1 + R_c\frac{\gamma_{2,0}}{2}\sum_k e_k^2}\right). \tag{3.9}$$

Since we use BPSK modulation, the components of the vector ***e*** can only take on the values 0,+2 and -2. More specifically, ***e*** takes on the value +2 for $d_2 - r_1$ positions, -2 for $d_e - r_1$ positions and zero for other positions. Therefore, the summation term in the argument of Q function can be written as,

$$\sum_k e_k^2 = 4(d_e + d_2 - 2r_1). \tag{3.10}$$

The average PEP is then given by,

$$PEP\left(c^{(1)} \to c^{(2)}\right) = \sum_{r_1} p_{R_1}(r_1) E_{\gamma_{1,0},\gamma_{2,0}}\left\{Q\sqrt{2R_c\left(\gamma_{10}.d_1 + \gamma_{2,0}(d_e + d_2 - 2r_1)\right)}\right\}, \tag{3.11}$$

where

$$Q(x)=\frac{1}{2\pi}\int_{x}^{\infty}e^{-t^2/2}dt\,. \tag{3.12}$$

In order to calculate the expectation in Eq. (3.11), we use an alternative representation for Q function which is,

$$Q(x)=\frac{1}{\pi}\int_{0}^{\pi/2}e^{-\frac{x^2}{2\sin^2\theta}}d\theta\ . \tag{3.13}$$

Let $E_{\gamma_{1,0},\gamma_{2,0}}\left\{Q\sqrt{2R_c\left(\gamma_{10}.d_1+\gamma_{2,0}\left(d_e+d_2-2r_1\right)\right)}\right\}=K$. Then, using Eq. (3.13), the result of this expectation becomes

$$K=\frac{1}{\pi}\int_{0}^{\pi/2}\left[\int_{0}^{\infty}e^{-\frac{R_c\gamma_{10}.d_1}{\sin^2\theta}}p(\gamma_{10})d\gamma_{10}\right]\times\left[\int_{0}^{\infty}e^{-\frac{R_c\gamma_{20}.(d_e+d_2-2r_1)}{2\sin^2\theta}}p(\gamma_{20})d\gamma_{20}\right]d\theta\,. \tag{3.14}$$

The inner integrals in Eq. (3.14) are in the form of moment generating functions (MGF) for the densities $p(\gamma_{10})$ and $p(\gamma_{20})$. The general formulation for MGF is,

$$M_x(s)=\int_{0}^{\infty}e^{sx}p(x)dx\,. \tag{3.15}$$

Rewriting Eq. (3.14) in the form of MGF's, we obtain,

$$K=\frac{1}{\pi}\int_{0}^{\pi/2}M_{\gamma_{1,0}}\left(-\frac{R_cd_1}{\sin^2\theta}\right)M_{\gamma_{2,0}}\left(-\frac{R_c\left(d_e+d_2-2r_1\right)}{\sin^2\theta}\right)d\theta\,. \tag{3.16}$$

For the case of Rayleigh fading, the MGF of instantaneous SNR is,

$$M_\gamma(-s)=\frac{1}{1+\gamma}\ . \tag{3.17}$$

As a result, we can rewrite Eq. (3.16) as,

$$K = \frac{1}{\pi}\int_0^{\pi/2}\left(1+\frac{R_c\gamma_{1,0}d_1}{\sin^2\theta}\right)^{-1}\left(1+\frac{R_c\gamma_{2,0}\left(d_e+d_2-2r_1\right)}{\sin^2\theta}\right)^{-1}d\theta\,. \tag{3.18}$$

Since the integrands in Eq. (3.18) is maximized for $\sin^2\theta = 1$, instead of obtaining a closed form solution, we express an upper bound as,

$$K \le \frac{1}{2}\left(\frac{1}{1+R_c d_1\gamma_{1,0}}\right)\left(\frac{1}{1+R_c\left(d_e+d_2-2r_1\right)\gamma_{2,0}}\right). \tag{3.19}$$

For fast fading channel PEP is defined as,

$$PEP\left(c^{(1)}\to c^{(2)}\right) = \sum_{r_1} p_{R_1}\left(r_1\right)E_{\gamma_{1,0},\gamma_{2,0}}\left\{Q\sqrt{2R_c\left(\sum_{n\in\eta_1}\gamma_{1,0}\left(n\right)+\sum_{n\in\eta_1}\gamma_{2,0}\left(n\right)\right)}\right\} \tag{3.20}$$

where the cardinalities of η_1 and η_2 are d_1 and $\left(d_e+d_2-2r_1\right)$, respectively. Consequently, *K* is expressed as,

$$K = \frac{1}{\pi}\int_0^{\pi/2}\left(1+\frac{R_c\gamma_{1,0}}{\sin^2\theta}\right)^{-d_1}\left(1+\frac{R_c\gamma_{2,0}}{\sin^2\theta}\right)^{-\left(d_e+d_2-2r_1\right)}d\theta \tag{3.21}$$

and the upper bound for *K* is obtained as,

$$K \le \frac{1}{2}\left(\frac{1}{1+R_c\gamma_{1,0}}\right)^{d_1}\left(\frac{1}{1+R_c\gamma_{2,0}}\right)^{\left(d_e+d_2-2r_1\right)}. \tag{3.22}$$

The conditional union bound, $p_{ub}\left(d_R\right)$, is expressed for both quasi-static and fast fading channels as,

$$p_{ub}\left(d_e\right) = \sum_{d_1}\sum_{d_2}\frac{i}{N}\frac{t_p^S\left(i,d'\right)t_p^R\left(i,d_2\right)}{\binom{N}{i}}\times PEP\left(c^{(1)}\to c^{(2)}\right). \tag{3.23}$$

3.2.3 Simulation Results

In the simulations, the BER performance of non-cooperative turbo system and that of DTCC system are evaluated. The 1/2 rated RSC encoder with generator matrix G = (1,5/7) is used as component code and BPSK modulation is employed at both users. For cooperative scheme, the SNR of the channel between the users, $\gamma_{1,2}$, is denoted as *iSNR* in the graphics. Also it is assumed that SNR's of user-destination links are equal, i.e. $\gamma_{1,0} = \gamma_{2,0}$. The frame length, N, is chosen as 1024.

The simulation results for slow fading channel are illustrated in Fig. 3.4. We observe that significant gain can be achieved with cooperation since it ensures diversity gain over non-cooperative system. In perfect inter-user channel case, the cooperative system performs 9 dB better than non-cooperative case at a BER level

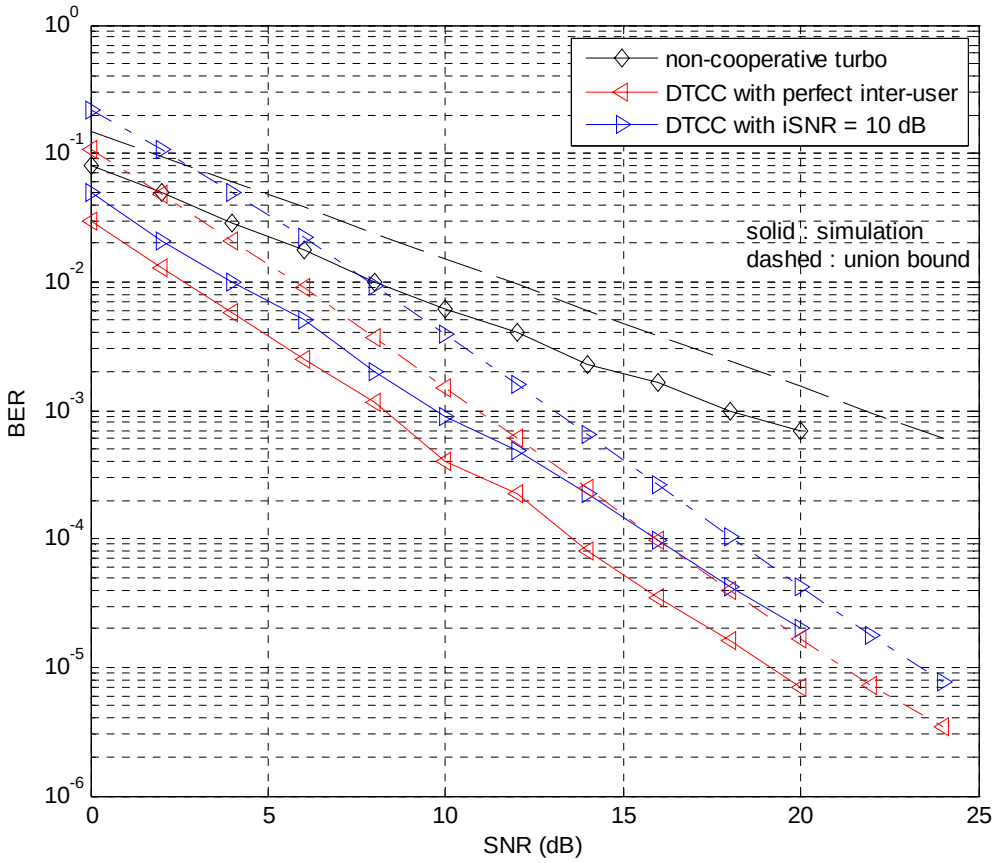

Figure 3.4 Performance evaluations of cooperative and non-cooperative system for quasi-static fading channel.

of 10^{-3}. When the inter-user channel has a SNR value of 10 dB, the gain decreases to 6 dB. It is also observed that, the upper bounds are moderate and match the simulation results.

The simulation results for fast fading channel are illustrated in Fig. 3.5. Again the user-destination SNR's are chosen as equal, i.e. $\gamma_{1,0} = \gamma_{2,0}$. Since no diversity gain exist for this case, cooperative and non-cooperative systems perform approximately the same. The gain at a BER level of 10^{-4} is only 0.3 dB. Additionally, we observe that the upper bounds obtained by union bounding technique are more tight for fast fading channel and support the simulation results.

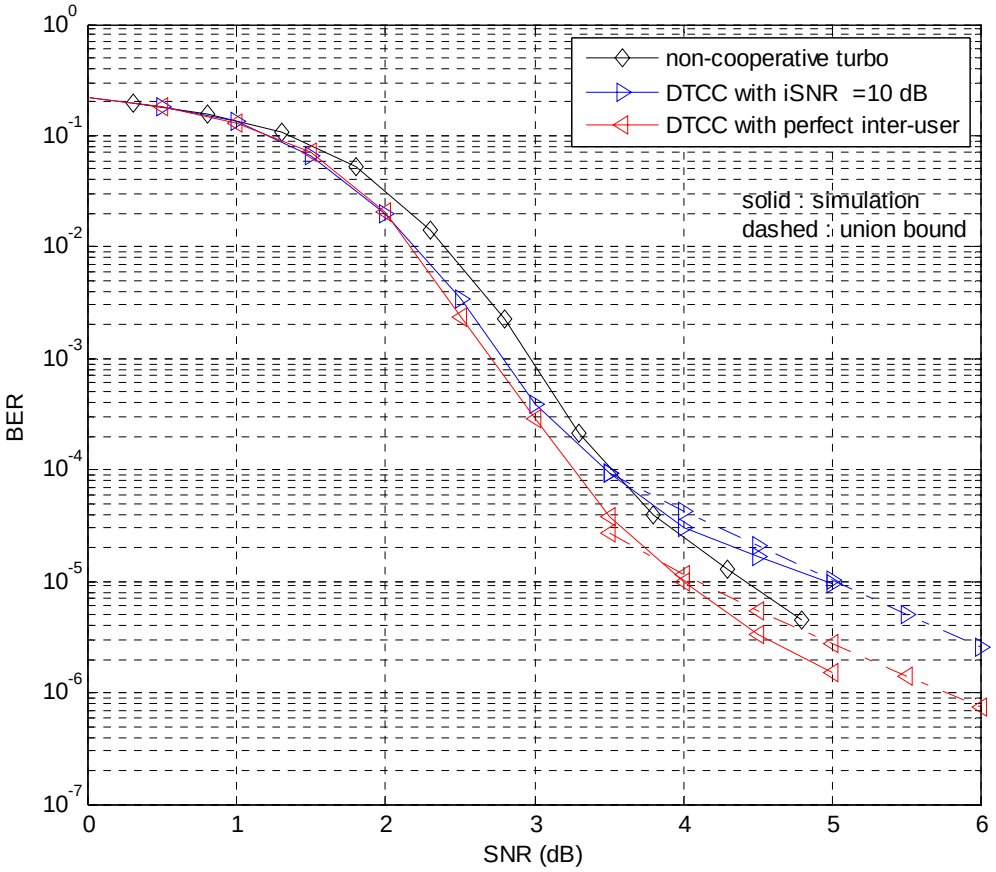

Figure 3.5 Performance evaluations of cooperative and non-cooperative systems for fast fading channel

3.3 Multilevel Codes

Convolutional codes designed for large minimum Euclidean distance performs poor for fading channels, because for fading channels, minimum symbol (Hamming) distance is the design criteria together with minimum product distance. Multilevel coding technique, originally proposed by Imai and Hirakawa (1977), combines multilevel binary codes with modulation using Ungerboeck's (1982) set partitioning rule, and has performance and bandwidth advantages over trellis coded modulation even with a suboptimal multistage decoder. There is a one-to-one correspondence between the minimum Hamming distance of component codes and the number of branches of time diversity in multilevel coding. Multilevel codes were shown to outperform Ungerboeck's codes for fully interleaved Rayleigh fading channel (Seshadri & Sundberg, 1993).

3.3.1 Encoder and Set Partitioning

The encoder employing PSK modulation is shown in Fig. 3.6. It is possible to use modulation techniques other than PSK as well. The overall rate of the code is the sum of individual rates of the codes constituting the multilevel scheme. Let the information rate per 2^m - PSK symbol be *K/L* bits which is also the bandwidth efficiency of the code. The mapping follows the set partitioning rule originially described by Ungerboeck. As an example, the set partitioning rule for a two level multilevel code with quadrature phase shift keying (QPSK) modulation is illustrated in Fig. 3.7. The bit $x^{(i)}$ partions the subset *i*, whose intraset distance $\Delta^{(i)}$. Since the performance of the code at level *i* depends on its intraset distance, assigning codes with higher gains and distances to levels with smaller $\Delta^{(i)}$ is crucial for overall performance. The overall rate constraint, $0 < K / L < m$ bits per 2^m - PSK symbol, should be fulfilled meanwhile.

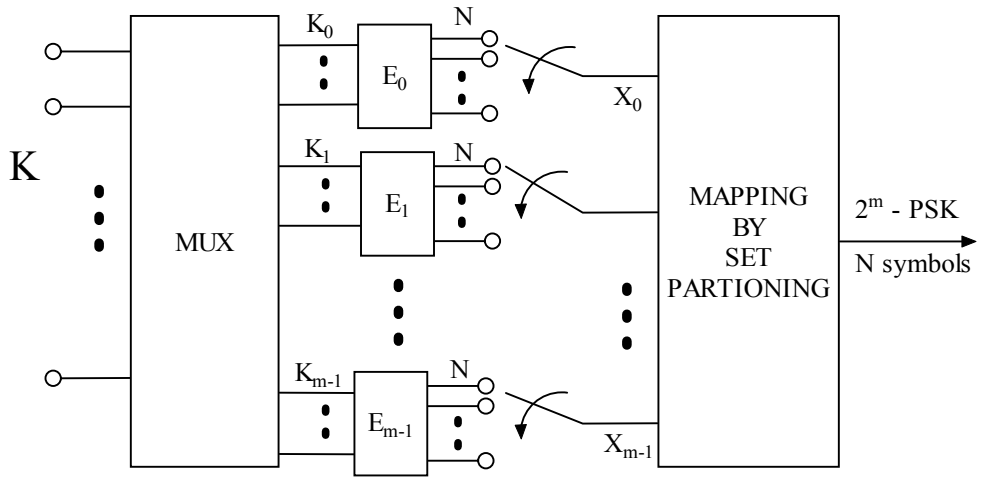

Figure 3.6 Encoding of multistage coded 2^m-phase modulation.

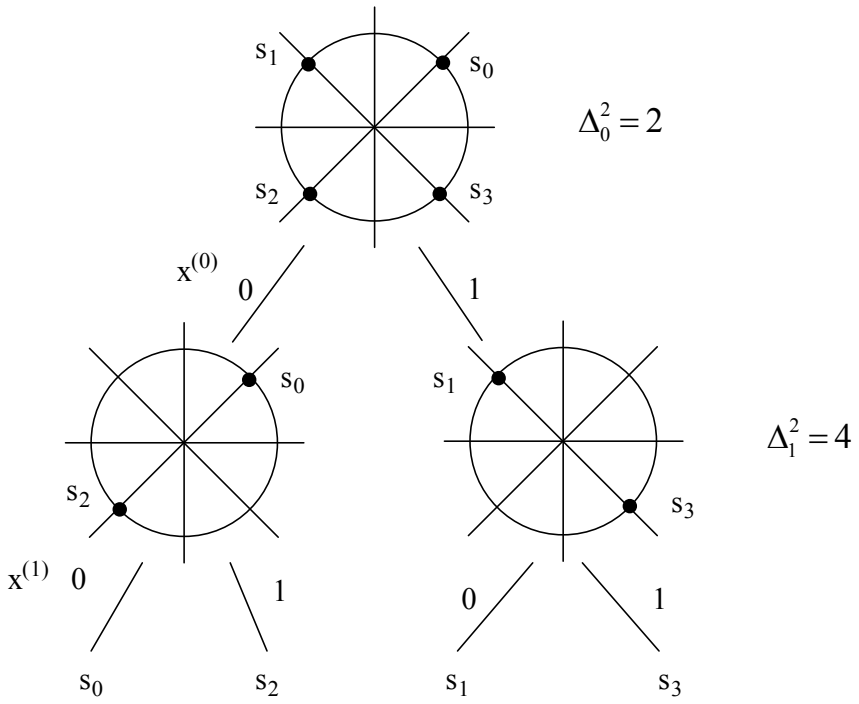

Figure 3.7 Set partitioning for multilevel coded QPSK.

3.3.2 Multistage Decoder

The multistage decoder, given in Fig. 3.8, is proposed by Imai & Hirakawa (1977). For each stage, a Viterbi decoder is applied to produce the estimated information sequence, $\hat{u}_k$ and code sequence.

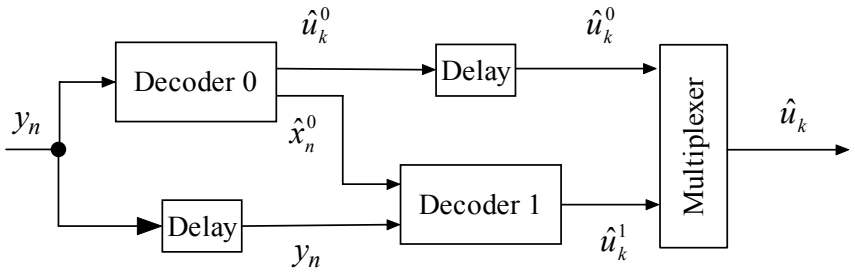

Figure 3.8 Multistage decoder.

The Viterbi algorithm calculates the metrics upon a signal set which is determined by the side information according to the set partitioning structure. The metrics associated with the code bits are simply the squared Euclidean distance between the received symbol and the symbol within the predetermined signal set. Since the codeword of a rate k/n convolutional code consists of n bits, the cooresponding branch metric is the summation of n consecutive metrics in the trellis diagram of the code.

Asymptotic coding gain (ACG) and effective coding gain are the two parameters that quantify the performance of a multilevel code. The latter gain also takes into account the error coefficients of the code. However the interaction between decoders in various stages makes it difficult to extend these error event bounds to obtain upper bounds on the decoded bit error probability. Assuming very small error rate the gain in bit-energy over noise density E_b/N_o relative to uncoded transmission is,

$$G = 10\log\frac{K/L}{m-1}\min_{0\le i\le m-1}\left\{\left(\frac{\Delta^{(i)}}{\Delta^{(1)}}\right)^2 d_H^{(i)}\right\}\ \ dB \tag{3.24}$$

where $d_H^{(i)}$ is the minimum or free distance of the code in stage *i*. For coded QPSK this gain is,

$$G = 10\log\frac{K}{L}\min\left(0.5d_H^{(0)}, d_H^{(1)}\right)\ . \tag{3.25}$$

3.3.3 Upper Bound for Probability of Error

In this section, multistage decoding of multilevel codes over an AWGN channel is considered. It is assumed that the components of the noise vector are independent Gaussian random variables with zero mean and variance $N_0/2$ in each dimension. The error performance evaluation method for PSK signals given in (Kofman, et. al. 1992) underlies the analysis here. If the side information carried by the decoders is always correct, the bit error probability of the decoder at the *i*th level ($i = 1,2, \ldots, M$) is upper bounded by

$$P_{bi} \le \frac{1}{k_i} Q\left(\sqrt{\frac{E_s\left(d_E^{(i)}\right)^2}{2N_0}}\right) \exp\left(\frac{E_s\left(d_E^{(i)}\right)^2}{4N_0}\right) \left.\frac{\partial T_i\left(W^{(i)}, I\right)}{\partial I}\right|_{I=1}, \tag{3.26}$$

where $\left(d_E^{(i)}\right)^2$, equals to $\left(d_H^{(i)}\right)^2 \Delta_{i-1}^2$, is the squared free Euclidean distance for i*th* level and E_s is the average energy per channel symbol. $T_i\left(W^{(i)}, I\right)$ denotes the transfer function of a convolutional code C_i with the rate k_i/n_i and given by

$$T_i\left(W^{(i)}, I\right) = \sum_{j=1}^{\infty} \sum_{d=d_H^{(i)}}^{\infty} a_{d_i} \left[W^{(i)}\right]^d I^j, \tag{3.27}$$

where a_{d_i} is the number of path pairs in the trellis diagram with distance *d*. The overall bit error probability is given by

$$P_b = \frac{\sum_{i=1}^{M} R_i P_{bi}}{\sum_{i=1}^{M} R_i}. \tag{3.28}$$

3.4 Multilevel Coded Cooperative System

The performance of multilevel codes on fading channels promises their use as component codes for coded cooperation. Bandwidth efficiency is also a key parameter in designing coded cooperative systems. Most of the works assume an orthogonal transmission (different frequency bands or different time slots) in order to uniquely detect the information. Mahinthan and Mark (2005) proposed a simple cooperative scheme which has the same power and bandwidth requirements with that of non-cooperative scheme. Similarly, we form orthogonal signaling via assigning the in-phase and quadrature components of the modulated signal to different users and thus transmit in the same frequency band and at the same time without sacrifying extra bandwidth for cooperation. Since we assign each dimension of the signal constellation to different users, it is also possible to detect the information bits of each user independently at the corresponding receivers.

We propose a coded cooperative system using multilevel coding technique. The performance of the multilevel coded cooperation (MCC) is compared with the multilevel coded (MC) system employing the same multilevel encoder and having two transmit antennas. In our scheme, each bit associated with corresponding level belongs to individual users, i.e. the first level is partitioned with user's own data and the remaining levels are with that of cooperating users.

3.4.1 System and Channel Model

The multilevel coded cooperative system considered here consists of two cooperating users equipped with single antenna and transmitting to the same destination. We denote cooperating two users as source and relay, respectively, in order to prevent confusion. Two convolutional codes with rates $R_1 = k_1 / n_1$ and $R_2 = k_2 / n_2$ are used as component codes and a two-level set partitioning is employed. Indeed, we can extend the system design for more than two users by increasing the number of levels in set partitioning. While encoder 1 with rate R_1

outputs the user's own codewords, the second encoder with rate R_2 produces the codewords of the relay that will be re-transmitted to destination. The two element signal vector formed by taking the outputs of the first and second encoders in order is mapped to one of the QPSK symbols based on set partitioning rule. Figure 3.9 shows the encoding and modulation process at one of the cooperating users. Let the data vectors of the source and relay at frame *i* be defined as $\boldsymbol{u}_s^{(i)}$ and $\boldsymbol{u}_r^{(i)}$, respectively. The outputs of the encoders are defined as $\boldsymbol{s}$ for the user and $\boldsymbol{r}$ for the relay. Finally, the transmitted channel signals at frame *i* is $\boldsymbol{x}_s^{(i)}$ and $\boldsymbol{x}_r^{(i)}$ for user and relay, respectively.

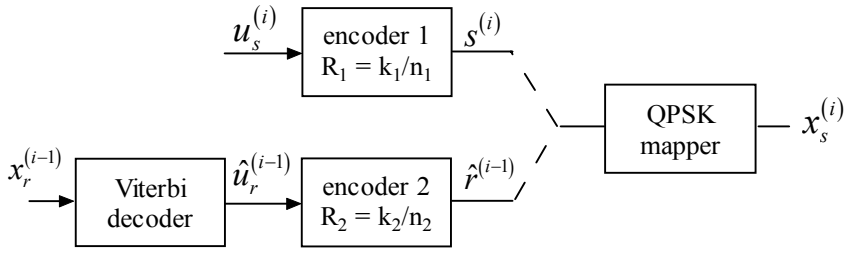

Figure 3.9 Encoder diagram of multilevel coded cooperative scheme.

Each user has two convolutional encoders as component codes of the two level system; the input of the first encoder is the data of the user itself and the code words at the output of this encoder constitutes the first level of the multilevel system. Since multilevel coded data are transmitted between the user and relay, the user also decodes (by Viterbi decoder or multistage decoder) and re-encodes the data received from the partner and obtains an estimate of the partner's code words. The outputs of the first and second encoder constitute the in-phase and quadrature components, respectively, in the signal constellation. The baseband representation of the transmitted channel signal is,

$$\boldsymbol{x}_s^{(i)} = \sqrt{E_b/2}\left(\boldsymbol{s}^{(i)} + j\hat{\boldsymbol{r}}^{(i-1)}\right). \tag{3.29}$$

For AWGN channel, the set partitioning method used in multilevel codes follows the Ungerboeck's set partitioning rule which maximizes the minimum intra-subset Euclidean distance. But for Rayleigh fading channels, multilevel coding scheme with Gray labeling outperforms the most known trellis codes because of increased diversity. Also in order to apply the orthogonal signaling, instead of Ungerboeck's set partitioning rule, the set partitioning shown in Fig. 3.10 was applied. Assuming a block size of N, the transmission scheme will be as given in Fig. 3.11. The minimum Euclidian distance is the same for two levels and is equal to $\Delta_0^2 = 2$.

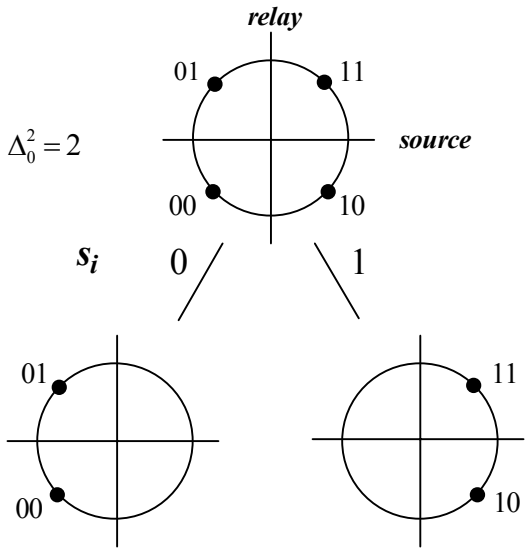

Figure 3.10. Set partitioning of QPSK.

	Frame (i-1)	Frame (i)	Frame (i+1)
S:	$s_1^{(i-1)}\ \hat{r}_1^{(i-2)} \ldots s_N^{(i-1)}\ \hat{r}_N^{(i-2)}$	$s_1^{(i)}\ \hat{r}_1^{(i-1)} \ldots s_N^{(i)}\ \hat{r}_N^{(i-1)}$	$s_1^{(i+1)}\ \hat{r}_1^{(i)} \ldots s_N^{(i+1)}\ \hat{r}_N^{(i)}$
R:	$\hat{s}_1^{(i-2)}\ r_1^{(i-1)} \ldots \hat{s}_N^{(i-2)}\ r_N^{(i-1)}$	$\hat{s}_1^{(i-1)}\ r_1^{(i)} \ldots \hat{s}_N^{(i-1)}\ r_N^{(i)}$	$\hat{s}_1^{(i)}\ r_1^{(i+1)} \ldots \hat{s}_N^{(i)}\ r_N^{(i+1)}$

Figure 3.11. Frame based cooperative transmission scheme.

Cooperative transmission introduces a transmit diversity to the system, hence the receiver at the destination applies optimal combining method; maximum ratio combining (MRC). Since the cooperation takes place in consecutive frames, the inputs of the combiner is the current symbol and the previous symbol obtained by delay element. The decoder operates on data with a diversity order of two for perfect inter-user channel (PIC). Multistage decoding, which has complexity

advantages over maximum likelihood decoding, is used at the destination. Since the relay constitutes the second level of multilevel signaling, a decrease in the bit error rate can be expected with multistage decoding. The block diagram of the receiver will be as given Fig. 3.12.

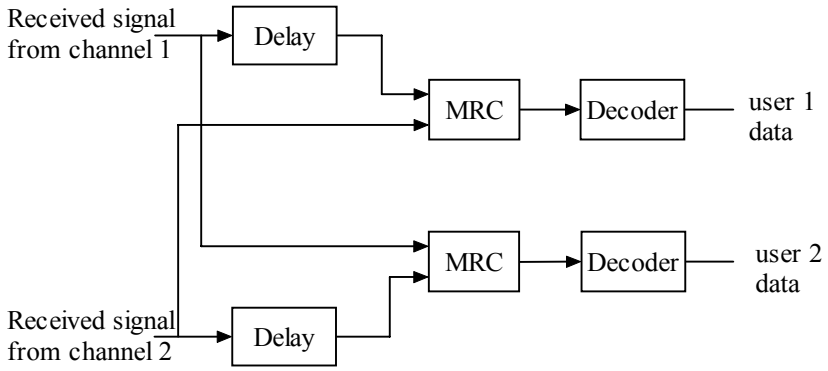

Figure 3.12 The block diagram of the receiver at the destination.

3.4.2 Pairwise Error Probability Analysis

Considering the two cooperative system with two users, we can define the faded received signal of single user at the destination as,

$$\boldsymbol{y}_{\mathrm{s}}^{(\mathrm{i})} = \boldsymbol{\alpha}_{\mathrm{s}}^{(\mathrm{i})} \boldsymbol{x}_{\mathrm{s}}^{(\mathrm{i})} + \boldsymbol{n}_{\mathrm{s}}^{(\mathrm{i})}. \tag{3.30}$$

Here, the fading coefficients, $\boldsymbol{\alpha}_s$'s, are zero mean complex Gaussian random variables with unit variance and the additive noise terms $\boldsymbol{n}_s$ are also zero mean complex Gaussian random variables with variance $N_0/2$. The fading coefficients are assumed to be known at the respective receivers and an error free transmission between the users is assumed. Receiver applies maximum likelihood decoding with MRC, so in order to decode the data $\boldsymbol{x}_s$, the received sequences $\boldsymbol{y}_{\mathrm{s}}^{(\mathrm{i})}$ and $\boldsymbol{y}_{\mathrm{r}}^{(\mathrm{i+1})}$ are processed jointly. Since PEP, defined as the probability that the transmitted sequence $\boldsymbol{x}_s$ is incorrectly decoded, depends on the fading

coefficients, the conditional PEP at the receiver can be expressed as

$$P\left(\mathbf{x}\to\hat{\mathbf{x}}\left|\boldsymbol{\alpha}\right.\right)=P\left(\sum_{j\in\eta}\left(M\left(x_s^{(i)}\left(j\right),x_r^{(i+1)}\left(j\right);\alpha_s^{(i)},\alpha_r^{(i+1)}\right)\right.\right.$$
$$\left.\left.-M\left(\hat{x}_s^{(i)}\left(j\right),\hat{x}_r^{(i+1)}\left(j\right);\hat{\alpha}_s^{(i)},\hat{\alpha}_r^{(i+1)}\right)\right)\geq 0\left|\alpha\right.\right), \tag{3.31}$$

where η is the index set with cardinality w for which $x_j\neq\hat{x}_j$, w is the Hamming distance between $\boldsymbol{x}$ and $\hat{\boldsymbol{x}}$, and $M\left(x_s^{(i)}\left(j\right),x_r^{(i+1)}\left(j\right);\alpha_s^{(i)},\alpha_r^{(i+1)}\right)$ is defined as,

$$M\left(x_s^{(i)}\left(j\right),x_r^{(i+1)}\left(j\right);\alpha_s^{(i)},\alpha_r^{(i+1)}\right)$$
$$=-\min_{x\in C_b}\left(\left|y_s^{(i)}\left(j\right)-\alpha_s^{(i)}x_s^{(i)}\left(j\right)\right|+\left|y_r^{(i+1)}\left(j\right)-\alpha_r^{(i+1)}x_r^{(i+1)}\left(j\right)\right|\right). \tag{3.32}$$

Without loss of generality, we can assume that the all-zero sequence is transmitted. Also we assume that the uplink SNR's are equal. The union bound yields the following expression for the first decoding stage for all the code sequences associated with $\boldsymbol{x}$ of weight w,

$$P\left(\boldsymbol{x}_s\to\hat{\boldsymbol{x}}_s\left|\boldsymbol{\alpha}\right.\right)=2^{-w}Q\left(\sqrt{\frac{2R_1E_b}{N_0}\nabla_0^2\left(\sum_{j\in\eta}\left(\alpha_s^{(i)}\right)^2+\sum_{j\in\eta}\left(\alpha_r^{(i+1)}\right)^2\right)}\right), \tag{3.33}$$

with E_b/N_0 denoting the energy-per-bit-to-noise ratio. Since for Rayleigh fading channel, the fading coefficients, $\boldsymbol{\alpha}$'s, are i.i.d. Rayleigh distributed random variables with $E\left(\alpha\right)=1$, the random variables $\beta_1=\sum_{j\in\eta}\left(\alpha_s^{(i)}\right)^2$ and $\beta_2=\sum_{j\in\eta}\left(\alpha_r^{(i+1)}\right)^2$ will have an w-Erlang distribution with parameter one, hence their pdf are,

$$f_{\mathrm{B}}\left(\beta\right)=\frac{1}{\left(w-1\right)!}\beta^{(w-1)}e^{-\beta},\quad \beta\geq 0. \tag{3.34}$$

Thus, the unconditional PEP is,

$$P\left(\mathbf{x}_s \to \hat{\mathbf{x}}_s\right) = \int_0^{\infty}\int_0^{\infty} 2^{-w} Q\left(\sqrt{\frac{2RE_b}{N_0}\nabla_0^2\left(\beta_1+\beta_2\right)}\right) f_{\mathrm{B}_1}\left(\beta_1\right) f_{\mathrm{B}_2}\left(\beta_2\right) d\beta_1 d\beta_2 . \tag{3.35}$$

To evaluate the double integral given in Eq. (3.35) in closed form, we again use the alternative form of Q function given by Eq. (3.13) and the pre-calculated integral result

$$\frac{1}{\pi}\int_0^{\pi/2}\left(\frac{\sin^2\theta}{\sin^2\theta+c}\right)^n d\theta = \frac{1}{2}\left(1-\sqrt{\frac{c}{1+c}}\right)^n \sum_{k=1}^{n-1}\binom{n-1+k}{k}\left(\frac{1}{2}\left(1+\sqrt{\frac{c}{1+c}}\right)\right)^k . \tag{3.36}$$

We obtain a closed form expression for pairwise error probability as,

$$P\left(\boldsymbol{x}_s \to \hat{\boldsymbol{x}}_s\right) = 2^{-w}\left(\frac{1-\delta}{2}\right)^{2w}\sum_{k=0}^{2w-1}\binom{2w-1+k}{k}\left(\frac{1+\delta}{2}\right)^k , \tag{3.37}$$

where

$$\delta = \sqrt{\frac{R_1E_b/N_0}{1+R_1E_b/N_0}} . \tag{3.38}$$

For slow fading channel, PEP equals to,

$$P\left(\boldsymbol{x}_s \to \hat{\boldsymbol{x}}_s\right) = 2^{-w+1}\left(\frac{1-w\delta}{2}\right)^2\left(\frac{1+w\delta}{2}\right). \tag{3.39}$$

Finally, the BER is upper bounded as,

$$P_b \le \sum_{w=w_{\min}}^{N}\frac{w}{N}A_w^{(1)}P\left(\boldsymbol{x}_s \to \hat{\boldsymbol{x}}_s\right) \tag{3.40}$$

where $A_w^{(1)}$ denotes the number of the codewords with weight *w* obtained from the transfer function of the corresponding encoder.

3.4.3 Simulation Results

We examined the performance of the two user multilevel cooperative system in Rayleigh flat fading environment for quasi-static and fast fading cases with simulations. 1/2 rated four state convolutional code with generator matrix (7,5) was chosen as component code in the two level encoder for both source and relay nodes. The outputs of the encoders then form the QPSK symbols based on the set partitioning rule and orthogonal signaling scheme given in section 3.4.1. Simulations were performed for both perfect and imperfect inter-user channel conditions but the theoretical union bound for bit error probability was evaluated for only perfect inter-user case. The analysis for erroneous inter-user transmission between the users has been left as a future work. The frame length was chosen as 256 for all cases. Since the aim of cooperation is to reach to the performance of non-cooperative single user system with same diversity gain, we also simulated a multilevel coded system with two transmit antennas. Total power used for two cases is fixed for a fair comparison. The signal to noise ratios for inter-user transmission is named as *iSNR*. Also the SNR values for the user-destination links are assumed to be equal.

In Fig. 3.13, the BER versus SNR for fast fading case is plotted along with the upper bound calculated with union bounding technique. Since the theoretical error probability analysis for non-cooperative system with two transmit antennas is the same with cooperative system with perfect inter-user channel, it is expected to see close performances of the two for a wide range of SNR. Also the upper bound obtained by union bounding technique coincides with the simulation results. Another observation from the simulation results is that with erroneous transmission between cooperating users, an error floor occurs after a definite SNR value. This error floor comes from the re-encoded symbols in error occurring at the relay.

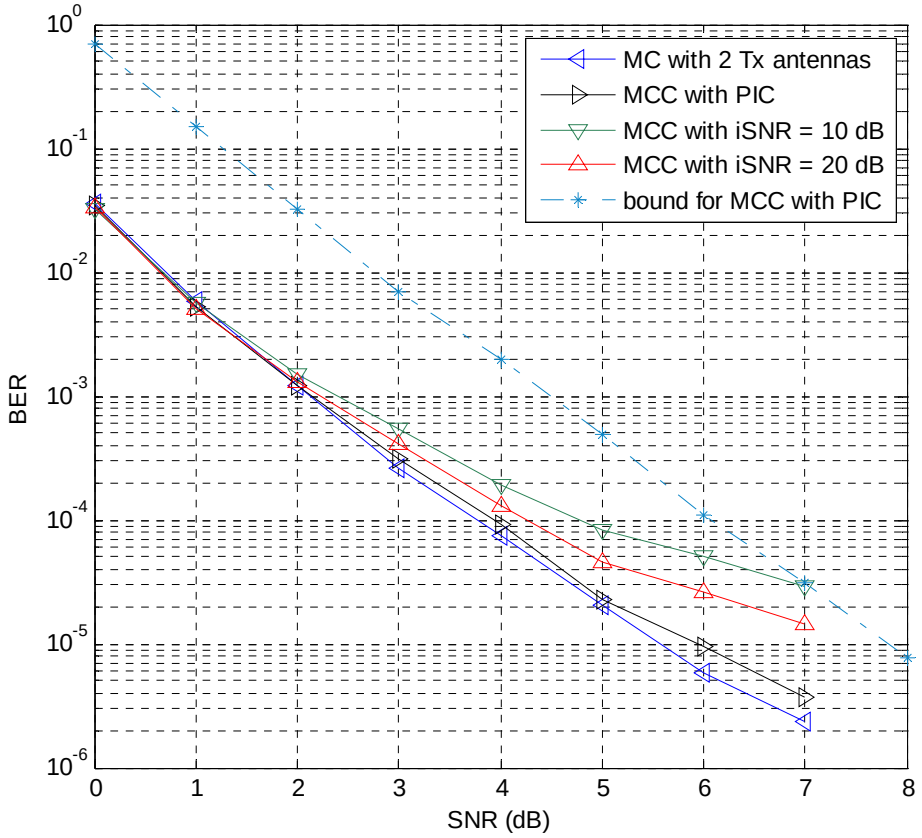

Figure 3.13 Performance evaluations of multilevel coded cooperative and non-cooperative systems for fast fading channel.

In order to reduce the error floor, turbo codes are applied at the first level of the multilevel code. The original 1/3 rated turbo encoder, generated with parallel concatenation of two (1,5/7) recursive systematic convolutional codes, is punctured to rate 1/2 and is used as the encoder of the first user. Both decoders at the relay and at the receiver apply an iterative turbo decoding based on MAP algorithm. The iteration number is set to 2 within the decoder at the destination and 3 within the decoder at the relay. We obtain the results in Fig. 3.14. It is observed that the error floor is removed and a gain of about 2.2 dB is achieved at a BER level of 10^{-4} for both *iSNR* values. Additional performance gain can be expected by increasing the iteration number within the MAP decoders.

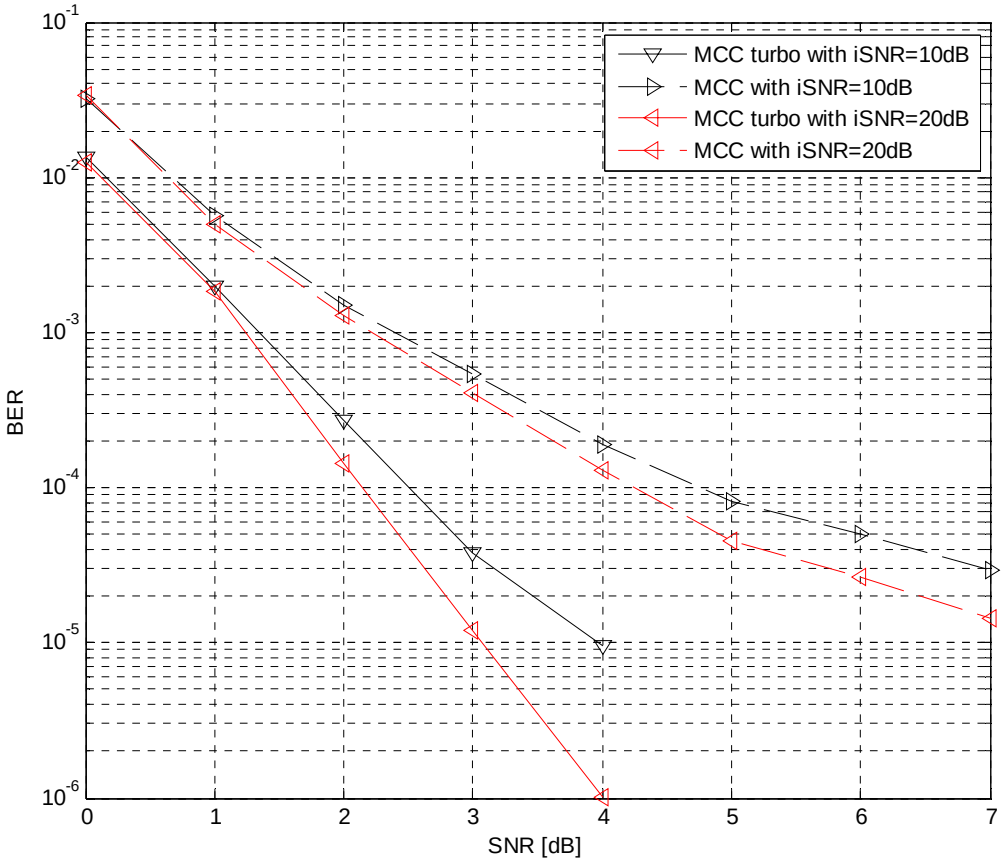

Figure 3.14 Performance evaluations of multilevel coded cooperative system with turbo component code for fast fading channel.

The simulation results for quasi-static Rayleigh fading case is given in Fig. 3.15. Again, the performance of multilevel coded cooperative case with perfect inter-user channel performs almost the same as non-cooperative multilevel coded system with two transmit antennas. The upper bound calculated with the derived Eq. (3.40), supports the simulation results.

3.5 Chapter Summary

The cooperative system in which turbo codes are applied distributively is shown to outperform non-cooperative counterpart for slow fading channel. However, since DTCC system does not offer a diversity gain for fast fading channel, no significant gain can be realized via cooperation. Supported by simulation results, the BER analysis including the inter-user channel condition gives accurate bounds on overall BER for a specific inter-user channel SNR.

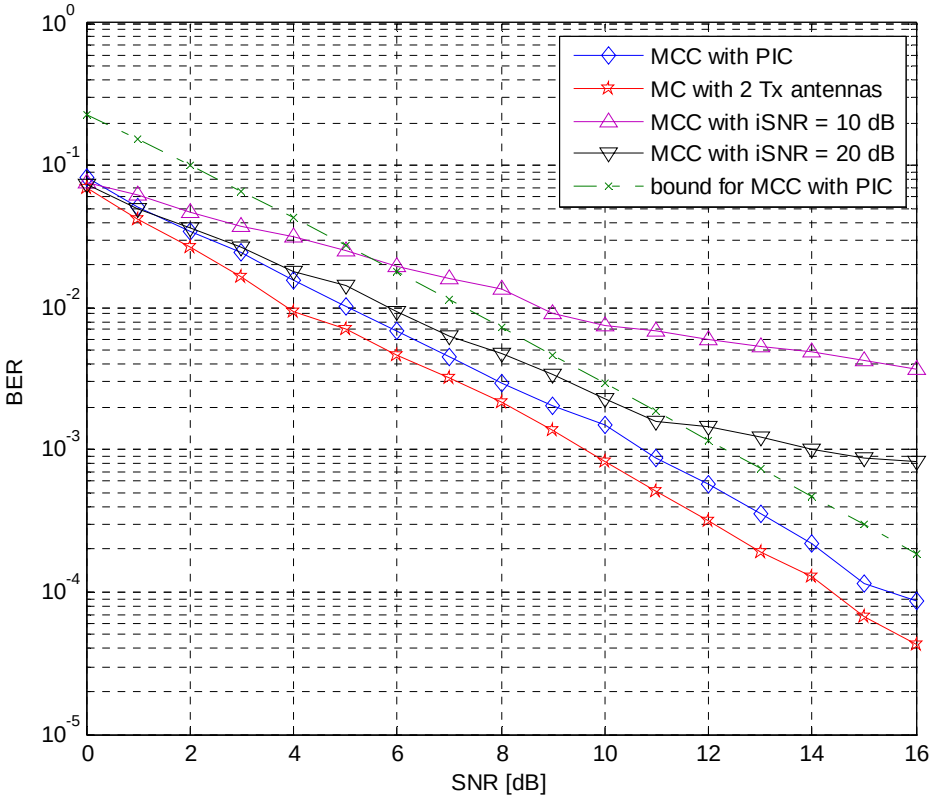

Figure 3.15 Performance evaluations of multilevel coded cooperative and non-cooperative systems for quasi-static Rayleigh fading channel.

Simulation results have shown that the MCC system with perfect inter-user channel achieves almost the same performance as the non-cooperative single user employing multilevel coding but with 2 transmit antennas for a wide SNR region. Also the theoretical bit error rate upper bound obtained by union bounding technique supports the simulation results. The error floor observed for non-perfect inter-user channel is shown to be removed by applying more protective turbo codes as the component code of the first level of multilevel code. The results presented in this chapter have been published in (Yılmaz & Yılmaz, 2008).

CHAPTER FOUR
LDPC CODED COOPERATION OVER WIRELESS RELAY CHANNELS

In this chapter, we analyze cooperation over wireless relay channel comparing various forwarding methods applied at the relay node. In particular, we construct LDPC coded cooperative scheme in which DF, DetF, and AF techniques are applied at the relay in order to assist the source transmission. Considering both half and full duplex modes, iterative detection/decoding based receiver is proposed and capacity bounds are defined. We perform simulations in order to obtain the BER performance of the proposed schemes and determine the most adequate forwarding method considering the complexity issue as a design criteria as well.

The chapter is organized as follows: We give an overview of relay channel in Section 4.1. The channel models for relay communication are introduced in Section 4.2, together with the analysis of capacity limits. In Section 4.3, we analyze LDPC coded cooperation over relay channel with different forwarding techniques employed at the relay. We present performance evaluation results for both half and full duplex cases. Finally, the conclusions are given in Section 4.4.

4.1 The Relay Channel

The relay channel proposed by Van der Meulen (1971), is a channel composed of three nodes, a source node N_s, a relay node N_r and a destination node N_d, as illustrated in Fig. 4.1. The relay node receives the signal from the source and generates a new signal to improve the transmission between the source and the destination. The destination node receives the superposition of the signals from the source and the relay nodes, and tries to recover the original information. Although only limited amount of work on relay systems is observed for over two decades after the work of Meulen, the relay channel have aroused interest with the work of Sendoranis et. al., (2003) where user cooperative diversity is introduced.

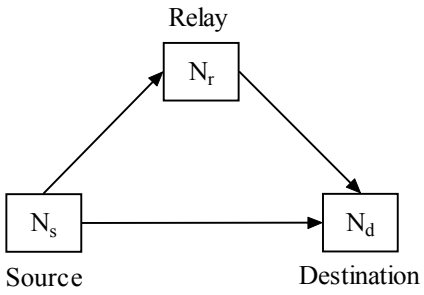

Figure 4.1. Classical relay channel model.

The incorporation of turbo and LDPC codes into the relay channel helps to approach the capacity limits of relay channel. In (Zhao & Valenti, 2003), distributed turbo coding scheme is proposed for the half-duplex relay channel. Later, an improved scheme by exploiting the channel adaptivity is developed in (Souryal & Vojcic, 2004). All these strategies consider an orthogonal channel between the source and the relay, which results in a simplified receiver structure but reduced spectral efficiency. To achieve a higher capacity, Zhang and Duman (2005, 2007) proposed several practical turbo coded cooperative schemes for both full-duplex relaying and time-division based half-duplex relaying where the transmitters work on the same channel, i.e. the source transmission and the relay transmission are superimposed with each other. By employing an appropriate multi-access channel detector and iterative decoding at the destination, these schemes are shown to approach the constrained capacity (bounds) very closely.

Hu & Duman, (2007) reconstructed the coded cooperative scheme by employing LDPC codes as an alternative to turbo codes for both half and full duplex cases. Carefully designed LDPC coded system is shown to outperform the turbo coded counterpart. In this chapter, we revisit this LDPC coded cooperative system and different from (Hu & Duman, 2007), we apply various forwarding methods introduced in Section 3.1.2. We try to figure out the most effective protocol over ergodic and non-ergodic fading channels for both half and full duplex modes via simulation results.

4.2 Cooperation over Wireless Relay Channel

In this part, we construct cooperative communication over the three terminal single relay channel. We assume that each node is equipped with only one transmit and/or receive antenna and that the relay can operate either in half or full duplex mode. We also assume that source and relay transmission are over the same channel. We next describe the mathematical models and transmission schemes for full-duplex and half-duplex modes.

4.2.1 Signaling and Channel Model for Full-Duplex Relaying

The full-duplex relay channel model is described in (Van der Meulen, 1971) and its channel model is shown in Fig. 4.2. The signals received at the relay and source are defined respectively as,

$$Y_r = \sqrt{K_1} H_{sr} X_s + Z_1, \tag{4.1}$$

$$Y_d = H_{sd} X_s + \sqrt{K_2} H_{rd} X_r + Z_2 \tag{4.2}$$

where X_s and X_r are the transmitted symbols from the source and the relay nodes, respectively. We assume individual power constraints P for both source and relay but a total power constraint can also be assumed and the total power can be distributed among source and relay nodes by applying optimization tool. H_{sd}, H_{sr} and H_{rd} are the independent channel coefficients with complex Gaussian distribution having zero mean and unit variance. Z_1 and Z_2 denote the additive

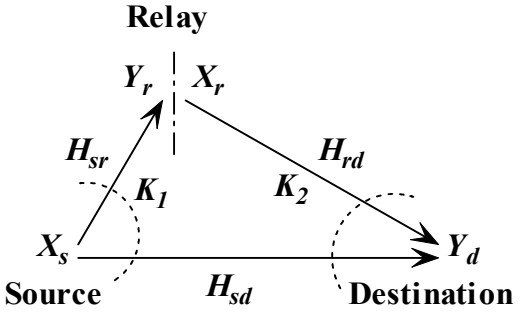

Figure 4.2 Channel model for full-duplex relaying.

white Gaussian noise terms with zero mean and variance of $N_0/2$ per dimension. K_1, K_2 are the relative gains of the source-relay link and the relay-destination link over the source-destination link. We assume that all the links are frequency-flat Rayleigh fading, and the channel coefficients are known only at the respective receivers. R_c is the rate of overall system and the SNR is defined as $P/(R_cN_0)$.

Now we will describe the transmission process for all protocols. What is common for all protocols is that the source and relay nodes transmit simultaneously at the same frequency band. In other words the destination node receives a superposition of the source and the relay signals. The use of non-orthogonal channels offers an increase in capacity and bandwidth efficiency compared to orthogonal channels. In DF protocol, the source node encodes its own information and transmits for each block of transmission. The relay node receives this information and at the same time transmits the codeword generated by decoding and re-encoding the source signal received in the previous block. In DetF mode, the relay only performs hard detection as opposed to decoding and re-encoding processes in DF mode. Clearly this method is less complex than the DF protocol. Finally, in AF mode, the relay node simply normalizes the received signal in order to set the average energy to unity and forwards to the destination without additional processing.

The capacity of full duplex relay channel is derived in (Cover & El Gamal, 1979) as,

$$C \le E\left[\max_{p(X_s,X_r)} \min\left\{I\left(X_s, X_r; Y_d\right), I\left(X_s; Y_r, Y_d \middle| X_r\right)\right\}\right], \tag{4.3}$$

where E denotes the expectation operator. The lower bound, which can also be viewed as the achievable rate is also given in (Cover & El Gamal, 1979) as,

$$C \ge E\left[\max_{p(X_s,X_r)} \min\left\{I\left(X_s, X_r; Y_d\right), I\left(X_s; Y_r \middle| X_r\right)\right\}\right]. \tag{4.4}$$

The capacity bounds given by Eq. (4.3) and Eq. (4.4) assume Gaussian distributed input signals. The achievable information rate bounds derived under the i.u.d. binary inputs constraint are defined as,

$$I^f \le \min\left\{E\left[I_b\left(X_s, X_r; Y_d\right)\right], E\left[I_b\left(X_s; Y_r, Y_d \middle| X_r\right)\right]\right\}, \tag{4.5}$$

$$I^f \ge \min\left\{E\left[I_b\left(X_s, X_r; Y_d\right)\right], E\left[I_b\left(X_s; Y_r \middle| X_r\right)\right]\right\}. \tag{4.6}$$

If we assume a perfect source-relay link, i.e. $K_1 = \infty$, the capacity bounds converge to,

$$C = E\left[\max_{p(X_s, X_r)} I\left(X_s, X_r; Y_d\right)\right], \tag{4.7}$$

$$I^f = \min\left\{E\left[I_b\left(X_s, X_r; Y_d\right)\right], 1\right\}. \tag{4.8}$$

The capacity and information rate curves for full duplex relay channel with perfect source-relay channel, i.e. $K_1 = \infty$, and $K_2 = 0$ dB, are plotted in Fig. 4.3. For a fair comparison, we used $2P$ as the power of direct transmission. We observe that there is a slight gain in capacity with relay assisted transmission. Moreover, the gain in achievable information rate is much higher when direct transmission is taken as benchmark. We plotted the bounds for capacity and constrained information rates using BPSK modulation for the case when K_1=12 dB and K_2= 3 dB in Fig. 4.4. In multi-hop transmission no direct link exists from source to destination, instead the transmission path tracks source-relay-destination nodes. For this case we notice an apparent gain in unconstrained capacity between the relay assisted and direct transmissions. Also the upper and lower bounds overlap for this case.

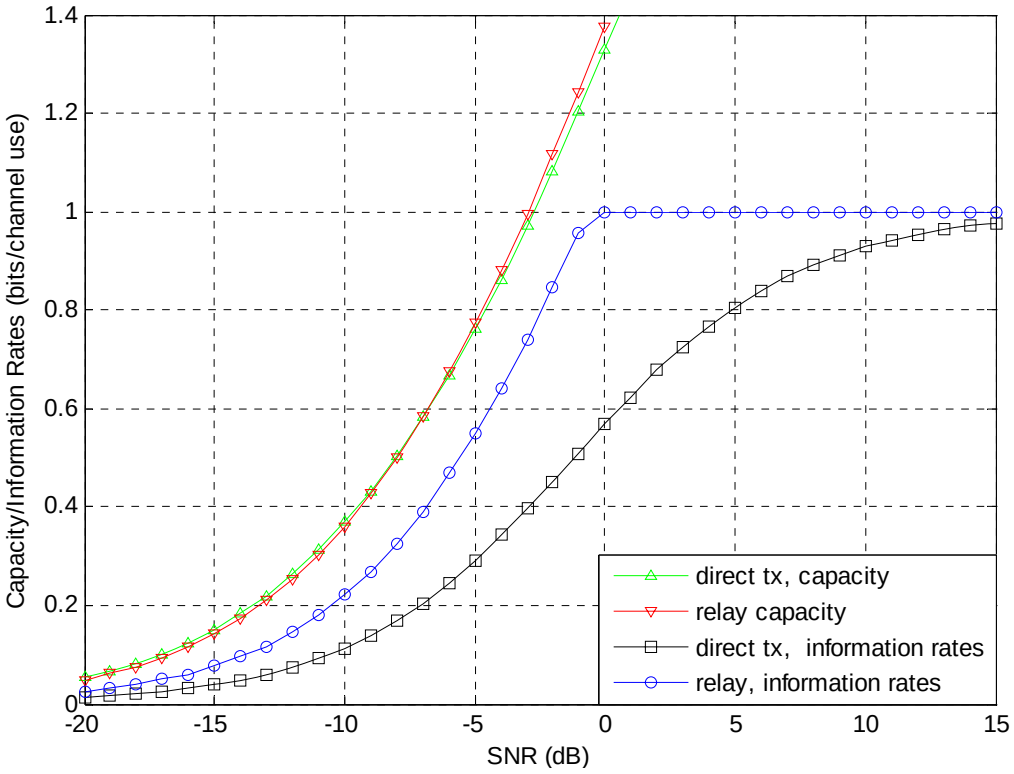

Figure 4.3 Capacity and information rate curves for full duplex relay channel.

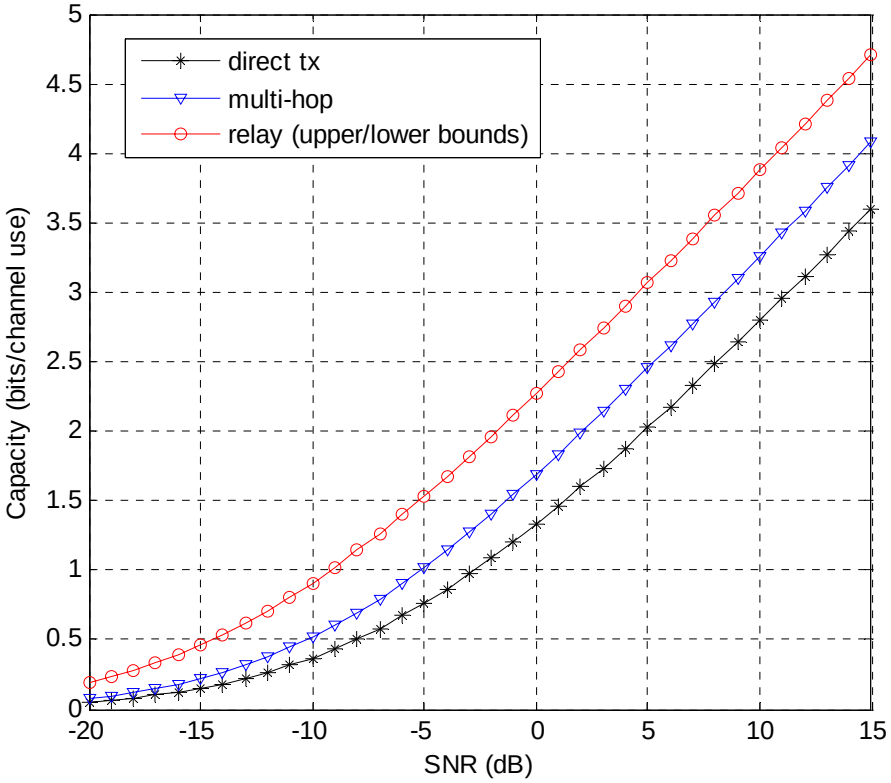

Figure 4.4 Unconstrained capacity of full duplex channel for K_1=12 dB and K_2= 3 dB.

4.2.2 Signaling and Channel Model for Half-Duplex Relaying

The transmit and receive chains of relay antenna should be isolated by a circulator in full duplex mode. But this causes self interference and limits the performance. When the conditions for full duplex operation are not met, relays transmit in half-duplex mode, either by time division or frequency division. The time division based half duplex channel model is depicted in Fig. 4.5. In this case, each transmission period of T is divided into two time slots. In DF mode, the source node transmits part of the coded bits during the first slot of duration, αT, while the relay node does not transmit but only receives. In the second slot of duration, $(1-\alpha)T$, the source node transmits another set of coded bits. Meanwhile, the relay node transmits its own codeword based on the source bits received in the first time slot.

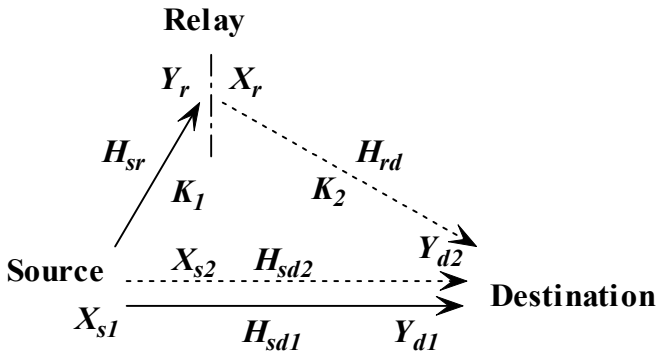

Figure 4.5 Channel model and transmission scheme for half-duplex relaying.

In DetF and AF modes, on the other hand, the codeword is partitioned into two parts. The source node transmits the first partition of length αN in the first time slot, where N is the length of the total codeword. The remaining partition is transmitted by the source node in the second time slot. While the relay node only listens in the first slot, it forwards the detected/amplified first partition in the second time slot in DetF and AF modes, respectively. For all 3 protocols, the coefficient α is a parameter that controls the time allocated between direct transmission and cooperation. In Fig. 4.5, the transmission during the first and second time slot is represented by solid lines and dotted lines, respectively.

Mathematically, the channel is given by

$$Y_r = \sqrt{K_1} H_{sr} X_{s1} + Z_r \tag{4.9}$$

$$Y_{d1} = H_{sd1} X_{s1} + Z_1, \tag{4.10}$$

$$Y_{d2} = H_{sd2} X_{s2} + \sqrt{K_2} H_{rd} X_r + Z_2, \tag{4.11}$$

where X_{s1} and X_{s2} are the transmitted signals from the source during the first and second slots, X_r is the transmitted signal from the relay during the second slot, Y_r is the received signal at the relay during the first slot, Y_{d1} and Y_{d2} are the received signals at the destination during the first and second slots. The individual power constraint, *P*, is also assumed in this case. Other definitions are the same as the full-duplex case.

In this time division based transmission scheme, the upper/lower bounds for the capacity are given by,

$$\begin{aligned} C \le E\Bigg[\max_{p(X_s, X_r)} \min \Big\{ & \alpha I\left(X_{s1}; Y_r, Y_{d1}\right) + (1-\alpha) I\left(X_{s2}; Y_{d2} \middle| X_r\right), \\ & \alpha I\left(X_{s1}; Y_{d1}\right) + (1-\alpha) I\left(X_{s2}, X_r; Y_{d2}\right) \Big\} \Bigg], \end{aligned} \tag{4.12}$$

$$\begin{aligned} C \ge E\Bigg[\max_{p(X_s, X_r)} \min \Big\{ & \alpha I\left(X_{s1}; Y_r\right) + (1-\alpha) I\left(X_{s2}; Y_{d2} \middle| X_r\right), \\ & \alpha I\left(X_{s1}; Y_{d1}\right) + (1-\alpha) I\left(X_{s2}, X_r; Y_{d2}\right) \Big\} \Bigg], \end{aligned} \tag{4.13}$$

where $X_s = \left[X_{s1}\ X_{s2}\right]$. The achievable information rates for i.u.d. binary input constraint can be expressed as,

$$\begin{aligned} I^h \le \min \Big\{ & E\Big[\alpha I\left(X_{s1}; Y_r, Y_{d1}\right) + (1-\alpha) I\left(X_{s2}; Y_{d2} \middle| X_r\right) \Big], \\ & E\Big[\alpha I\left(X_{s1}; Y_{d1}\right) + (1-\alpha) I\left(X_{s2}, X_r; Y_{d2}\right) \Big] \Big\} \end{aligned} \tag{4.14}$$

$$I^h \geq \min\left\{E\left[\alpha I\left(X_{s1};Y_r\right)+\left(1-\alpha\right)I\left(X_{s2};Y_{d2}\left|X_r\right.\right)\right],\right.$$
$$\left.E\left[\alpha I\left(X_{s1};Y_{d1}\right)+\left(1-\alpha\right)I\left(X_{s2},X_r;Y_{d2}\right)\right]\right\}. \tag{4.15}$$

For perfect source-relay link the capacity and information rates converge to

$$C = E\left[\max_{p(X_{s1},X_r)}\left\{\alpha I\left(X_{s1};Y_{d1}\right)+\left(1-\alpha\right)I\left(X_{s2},X_r;Y_{d2}\right)\right\}\right], \tag{4.16}$$

$$I^h = \min\left\{1, E\left[\alpha I\left(X_{s1};Y_{d1}\right)+\left(1-\alpha\right)I\left(X_{s2},X_r;Y_{d2}\right)\right]\right\}. \tag{4.17}$$

The upper and lower bounds for half duplex channel for K_1=12 dB and K_2= 3 dB is plotted together with perfect inter-user case and direct transmission in Fig. 4.6. We observe that relay channel has the potential to achieve a higher capacity than the direct transmission.

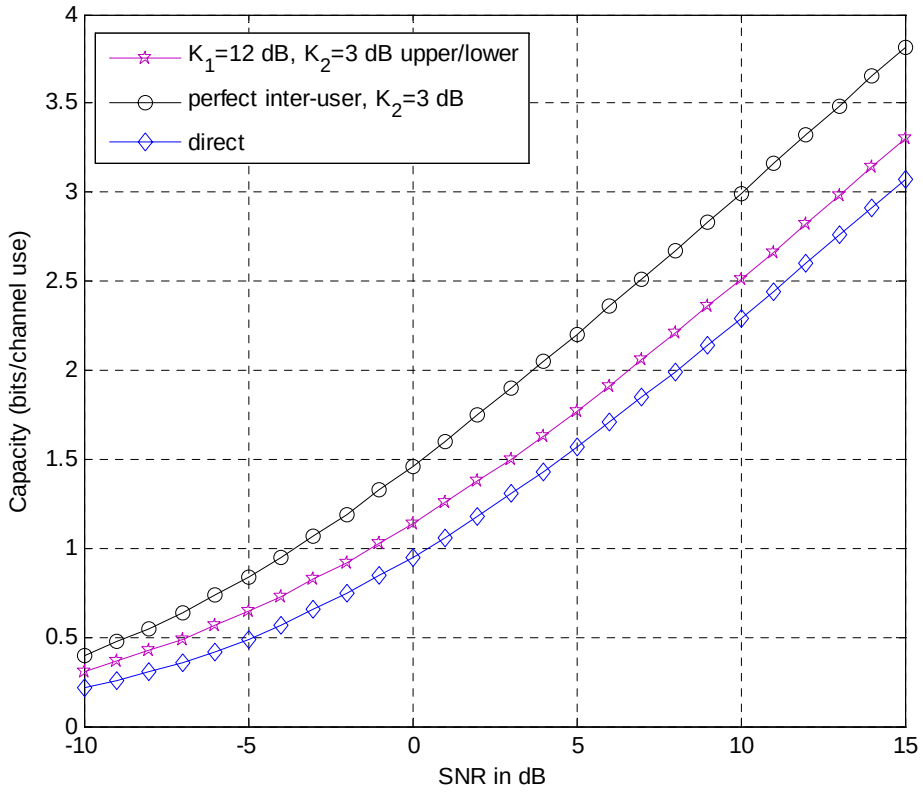

Figure 4.6 Unconstrained capacity of half duplex channel.

4.3 LDPC Coded Cooperation over Relay Channel

In this section, we construct specific LDPC coded full-duplex and half-duplex relay systems and apply three different protocols at the relay node. The performance evaluations of all protocols are realized under ergodic and non-ergodic fading cases.

4.3.1 Full-Duplex System

For full duplex case, we propose symmetric information combining (SIC) scheme in which the relay retransmits the information it receives from the source in block *k*-1 during block *k*. At the source node, the data sequence is divided into several consecutive blocks. For each block, the source encodes and broadcasts the data to both the relay and the destination. The relay node listens and receives/detects/decodes the source signal in AF/DetF/DF modes respectively, while at the same time, it transmits its signal corresponding to the source information in the previous block. This process is illustrated in Fig. 4.7.

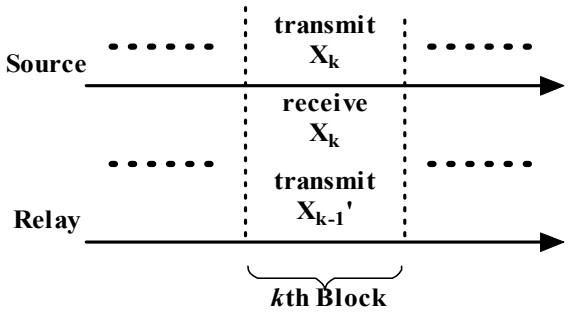

Figure 4.7 Transmission scheme for full duplex case.

The signals used by the source and relay are identical for the SIC scheme. Therefore the rate of overall system is equal to the rate of the LDPC code applied at the source node. But it is also possible to puncture half of the coded bits and transmit the punctured bits by the relay during the following transmission block after proper decoding and re-encoding in DF mode. However, since DetF and AF modes do not involve decoding and re-encoding, SIC schemes are adequate for DetF and AF modes.

The detection and decoding process of a single block at the destination is as follows. The signals of the source and the relay nodes are combined in order to obtain the original source data. The receiver structure is shown in Fig. 4.8. The major components of the receiver are the multiple access channel detector and the LDPC decoder. The detector and decoder are both SISO modules which can exchange extrinsic information in an iterative manner similar to "turbo equalization".

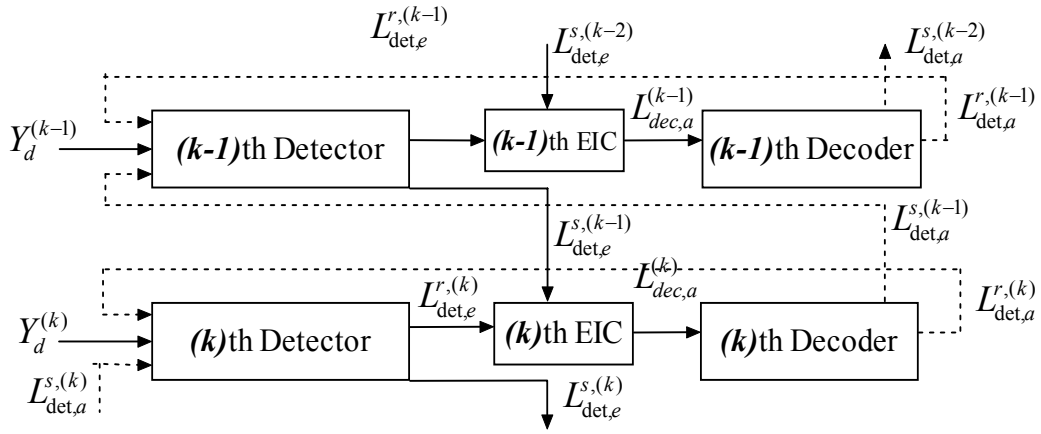

Figure 4.8 Receiver diagram for full duplex case.

The M bits (denoted by $B = \{b_1, b_2, \ldots, b_M\}$) of a 2^M-ary modulation signal are mapped to a constellation point, denoted by X, i.e. $X = g(B)$. At each time instant, there are two channel inputs X_s and X_r and two groups of M bits B_s and B_r corresponding to X_s and X_r. The channel output Y_d is given by (4.2). A soft output MAP detector computes the soft information about the transmitted source and relay bits using the noisy channel observation Y_d and the available a priori information $L_{det,a}$ for each bit. The LLR for the kth source bit b_s^k is computed as

$$
\begin{aligned}
L_{\text{det}}\left(b_s^k\right) &= \log \frac{P\left(b_s^k = 0 \middle| Y_d\right)}{P\left(b_s^k = 1 \middle| Y_d\right)} \\
&= \log \frac{\sum_{B_s^i : b_s^k = 0} \sum_{B_r^j} p\left(Y_d \middle| X_s^i = g\left(B_s^i\right), X_r^j = g\left(B_r^j\right)\right) e^{\sum_{m \in \Psi_s} L_{\text{det},a}\left(b_s^m\right) + \sum_{n \in \Psi_r} L_{\text{det},a}\left(b_r^n\right)}}{\sum_{B_s^i : b_s^k = 1} \sum_{B_r^j} p\left(Y_d \middle| X_s^i = g\left(B_s^i\right), X_r^j = g\left(B_r^j\right)\right) e^{\sum_{m \in \Psi_s} L_{\text{det},a}\left(b_s^m\right) + \sum_{n \in \Psi_r} L_{\text{det},a}\left(b_r^n\right)}},
\end{aligned}
\tag{4.18}
$$

where $k = 1, \ldots, M$, and $\Psi_s\left(\Psi_r\right)$ is the set of indices with source (relay) bit 0. $L_{\mathrm{det},a}\left(b_s^m\right)$ and $L_{\mathrm{det},a}\left(b_r^n\right)$ are the a priori information on the mth source and the nth relay bits, respectively, $m,n \in \{1,2,...,M\}$ which are provided by the output of the LDPC decoder in the previous iteration step. The log likelihood ratio for the kth relay bit b_r^k can be calculated similarly by changing all the indices 's' in Eq. (4.18) with 'r' and 'r' with 's'.

The output extrinsic information is given by

$$L_{\mathrm{det},e}\left(b_s^k\right) = L_{\mathrm{det}}\left(b_s^k\right) - L_{\mathrm{det},a}\left(b_s^k\right). \tag{4.19}$$

The extrinsic information $L_{\mathrm{det},e}\left(b_r^k\right)$ is computed in a similar way. In the block diagram, the role of the module named EIC (which stands for extrinsic information combining) is to combine the soft information provided by the source and the relay nodes. In other words, the EIC sums up the likelihood information from the source and the relay nodes corresponding to the same data block and the LLR information for the original codeword is generated.

The log-domain belief propagation algorithm is used at the decoder and the soft information received from the detector through EIC is used as input. Specifically, at a variable node with degree d_v, the message passed to its incident check node k is

$$L_v^k = L_{dec,a}^k + \sum_{j=0, j\neq k}^{d_v-1} L_c^j, \quad k = 0,...,d_v - 1, \tag{4.20}$$

where $L_{dec,a}^k$ is the soft output of EIC, and L_c^j is set to 0 at the first local iteration. At a check node with degree d_c, the message passed to its incident variable node k satisfies the *tanh* rule, i.e.

$$\tanh\left(L_c^k/2\right)=\prod_{j=0,j\neq k}^{d_c-1}\tanh\left(L_v^j/2\right),\quad k=0,...,d_c-1. \tag{4.21}$$

The same procedure continues until all the parity check equations are satisfied or a predetermined number of local iterations is met. We denote the number of iterations in the decoder as Q_d. The output LLR for coded bit *I* is

$$L_{dec}^i=\sum_{j=0}^{d_v-1}L_c^j+L_{dec,a}^i,\quad i=0,...,N-1, \tag{4.22}$$

where N is the codeword length. One global iteration is accomplished when the extrinsic information

$$\begin{aligned}L_{\mathrm{det},a}^{i,s}&=L_{dec}^i-L_{\mathrm{det},e}^{i,s},\\ L_{\mathrm{det},a}^{i,r}&=L_{dec}^i-L_{\mathrm{det},e}^{i,r},\quad i=0,...,N-1,\end{aligned} \tag{4.23}$$

is sent back to the detector. We denote the number of global iterations as Q_g.

In order to gain insight about the performances of three different protocols, we performed Monte Carlo simulations for both ergodic and non-ergodic fading channels. The system proposed for DF mode applies a (64800, 32400) irregular LDPC code of rate $R_c=1/2$. The K_1 and K_2 gains are 12 dB and 3 dB, respectively. The simulation results for ergodic fading channel is illustrated in Fig. 4.9. The channel gains are independent of each other and varied for each symbol in a single block for ergodic fading. For this reason this type of fading is named as ‘fast fading’ as well. Since no additional gain is observed after 2 global iterations, we plot the results for $Q_g=2$.

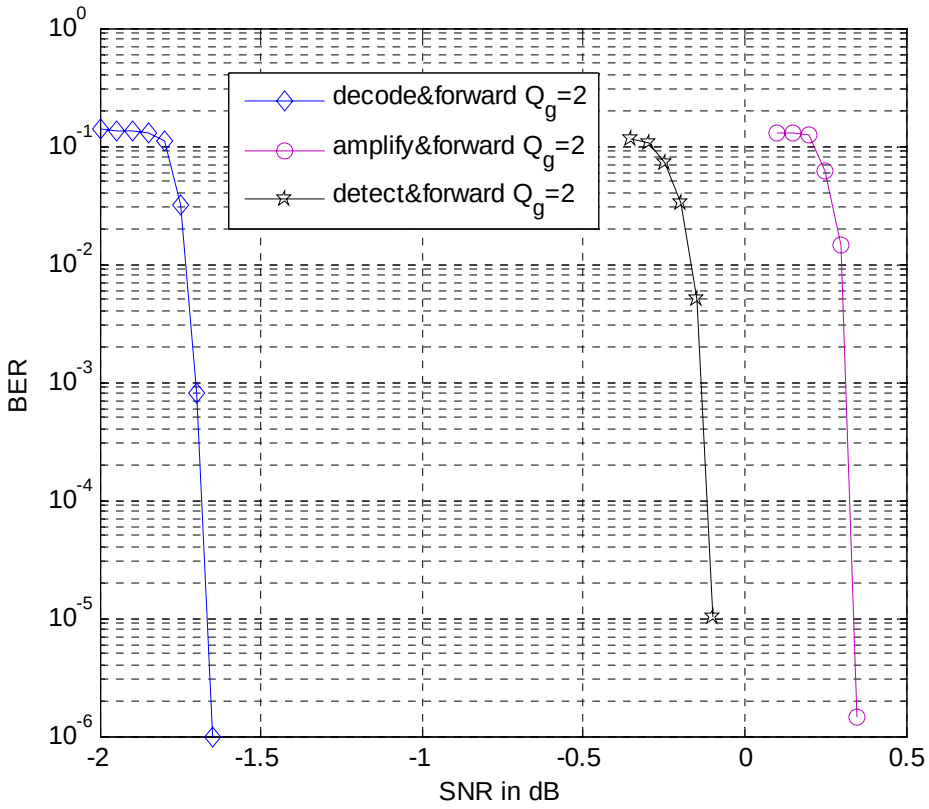

Figure 4.9 Performance evaluations for full duplex case over ergodic fading channel.

We observe that the DF protocol has superior performance compared to DetF and AF protocols. At a BER level of 10^{-4}, DF has a gain of approximately 1.5dB and 2 dB over DetF and AF protocols. The gain of DetF over AF is 0.5 dB at the same BER value. DF is expected to outperform DetF and AF as long as the relay successfully decodes source codeword. Also, it is expected that DetF and AF protocols would have poor performances at low SNR.

For non-ergodic fading channel, we assume that the fading coefficients remain the same for entire single block and change block by block. The simulation results for this case are plotted in Fig. 4.10. Maximum achievable diversity order for full duplex case compared to SISO transmission is two since only one relay is deployed. We also plot the performance of direct transmission for comparison.

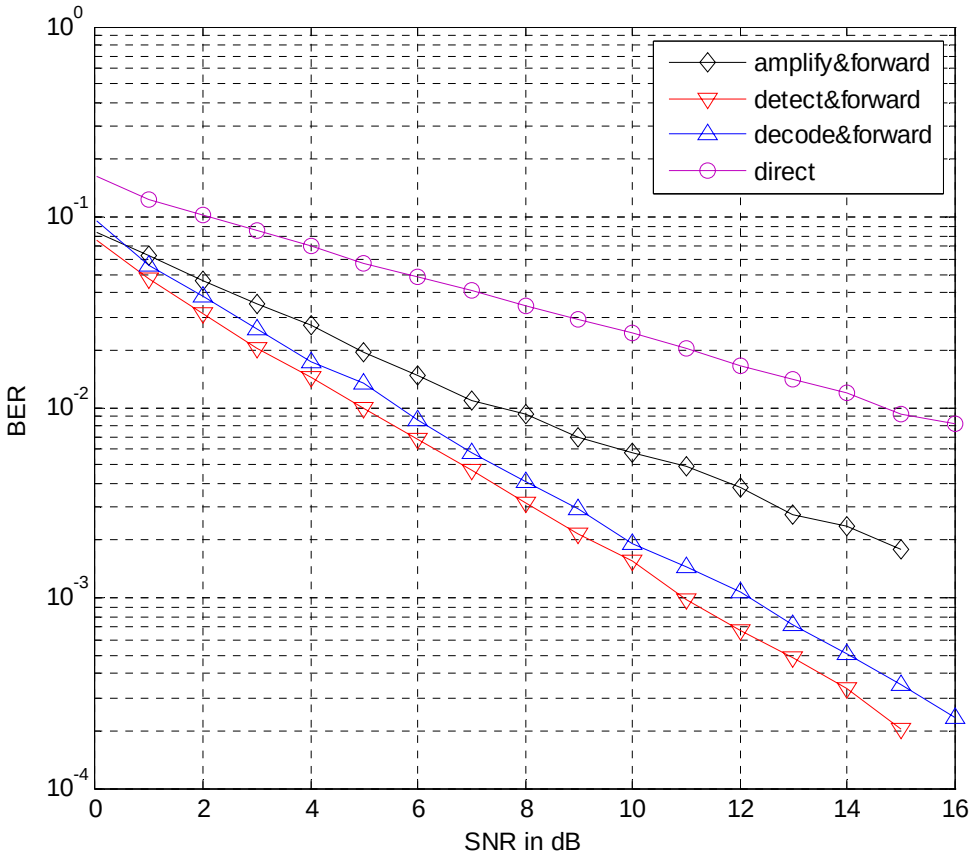

Figure 4.10 Performance evaluations for full duplex case over non-ergodic fading channel.

The simulation results point out that the DetF protocol achieves the lowest bit error probability for a fixed SNR value as compared to DF and AF modes. The performance loss with erroneous source-relay transmission is higher in DF mode, so the deep fades cause DF mode to have an inferior performance to DetF at non-ergodic fading channel. We also observe that the diversity order attained with AF mode is less than that of DetF and DF modes, and, as a result, the latter two modes outperform AF mode in BER performance.

4.3.2 Half-Duplex System

In half duplex transmission, a frame based time division multiplexed transmission protocol is applied where each frame transmission period, T, is divided into two time slots corresponding to direct transmission and cooperation. The length of these time slots are controlled by the parameter α. First let us give the details of DF mode. In DF protocol, the coded bits of a (N,K) LDPC code with

rate R_c^1 are subdivided into three groups of codewords denoted as Φ_1, Φ_2 and Φ_3. The lengths of these groups are $\alpha N/(2-\alpha)$, $(1-\alpha)N/(2-\alpha)$ and $(1-\alpha)N/(2-\alpha)$, respectively. The overall code rate of the system is $R_c = R_c^1(2-\alpha)$. During the first slot of duration, αT, the source node transmits Φ_1, while the relay node only listens. In the second time slot of duration, $(1-\alpha)T$, the source node continues its transmission with the other set of coded bits, Φ_2. Meanwhile, the relay node transmits Φ_3, obtained by decoding and re-encoding the group received in the first time slot.

Depending on α, optimum allocation of three groups of bits is considered for two cases in (Hu & Duman, 2007). Although not essential, the use of systematic codes is assumed for both cases therein. For the case of $\alpha \geq R_c$, the parity bits are grouped into three groups with periodic puncturing. All the systematic bits and the first group of parity bits form Φ_1. The remaining two groups of parity bits form Φ_2 and Φ_3, respectively. For $\alpha < R_c$, only a part of the systematic bits can be transmitted at the first time slot and the design of LDPC code is more challenging. Since we are not interested in optimum code design, we choose $\alpha \geq R_c$ and apply the corresponding allocation rule.

For DetF and AF schemes, a (*N*,*K*) LDPC code with rate R_c is partitioned into two groups, Φ_1 and Φ_2. The source sequentially transmits these partitions in two slots. The relay, on the other hand, transmits the first partition Φ_1 in the second time slot. If $\alpha < 1/2$, the relay transmits Φ_1 in the $\alpha/(1-\alpha)$ portion of second time slot and remains silent in the remaining $(1-2\alpha)/(1-\alpha)$. In the optimum case, $\alpha = 1/2$, the relay is active during the whole second time slot. If $\alpha > 1/2$, then the relay transmits $(1-\alpha)/\alpha$ portion of Φ_1 in the second time slot.

The receiver block diagram at the destination node is illustrated in Fig. 4.11. In the first time slot, the simple MAP detector for point-to-point communication,

"Detector One", extracts the soft information from the received source signal. In the second time slot, "Detector Two" extracts soft information of source and relay signal components from the noisy multiple access channel.

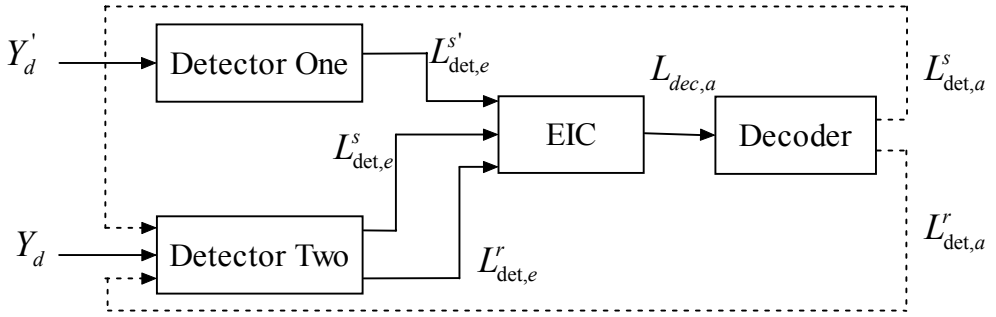

Figure 4.11 Block diagram of the receiver design for half-duplex relay system.

The EIC module collects the soft information from both the source and relay nodes and from both the first and second time slots. In DF mode it demultiplexes the three groups of likelihood information $\left(\text{about}\,\Phi_1, \Phi_2\, \textit{and}\, \Phi_3\right)$ to form one codeword observation for the (*N,K*) code and sends it to the LDPC decoder, which is again implemented using the log-domain BP algorithm. In DetF and AF modes, on the other hand, it sums up the information about Φ_1 obtained from the Detector One in the first slot and from detector two in the second slot similar to full duplex case. Finally, the information about Φ_1 and Φ_2 is demultiplexed to be decoded by LDPC decoder. Clearly, we can also perform iterations between the detector and the decoder similar to the full duplex case in order to improve the overall performance of the system.

We employ an irregular (64800, 32400) LDPC code and consider the case $\alpha = 3/4$, $K_1 = 12$ dB and $K_2 = 3$ dB. This yields an overall system rate of $R_c = 5/8$. The simulation results for ergodic fading case are given in Fig. 4.12. The performance improvement for iteration number higher than 3 is negligible. Accordingly, we present the results for an iteration number of maximum 3. However, there exists a significant improvement by increasing the iteration number up to 3. The DF protocol is observed to outperform AF and DetF

protocols by 0.5 dB and 0.7 dB, respectively, at a BER level of 10^{-4}. The gain attained by AF mode over DetF is about 0.2 dB at the same BER level.

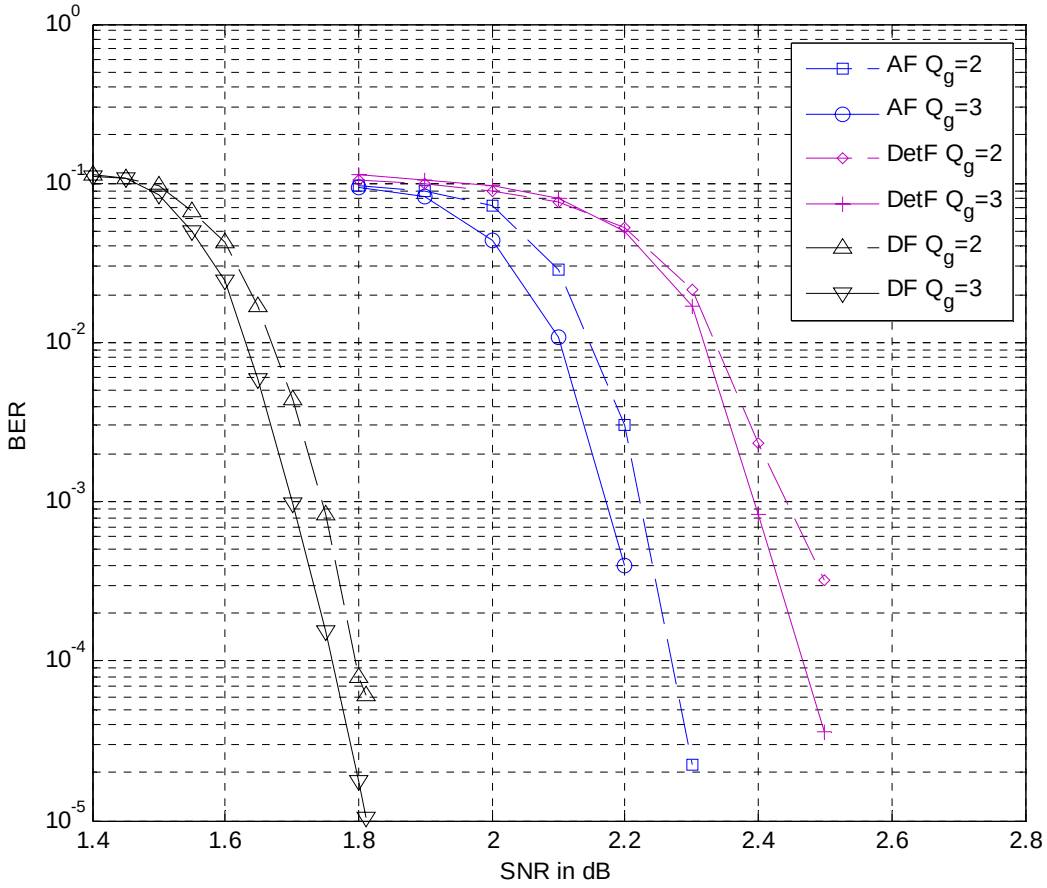

Figure 4.12 Performance evaluations for half duplex case over ergodic fading channel.

The superior performance of DF is expected to last for ergodic fading channel as long as an error free source-relay channel exists. Since the relative channel gains reflect the quality of the corresponding channels, a series of simulations are performed using various relative gains in order to investigate their effects on different protocols. Two cases are considered; K_1=10 dB, K_2=0 dB (case 1) and K_1=5 dB, K_2=0 dB (case 2), and the same (64800, 32400) irregular code is applied with $\alpha = 3/4$. The performance of direct transmission between source and destination is plotted for comparison. The results are presented in Fig. 4.13.

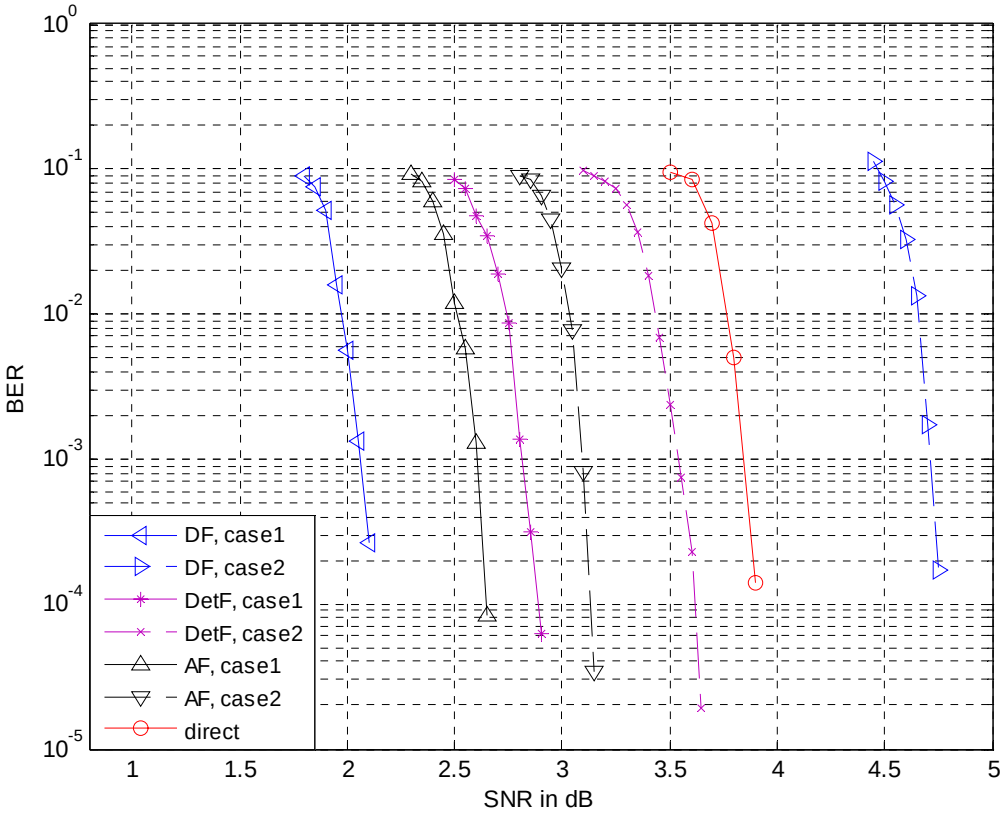

Figure 4.13 Performance evaluations for half duplex case with different relative gains.

Observing the results in Fig. 4.13, we notice the superior performance of DF for case 1, i.e. K_1=10 dB, K_2=0 dB. When K_1 is decreased to 5 dB, on the other hand, the performances reverse this time. Since the source-relay channel cannot provide an error free transmission, the AF and DetF protocols outperform DF mode. Although both AF and DetF protocols are better than direct transmission for both cases, DF is worse than direct transmission and it is not possible to benefit from relay channel in DF mode for case 2. The simulation results for non-ergodic fading channel are presented in Fig. 4.14. We observe similar results like full duplex case. The DetF protocol is superior to DF and outperforms both DF and AF protocols.

4.4 Chapter Summary

In this chapter we investigate the performances of three different forwarding protocols, namely DF, DetF and AF, on LDPC coded cooperative communication

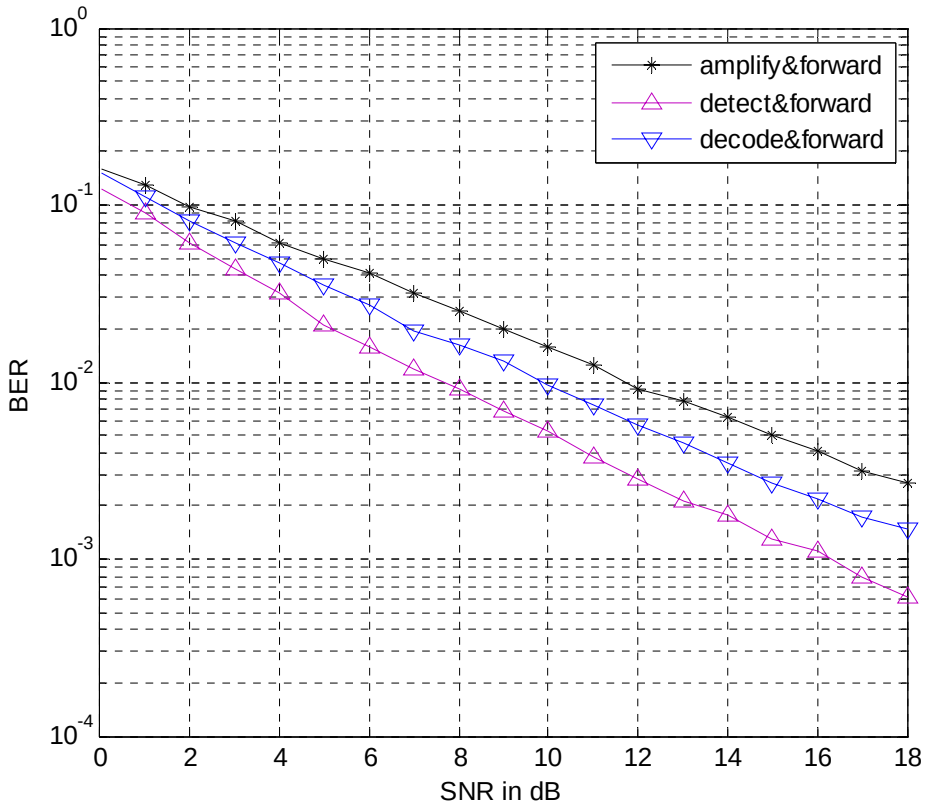

Figure 4.14 Performance evaluations for half duplex case over non-ergodic fading channel.

over wireless relay channel. We proposed appropriate transmission schemes and signaling for both half and full duplex cases and evaluated the performance for both ergodic and non-ergodic fading environment. For ergodic fading, the DF protocol achieves a superior performance compared to other two protocols for both half and full duplex modes. The gain of DF over DetF and AF increases up to 1.5 dB and 2 dB, respectively, for the implemented full duplex mode. The gain is less for half duplex case. The error free transmission between the source and relay nodes in DF mode contributes to its superiority. However, for non-ergodic fading channel, the DF protocol is superior to AF mode, while the DetF protocol has the best performance.

CHAPTER FIVE
ASYNCHRONOUS COOPERATION
OVER WIRELESS RELAY CHANNELS

In this chapter, we focus on cooperation over wireless relay channel with emphasis on synchronism issue. We apply relaying schemes based on LDPC codes and investigate the effects of time delay and phase offset between the source and relay transmission. Capacity bounds are determined using information theoretical analysis. The convergence analysis of practical schemes are evaluated as a tool to determine the overall system performance. In order to suppress the detrimental effects of asynchronous communication, we propose iterative detection techniques and perform simulations.

The chapter is organized as follows: We define asynchronous cooperative communication system and present the results of related previous works in Section 5.1. We introduce asynchronous transmission over relay channel and present mathematical definitions of signals in Section 5.2. We present the capacity analysis of asynchronous transmission for both half and full duplex cases in Section 5.3. We propose an iterative detector and illustrate the receiver diagram in Section 5.4. We also propose a reduced complexity receiver employing minimum mean square error (MMSE) criteria at the detector. As a performance evaluation tool, we employ convergence analysis using EXIT chart method in Section 5.5. We also present the performance evaluations obtained by simulations in Section 5.5. The chapter is concluded in Section 5.6.

5.1 Asynchronous Relay Systems

Almost all these schemes assume that perfect timing and carrier synchronization are available between the terminals. However, the lack of a central controller and the distributed nature of schemes complicate the coordination of the terminals. It is also difficult to achieve synchronization when the received signal is a combination of signals from different users transmitting at different times. Such a reception results with the interference of the data blocks. Despite this interference, it is

shown in (Cover, McEliece, & Posner, 1981) that asynchronism does not decrease the multi-access channel capacity when compared with its synchronous counterpart.

In the context of multiple access channels, another issue to be considered is the impact of discrete sufficient statistics on system performance. For the case of the lack of sufficient statistics, the term approximate statistics is introduced in (Mantravadi & Veeravalli, 2001) and it is shown that both the finite set of discrete sufficient statistics produced via correlation and the finite set of approximately sufficient statistics obtained by matched filtering followed by Nyquist sampling achieve nearly the same performance. For the case of asynchronous relay channel, it is possible to obtain sufficient statistics by passing the received signal through two matched filters synchronized with source and relay signals individually. But optimum usage of this discrete statistics requires sequence detection, i.e. Viterbi algorithm. Hence detection of each symbol considering the received signal only in the interval corresponding to that symbol is suboptimal. But it is reasonable to expect a limited performance loss due to this sub-optimality in light of the results in (Mantravadi & Veeravalli, 2001).

5.1.1 System and Channel Model

In this part, we introduce asynchronism between the source and relay transmission in the classical relay channel. Since asynchronism occurs only when both source and relay nodes are in transmission, which is always the case in full duplex mode, it takes place only in the second time slot of half duplex mode. However, the mathematical definitions given in this part are applicable for both cases whenever a superimposed asynchronous signal is present at the detector. Thus, we will give a single mathematical framework considering a relay channel where both source and relay nodes transmit. The detector is modified to mitigate the ISI appearing as a result of the non-ideal sampling at the destination. We predict the convergence threshold of the asynchronous system based on mutual information transfer between detector and decoder.

The superimposed source and relay signals are received at the destination as

$$y_d(t) = h_{sd}(t)x_s(t) + \sqrt{K_2}h_{rd}x_r(t) + n_d(t), \tag{5.1}$$

where $x_s(t)$ and $x_r(t)$ are the transmitted signals from the source and relay nodes, respectively, both with the same power *P*. The baseband representations of these multiple access channel signals are

$$x_s(t) = \sum_k b_s^k g_T(t - kT), \tag{5.2}$$

$$x_r(t) = \sum_k b_r^k g_T(t - kT), \tag{5.3}$$

where b_s^k and b_r^k are the k*th* coded bit from the source and the relay, respectively, and $g_T(t)$ is the impulse response of the pulse shaping filter which is normalized to have unit energy.

For the synchronous case, if we use a filter matched to the transmitter pulse shaping filter $g_R(t) = g_T(T - t)$, and assume that the output of the filter matched to the pulse waveform satisfies the Nyquist zero ISI property, the discrete model for the sampled output of the matched filter is

$$y_d^k = b_s^k h_{sd}^k + \sqrt{K_2}b_r^k h_{rd}^k + n_d^k, \tag{5.4}$$

where n_d^k is defined as

$$n_d^k = \int_{-\infty}^{\infty} n_d(t)g_T(t - kT)dt. \tag{5.5}$$

For the asynchronous system, the above model becomes rather complicated since the signal from the relay is delayed relative to the signal from the source. The received signal at the destination is defined as,

$$\begin{aligned} y_d(t) &= h_{sd}(t)x_s(t) + \sqrt{K_2}h_{rd}(t)x_r(t-\varepsilon T)e^{j\theta(t)} + n_d(t), \\ &= h_{sd}(t)\sum_k b_s^k g_T(t-kT) + \sqrt{K_2}h_{rd}(t)\sum_k b_r^k g_T(t-kT-\varepsilon T)e^{j\theta(t)} + n_d(t) \end{aligned} \tag{5.6}$$

where εT is the relative delay between the relay and source signals. We assume that this timing offset ε is constant during each frame and varies between the frames. $\theta(t)$ is the phase offset error assuming the receiver is locked perfectly to the source signal. Here, we assume it is a random variable that changes independently for each symbol and it is uniform on $[0, 2\pi)$.

If the receiver filter at the destination is synchronized with the pulse shaping filter of the source, then the discrete time representation of the signal at the output of this matched filter is,

$$y_{d1}^k = b_s^k h_{sd}^k + \sqrt{K_2}\sum_n b_r^n G_{k-n}(\varepsilon)e^{j\theta_k}h_{rd}^k + n_{d1}^k, \tag{5.7}$$

where

$$G_n(\varepsilon) = \int_{-\infty}^{\infty} g_T(t)\,g_T(t+nT-\varepsilon T)\,dt\,. \tag{5.8}$$

It can be noticed that the Nyquist criterion for zero-ISI is still satisfied for $G_n(\varepsilon)$ when $\varepsilon = 0$, i.e. $G_n(0) = 1$ for $n = 0$ and $G_n(0) = 0$ for $n \neq 0$.

The source and relay signals should be independently detected at the destination node since both the information from the source and the relay contribute to the

successful decoding of the original information. Hence, if we are only synchronized with the source signal, the relay signal may suffer from severe ISI and the system performance will be greatly degraded. If we consider the other case, i.e. assuming that the receiver is perfectly synchronized and phase locked with the relay signal, the discrete model for the resulting output becomes

$$y_{d2}^{k} = \sqrt{K_2} b_r^k h_{rd}^k + \sum_n b_s^n G_{k-n}(-\varepsilon) e^{j\phi_k} h_{sd}^k + n_{d2}^k, \tag{5.9}$$

where ϕ_k stands for the phase offset error assuming the receiver is locked to the relay signal and is assumed to be uniform on $[0, 2\pi)$. From Eq. (5.9), we can deduce that y_{d2}^k is the noisy relay signal interfered with the source signal. This signal is used to detect the relay component from the multi-access channel signal.

It can be stated from (5.7) and (5.9) that the lack of synchronization directly results in both ISI and phase variations. The exact characterization of this ISI and its impact on the whole system requires evaluating Eq. (5.8) for particular type of pulse shaping filter. Specifically, we will consider two ensembles of pulse shaping filters: rectangular and square root raised cosine (SQRC) pulse shaping filters. Although the former model is not very practical in real systems, it can provide us with some insights into the problem. The SQRC pulse is more representative of what happens in real systems, though it complicates the analysis.

For the case of a rectangular pulse, if we have perfect timing and phase synchronization with the source signal, we obtain the received signal as

$$y_{d1}(t) = \begin{cases} b_s^k h_{sd}(t) + \sqrt{K_2} b_r^{k-1} e^{j\theta(t)} h_{rd}(t) + n_{d1}(t), & kT \le t < kT + \varepsilon T \\ b_s^k h_{sd}(t) + \sqrt{K_2} b_r^k e^{j\theta(t)} h_{rd}(t) + n_{d1}(t), & kT + \varepsilon T \le t < (k+1)T \end{cases} \tag{5.10}$$

where we assume that ε is a random variable uniformly distributed on [0,1]. The discrete time representation of the output signal is

$$y_{d1}^{k} = b_s^k h_{sd}^k + \sqrt{K_2}\left[(1-\varepsilon)b_r^k + \varepsilon b_r^{k-1}\right]e^{j\theta_k} h_{rd}^k + n_{d1}^k . \tag{5.11}$$

All the relay signal components in Eq. (5.11) are interference for the source signal. Similarly, if we consider perfect timing and phase synchronization with the relay signal, then we obtain

$$\begin{aligned} y_{d2}(t) &= h_{sd}(t+\varepsilon T)x_s(t)e^{j\phi(t)} + \sqrt{K_2}h_{rd}(t)x_r(t) + n_{d2}(t), \\ &= \begin{cases} b_s^k h_{sd}(t)e^{j\phi(t)}(t) + \sqrt{K_2}b_r^k h_{rd}(t) + n_{d2}(t), & kT \le t < (k+1)T - \varepsilon T, \\ b_s^{k+1} h_{sd}(t)e^{j\phi(t)}(t) + \sqrt{K_2}b_r^k h_{rd}(t) + n_{d2}(t), & (k+1)T - \varepsilon T \le t < (k+1)T \end{cases} \end{aligned} \tag{5.12}$$

and the discrete time representation of the output signal from the matched filter is

$$y_{d2}^{k} = \sqrt{K_2}b_r^k h_{rd}^k + \left[(1-\varepsilon)b_s^k + \varepsilon b_s^{k+1}\right]e^{j\phi_k} h_{sd}^k + n_{d2}^k . \tag{5.13}$$

A more practical and commonly used zero-ISI pulse is the raised cosine pulse. It is usually realized as a cascade of two filters, one of which is employed at the transmitter side and the other at the receiver side. The impulse response of the filter is given by,

$$p_{SQRC}(t) = 4\beta \frac{\cos\left[(1+\beta)\pi t/T\right] + \sin\left[(1-\beta)\pi t/T\right](4\beta t/T)^{-1}}{\pi\sqrt{T}\left[1-16\beta^2 t^2/T^2\right]}, \tag{5.14}$$

where T is the symbol period and β is the roll-off factor. When transmit and receive filters are perfectly aligned, they will form the raised cosine pulse which satisfies the Nyquist principle for zero-ISI and becomes zero at any timing instant

$t = nT$ except for $n = 0$. However, if they are misaligned, the discrete output is not zero at any timing instant and thus causes ISI between information symbols. We cannot simplify $G_n(\varepsilon)$ as in the case of the rectangular pulse, yet Eq. (5.7) still holds.

5.2 Capacity Analysis

5.2.1 Full Duplex Case

Throughout this section, we assume that the pulse shaping filter, $g_T(t)$, is defined only in the interval $[0,T]$. Consequently the discrete time representation of the filtered signal at the destination is,

$$y_d^k = b_s^k h_{sd} + \sqrt{K_2} h_{rd} \left(\delta_1 b_r^k + \delta_2 b_r^{k-1} \right) e^{j\theta_k} + n_d^k , \tag{5.15}$$

where

$$\delta_1 = \int_0^T g(t)\, g(t - \varepsilon T) dt , \tag{5.16}$$

$$\delta_2 = \int_0^T g(t)\, g(t + T - \varepsilon T) dt . \tag{5.17}$$

Using max-flow min-cut theorem, the upper/lower bounds for the full duplex relay channel is given as (Cover & El Gamal, 1979),

$$C \le \lim_{N\to\infty} \frac{1}{N} \max_{p(X_s, X_r)} \min \left\{ I(X_s, X_r; Y_d), I(X_s; Y_r, Y_d \,|\, X_r) \right\}. \tag{5.18}$$

where the sequences of source and relay signals in a single frame are defined as $X_s = \left[b_s^1 b_s^2 \ldots b_s^N \right]$ and $X_r = \left[b_r^1 b_r^2 \ldots b_r^N \right]$. The individual mutual information terms in (5.18) can be calculated as,

$$I\left(X_s, X_r; Y_d\right) = H\left(Y_d\right) - H\left(Y_d \middle| X_s, X_r\right),$$
$$= E\left[\mathsf{C}\left(\left|h_{sd}\right|^2 P_s + K_2\left(\delta_1^{\,2} + \delta_2^{\,2}\right)\left|h_{rd}\right|^2 P_r + 2\rho_{s,r}\left(\delta_1 + \delta_2\right) h_{sd} h_{rd} \cdot \sqrt{K_2 P_s P_r} + 2\delta_1\delta_2 R_r\left(1\right)\right) \Big/ N_0\right)\right] \tag{5.19}$$

where $\mathsf{C}(x) = \log_2(1+x)$, $E[.]$ denotes the expectation over the random variables in parentheses and ρ_{sr} and $R_r(k)$ are defined as

$$\rho_{s,r} = \left| \frac{E\left[X_s X_r^*\right]}{\sqrt{E\left[\left|X_s^{\,2}\right|\right]}\sqrt{E\left[\left|X_r^{\,2}\right|\right]}} \right|, \tag{5.20}$$

$$R_r\left(k\right) = E\left[X_r^m X_r^{m-k}\right], \tag{5.21}$$

$$I\left(X_s; Y_d, Y_r \middle| X_r\right) = H\left(Y_d, Y_r \middle| X_r\right) - H\left(Y_d, Y_r \middle| X_s, X_r\right),$$
$$= E\left[\mathsf{C}\left(\left(\left|h_{sd}\right|^2 + K_1\left|h_{sr}\right|^2\right)\frac{\left(1-\rho_{s,r}^2\right)P_s}{N_0}\right)\right]. \tag{5.22}$$

We notice that the multiple access cut given by Eq. (5.19) is an increasing function of $R_r(1)$ and can take a maximum value of P_r. Also, since Eq. (5.19) is also an increasing function of $\rho_{s,r}$, whereas Eq. (5.22) is decreasing, we perform a maximization over $\rho_{s,r}$ in order to determine the bounds. The unconstrained upper bound for capacity of a full duplex asynchronous relay channel for equal source and relay power and various relative channel gains is illustrated in Fig. 5.1. A fixed relative time delay of $T/2$ between the source and relay transmission is assumed for asynchronous case. We observe that when source-relay channel has no relative gain over the source-destination link, the synchronous and asynchronous systems achieve the same capacity. On the other hand, when source-relay link is better than the source-destination channel, a small reduction on the capacity arises similar to the case of Gaussian multiple access channels (Cheng & Verdu, 1992). We should also note that, although we did not plot in Fig. 5.1, when K_1=0 dB and K_2 is positive, the bound is still the same with the case when K_1=0 dB, K_2=0 dB.

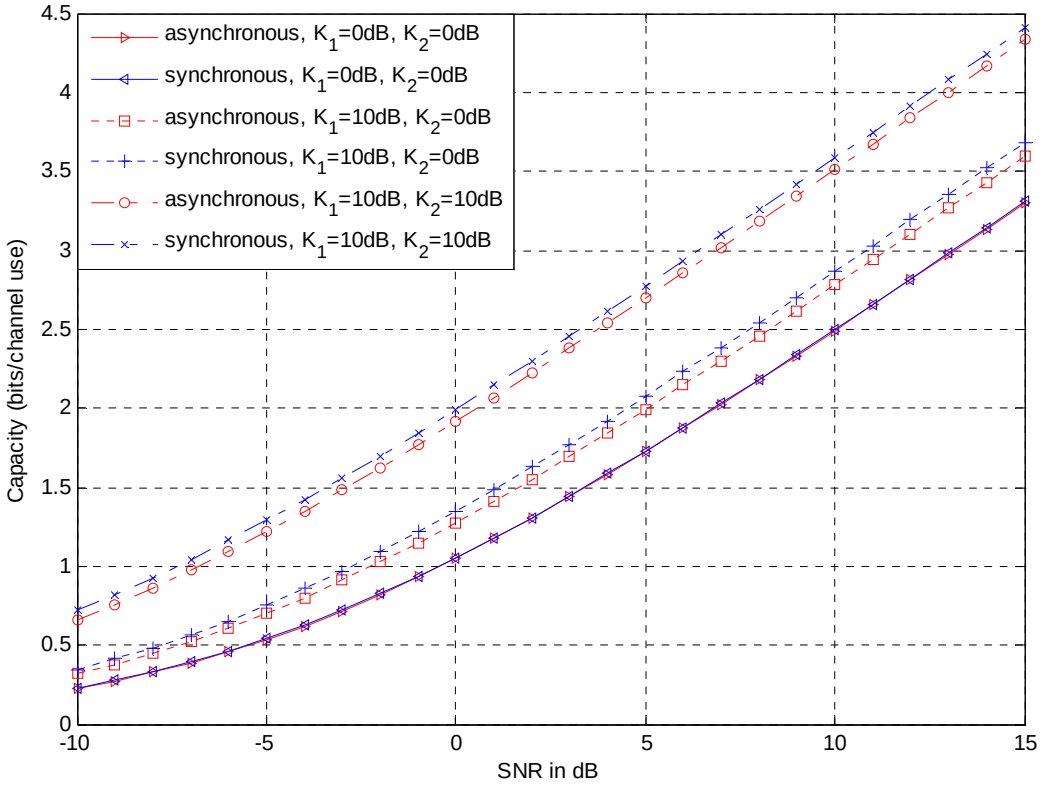

Figure 5.1 Capacity upper bound of full duplex asynchronous system.

5.2.2 Half Duplex Case

In half duplex case, we define x_{s1}, x_{s2} as the transmitted signals from the source during the first and second slots, x_r is the transmitted signal from the relay during the second slot. Powers of the source signal in the first and second slots are assumed to be $P_1^{(1)}$ and $P_1^{(2)}$, respectively. The relay node transmits with power P_2. Y_r is the received signal at the relay during the first slot, Y_{d1} and Y_{d2} are the received signals at the destination during the first and second slots. Similar to full duplex case, we define the sequences of source and relay signals in a single frame as $X_{s1} = \left[x_{s1}^1 \, x_{s1}^2 \ldots x_{s1}^{\alpha N} \right]$, $X_{s2} = \left[x_{s2}^1 \, x_{s2}^2 \ldots x_{s2}^{(1-\alpha)N} \right]$ and $X_r = \left[x_r^1 \, x_r^2 \ldots x_r^{(1-\alpha)N} \right]$. Based on this time division transmission scheme, the upper bound for the capacity is given by (Cover & El Gamal, 1979),

$$C \le \lim_{N\to\infty} \frac{1}{N} \max_{p(X_s,X_r)} \min\Big\{\alpha I\left(X_{s1};Y_r,Y_{d1}\right)+\left(1-\alpha\right) I\left(X_{s2};Y_{d2}\left|X_r\right.\right), \\ \alpha I\left(X_{s1};Y_{d1}\right)+\left(1-\alpha\right) I\left(X_{s2},X_r;Y_{d2}\right)\Big\}. \tag{5.23}$$

The mutual information terms in the capacity expression above can be defined as follows,

$$I\left(X_{s1};Y_r,Y_{d1}\right)=\frac{1}{2}E\left[\mathsf{C}\left(\left(\left|h_{sd1}\right|^2+K_1\left|h_{sr}\right|^2\right)\frac{P_1^{(1)}}{N_0}\right)\right], \tag{5.24}$$

$$I\left(X_{s2};Y_{d2}\left|X_r\right.\right)=\frac{1}{2}E\left[\mathsf{C}\left(\left(1-\rho_{s2,r}^2\right)\left|h_{sd2}\right|^2\frac{P_1^{(2)}}{N_0}\right)\right], \tag{5.25}$$

$$I\left(X_{s1};Y_{d1}\right)=\frac{1}{2}E\left[\mathsf{C}\left(\left|h_{sd1}\right|^2\frac{P_1^{(1)}}{N_0}\right)\right], \tag{5.26}$$

$$I\left(X_{s2},X_r;Y_{d2}\right)=\frac{1}{2}E\left[\mathsf{C}\left(\left|h_{sd2}\right|^2\frac{P_1^{(2)}}{N_0}+K_2\left(\delta_1{}^2+\delta_2{}^2\right)\left|h_{rd}\right|^2\frac{P_2}{N_0} \right.\right. \\ \left.\left. +2\rho_{s2,r}\left(\delta_1+\delta_2\right)\left|h_{sd2}\right|\left|h_{rd}\right|\frac{\sqrt{K_2P_1^{(2)}P_2}}{N_0}+\frac{2\delta_1\delta_2R_r\left(1\right)}{N_0}\right)\right]. \tag{5.27}$$

The definitions of ρ_{sr} and $R_r\left(k\right)$ are already given in Eq. (5.20) and Eq. (5.21), respectively. The unconstrained upper bound for capacity of a half duplex asynchronous relay channel is illustrated in Fig. 5.2. Equal source and relay powers and a fixed relative time delay of *T*/2 are assumed as in the full duplex case. We observe similar results as for the full duplex case, i.e. a reduction on the capacity is observed for asynchronous case with positive relative gains. Synchronous and asynchronous systems again attain the same bound for equal source-relay and source-destination channels. Otherwise a small degradation in the capacity arises.

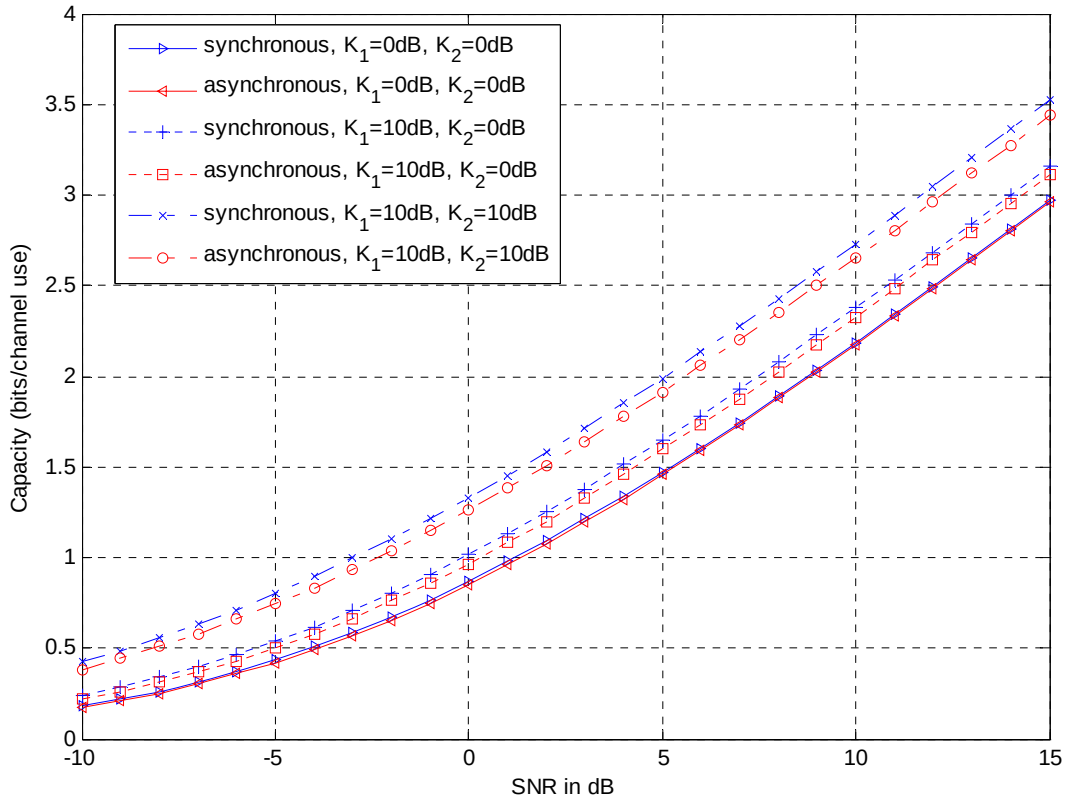

Figure 5.2 Capacity upper bound of half duplex asynchronous system.

5.3 Receiver Design and Detection Technique

For the asynchronous system, the received signal $y_d(t)$ is applied to two separate matched filters which are synchronized with the source and relay signals individually as shown in Fig. 5.3 for half duplex system. We notice that different from the receiver for synchronous case (Fig. 4.11), Detector Two is replaced with two individual matched filters in series with two detectors. A similar modification is also realized for full duplex case and the single detector is replaced with two individual detectors. The soft information of the source and relay bits are produced considering one as the interference signal for the other. We assume that the delay information and phase offset are both available at the receiver side perfectly, so that the detector incorporates and uses the delay and phase information into the detection.

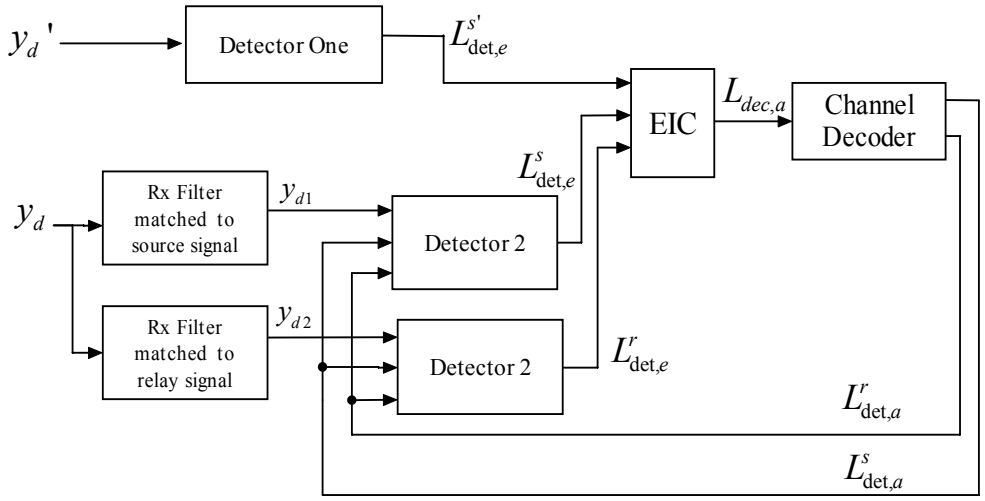

Figure 5.3 Receiver diagram for the asynchronous case.

For the case of a rectangular pulse and BPSK modulation, the LLR of the source signal is produced as

$$\begin{aligned} L^{s,k}_{\text{det}} &= \log \frac{P\left(b^k_s = 0 \middle| y^k_{d1}\right)}{P\left(b^k_s = 1 \middle| y^k_{d1}\right)}, \\ &= \log \frac{\sum_{b^{k-1}_r, b^k_r \in \{0,1\}} p\left(y^k_{d1} \middle| b^k_s = 0, b^k_r, b^{k-1}_r\right) P\left(b^k_s = 0, b^k_r, b^{k-1}_r\right)}{\sum_{b^{k-1}_r, b^k_r \in \{0,1\}} p\left(y^k_{d1} \middle| b^k_s = 1, b^k_r, b^{k-1}_r\right) P\left(b^k_s = 1, b^k_r, b^{k-1}_r\right)}. \end{aligned} \tag{5.28}$$

Similarly the LLR of the relay signal is given as

$$\begin{aligned} L^{r,k}_{\text{det}} &= \log \frac{P\left(b^k_r = 0 \middle| y^k_{d2}\right)}{P\left(b^k_r = 1 \middle| y^k_{d2}\right)}, \\ &= \log \frac{\sum_{b^k_s, b^{k+1}_s \in \{0,1\}} p\left(y^k_{d2} \middle| b^k_r = 0, b^k_s, b^{k+1}_s\right) P\left(b^k_r = 0, b^k_s, b^{k+1}_s\right)}{\sum_{b^k_s, b^{k+1}_s \in \{0,1\}} p\left(y^k_{d2} \middle| b^k_r = 1, b^k_s, b^{k+1}_s\right) P\left(b^k_r = 1, b^k_s, b^{k+1}_s\right)}. \end{aligned} \tag{5.29}$$

We should restate here that, as pointed out in the introduction part, optimum detection of *kth* symbol requires processing the whole discrete statistics, but the

performance loss with the above detection algorithm is limited. The length of the ISI increases with the number of nonzero valued $G_n(\varepsilon)$ for the case of SQRC pulse, so we can deduce from Eq. (5.28) that, the MAP detector for the asynchronous system has an exponential complexity with the length of ISI. The other complexity issue to be considered is the modulation level. Since the summations in the numerator and denumerator of Eq. (4.18) depend on the cardinality of the groups B_s and B_r, the complexity increases with the modulation level, M. Therefore we consider MMSE based linear symbol estimator at the destination node. We employ SISO-type detector which can incorporate a priori information and generate soft output suitable for turbo processing. A SISO-type MMSE equalizer is proposed in (Tuchler, Singer, & Koetter, 2002) for combatting ISI. The idea is using the estimated transmitted symbols rather than the received symbols while computing LLR's. We will set up the algorithm for estimating the source signal interfered with relay components but the other case, i.e. estimating the relay signal, is similar. If we limit the summation index in Eq. (5.7) from $-L$ to L, (total number of relay signals interfering with source signal is limited to $2L+1$) we set up the following set of observation equations in order to estimate x_s,

$$\underbrace{\begin{bmatrix} y_{d1}^{k-W_2} \\ \vdots \\ y_{d1}^{k+W_1} \end{bmatrix}}_{\mathrm{Y}_{d1}^{k}} = \underbrace{\begin{bmatrix} h_{sd}^{k-W_2} & 0 & \cdots & 0 & 0 \\ 0 & h_{sd}^{k-W_2+1} & 0 & \cdots & 0 \\ \vdots & & \ddots & & \vdots \\ 0 & \cdots & 0 & 0 & h_{sd}^{k+W_1} \end{bmatrix}}_{\mathrm{H}_{sd}^{k}} \times \underbrace{\begin{bmatrix} x_s^{k-W_2} \\ \vdots \\ x_s^{k+W_1} \end{bmatrix}}_{\mathrm{X}_{s}^{k}} + \underbrace{\begin{bmatrix} n_{d1}^{k-W_2} \\ \vdots \\ n_{d1}^{k+W_1} \end{bmatrix}}_{N_{d1}^{k}}$$

$$+ \underbrace{\begin{bmatrix} h_{rd}^{k-W_2} G_L(\varepsilon) & \cdots & h_{rd}^{k-W_2} G_{-L}(\varepsilon) & \cdots & 0 \\ 0 & h_{sd}^{k-W_2+1} G_L(\varepsilon) & \cdots & h_{rd}^{k-W_2} G_{-L}(\varepsilon) & 0 \\ \vdots & & \ddots & & \vdots \\ 0 & \cdots & h_{sd}^{k+W_1} G_L(\varepsilon) & \cdots & h_{sd}^{k+W_1} G_{-L}(\varepsilon) \end{bmatrix}}_{\mathrm{H}_{rd}^{k}} \times \underbrace{\begin{bmatrix} x_r^{k-W_2-L} \\ \vdots \\ x_r^{k} \\ \vdots \\ x_r^{k+W_1+L} \end{bmatrix}}_{\mathrm{X}_{r}^{k}} \tag{5.30}$$

where W_1, W_2 and $W = W_1 + W_2 + 1$ denote length of the noncausal part, length of the causal part and overall length of the estimator fitler, respectively. Rewriting in short form we obtain the channel model as,

$$\mathrm{Y}_{d1}^{k} = \mathrm{H}_{sd}\mathrm{X}_{s}^{k} + \mathrm{H}_{rd}\mathrm{X}_{r}^{k} + N_{d1}^{k}. \tag{5.31}$$

When we apply the well-known LMMSE algorithm, we can get $\hat{x}_s^k$ and $\hat{x}_r^k$ as,

$$\hat{x}_s^k = \mathrm{A}_k^H \mathrm{Y}_{d1}^k + e_k, \tag{5.32}$$

$$\hat{x}_r^k = \mathrm{C}_k^H \mathrm{Y}_d^k + d_k. \tag{5.33}$$

To minimize the mean square error (MSE) of the estimator, i.e. to minimize both $E\left(\left|x_s^k - \hat{x}_s^k\right|^2\right)$ and $E\left(\left|x_r^k - \hat{x}_r^k\right|^2\right)$, the estimator coefficients are calculated by,

$$\mathrm{A}_k = Cov\left(\mathrm{Y}_{d1}^k, \mathrm{Y}_{d1}^k\right)^{-1} Cov\left(Y_{d1}^k, x_s^k\right), \tag{5.34}$$

$$e_k = E\left(x_s^k - \mathrm{A}_k^H E\left(\mathrm{Y}_{d1}^k\right)\right). \tag{5.35}$$

It is easy to show that

$$Cov\left(Y_{d1}^k, x_s^k\right) = J_s Cov\left(x_s^k, x_s^k\right)^H, \tag{5.36}$$

and

$$Cov\left(\mathrm{Y}_{d1}^k, \mathrm{Y}_{d1}^k\right) = \mathrm{H}_{sd}^k \left(Cov\left(x_s^k, x_s^k\right)\right)^H \left(\mathrm{H}_{sd}^k\right)^H + \mathrm{H}_{rd}^k \left(Cov\left(x_r^k, x_r^k\right)\right)^H \left(\mathrm{H}_{rd}^k\right)^H + N_0 \mathrm{I}_K, \tag{5.37}$$

where $\mathrm{J}_s = \mathrm{H}_{sd}^k \left[0_{1\times K_1} \;\; 1 \;\; 0_{1\times K2}\right]^T$, $\mathrm{J}_r = \mathrm{H}_{rd}^k \left[0_{1\times K_1} \;\; 1 \;\; 0_{1\times K2}\right]^T$ and I_K is the identity matrix with dimension $K \times K$. To simplify the notations, we use $\overline{x}_u^k$ and v_u^k to denote the mean and covariance of x_u, with $u \in \{r, s\}$. Then the estimator is given by

$$\hat{x}_s^k = \overline{x}_s^k + \mathrm{V}_s^k \mathrm{J}_s^H \left(\Lambda_k^{-1}\right)^H \left(\mathrm{Y}_{d1}^k - \overline{\mathrm{Y}}_{d1}^k\right), \tag{5.38}$$

$$\hat{x}_r^k = \overline{x}_r^k + \mathrm{V}_r^k \mathrm{J}_r^H \left(\Lambda_k^{-1}\right)^H \left(\mathrm{Y}_{d1}^k - \overline{\mathrm{Y}}_{d1}^k\right), \tag{5.39}$$

where

$$\overline{Y}_{d1}^k = \left[\, \overline{y}_{d1}^{k-K_2} \ldots \overline{y}_{d1}^{k+K_1} \,\right]^T, \tag{5.40}$$

$$\mathrm{V}_\mathrm{s}^\mathrm{k} = diag\left[\, v_s^{k-L-K_2+1} \ldots v_s^{k+K_1} \right], \tag{5.41}$$

$$\mathrm{V}_\mathrm{r}^\mathrm{k} = diag\left[\, v_r^{k-L-K_2+1} \ldots v_r^{k+K_1} \right], \tag{5.42}$$

$$\Lambda_k = \mathrm{H}_{sd}^k \mathrm{V}_s^k \left(\mathrm{H}_{sd}^k\right)^H + \mathrm{H}_{rd}^k \mathrm{V}_r^k \left(\mathrm{H}_{rd}^k\right)^H + N_0 \mathrm{I}_K \,. \tag{5.43}$$

Here, the mean vector $\overline{Y}_{d1}^k$ is defined as,

$$\overline{Y}_{d1}^k = h_{sd}^k \overline{x}_s^k + \sum_{i=-L}^{L} G_i\left(\varepsilon\right) h_{rd}^k \overline{x}_r^{k-i} + n_d^k \,. \tag{5.44}$$

In order to derive a SISO detector, we need to incorporate the a priori information into the estimator and generate suitable extrinsic information for the decoder. Here, we follow (Tuchler, et. al., 2002) and use a method which decomposes the estimation and the soft output generation. Basically, the received signal is first passed through the estimator and then the a posteriori LLR is generated based on the estimator output. In order for the iterative turbo equalization to work, we need to make sure that $\hat{x}_s\left(k\right)$ is independent of $L_a^s\left(k\right)$, the a priori LLR information about $x_s\left(k\right)$, i.e. we need to set $L_a^s\left(k\right) = 0$ when computing $\hat{x}_s\left(k\right)$. Therefore, by using similar computations as in (Tuchler, et. al., 2002), we have

$$\hat{x}_s\left(k\right) = \left(1 + \left(1 - V_s^k\right)\psi_s^k J_s\right)^{-1} \psi_s^k \left(Y_{d1}^k - \overline{Y}_{d1}^k + \overline{x}_s^k J_s\right), \tag{5.45}$$

where $\psi_s^k = J_s^H \left(\Lambda_k^{-1}\right)^H$. Assuming Gaussian approximation for the probability density function (PDF) of $P\left(\hat{x}_s\left(k\right)\middle|x_s\left(k\right)\right)$, the soft extrinsic information for the source signal is

$$\begin{aligned} L_s^e\left(k\right) &= \log\frac{P\left(\hat{x}_s^k \middle| x_s^k = +1\right)P\left(x_s^k = +1\right)}{P\left(\hat{x}_s^k \middle| x_s^k = -1\right)P\left(x_s^k = -1\right)} - L_s^a\left(k\right), \\ &= -\frac{\left|\hat{x}_s^k - \varphi_s^k\right|^2}{\left(\sigma_s^k\right)^2} + \frac{\left|\hat{x}_s^k - \varphi_s^k\right|^2}{\left(\sigma_s^k\right)^2} = \frac{4\,\mathrm{Re}\left\{\hat{x}_s^k\left(\varphi_s^k\right)^H\right\}}{\left(\sigma_s^k\right)^2} \end{aligned} \tag{5.46}$$

where φ_s^k and σ_s^k are defined as

$$\varphi_s^k = \left(1 + \left(1 - V_s^k\right)\psi_s^k J_s\right)^{-1}\psi_s^k J_s\,, \tag{5.47}$$

$$\sigma_s^k = \left(1 + \left(1 - V_s^k\right)\psi_s^k J_s\right)^{-2}\left(\psi_s^k J_s - V_s^k \psi_s^k J_s J_s^H \left(\psi_s^k\right)^H\right). \tag{5.48}$$

The final soft output of the detector is given by (after some simplifications)

$$L_s^e\left(k\right) = \frac{4}{1 - V_s^k J_s^H \left(\psi_s^k\right)^H}\mathrm{Re}\left\{\psi_s^k\left(Y_{d1}^k - \overline{Y}_{d1}^k + \overline{x}_s^k J_s\right)\right\}. \tag{5.49}$$

The same procedure can be applied for x_r^k resulting in

$$L_r^e\left(k\right) = \frac{4}{1 - V_r^k J_r^H \left(\psi_r^k\right)^H}\mathrm{Re}\left\{\psi_r^k\left(Y_{d2}^k - \overline{Y}_{d1}^k + \overline{x}_r^k J_r\right)\right\} \tag{5.50}$$

5.4 Convergence Analysis and Simulation Results

Tracking the average mutual information between a specific bit and its corresponding LLR value is a useful tool to predict the convergence behavior of a

soft input soft output detector/decoder. In this context, we obtain the transfer functions of detector and decoder modules individually and track the information flow between these two modules. We can define the transfer functions of DET (detector module) and DEC (decoder module) respectively as,

$$\left(I^{s}_{\mathrm{dec},a}, I^{r}_{\mathrm{dec},a}\right) = \left(I^{s}_{\mathrm{det},e}, I^{r}_{\mathrm{det},e}\right) = f_1\left(I^{s}_{\mathrm{det},a}, I^{r}_{\mathrm{det},a}, SNR, R_c\right), \tag{5.51}$$

$$\left(I^{s}_{\mathrm{dec},e}, I^{r}_{\mathrm{dec},e}\right) = \left(I^{s}_{\mathrm{det},a}, I^{r}_{\mathrm{det},a}\right) = f_2\left(I^{s}_{\mathrm{det},e}, I^{r}_{\mathrm{det},e}\right) \tag{5.52}$$

where the subscript '*a*' ('*e*') denotes the average mutual information between *a priori* (extrinsic) LLR information and the corresponding transmitted bit. The transfer function of DET is obtained by both modeling the $L^{s}_{\mathrm{det},a}\left(b_s\right)$ and $L^{r}_{\mathrm{det},a}\left(b_r\right)$ as Gaussian distributed random variables conditioned on the information bit they represent. The mean and the variance of $L^{s}_{\mathrm{det},a}\left(b_s\right)$ are $\left(1-2b_s\right)\sigma^2_{L^{s}_{\mathrm{det},a}}/2$ and $\sigma^2_{L^{s}_{\mathrm{det},a}}$ respectively, where

$$\sigma^2_{L^{s}_{\mathrm{det},a}} = J^{-1}\left(I^{s}_{\mathrm{det},a}\right), \tag{5.53}$$

with

$$J\left(\sigma\right) = 1 - \int_{-\infty}^{\infty} \frac{e^{-\left(\left(\zeta-\sigma^2\right)/2\sigma^2\right)}}{\sqrt{2\pi}\sigma} \log_2\left(1+e^{-\zeta}\right) d\zeta\,. \tag{5.54}$$

The parameters of $L^{r}_{\mathrm{det},a}\left(b_r\right)$ are defined in the same way. The extrinsic information of detector is produced using this a priori information at specific SNR and rate. Since the mutual information between the extrinsic information L and the corresponding bit cannot be assumed as Gaussian distributed, it is calculated as

$$I_L = \frac{1}{2}\sum_{x=\pm 1}\int_{-\infty}^{\infty} p_L\left(\zeta \middle| X=x\right).\log_2 \frac{p_L\left(\zeta \middle| X=x\right)}{p_L\left(\zeta \middle| X=-1\right)+p_L\left(\zeta \middle| X=1\right)} d\zeta\,, \tag{5.55}$$

As pointed out in (Hu & Duman, 2007), the curves for f_1 and f_2 are four dimensional and difficult to analyze directly. Alternatively, for the special case $K_1 = \infty$ (perfect source-relay channel) and $K_2 = 0$ dB, the inputs and outputs are symmetric and the transfer functions can be analyzed via two dimensional curves. Therefore we can omit the superscripts '*s*' and '*r*' for this special case. Additionally, the transfer function of DEC can be calculated analytically for this special case via the procedure relying on the information transfer between the variable node decoder and check node decoder (ten Brink, et. al., 2004). Specifically, the EXIT functions of a degree d_v variable node and a degree d_c check node are

$$I_{VND,e}\left(I_A, d_v\right) = J\left(\sqrt{\left(d_v - 1\right)\left[J^{-1}\left(I_A\right)\right]^2 + \sigma_{L_{dec,a}}^2}\right), \tag{5.56}$$

$$I_{CND,e}\left(I_A, d_c\right) \approx 1 - J\left(\sqrt{d_v - 1} J^{-1}\left(1 - I_A\right)\right) \tag{5.57}$$

where $\sigma_{L_{dec,a}}^2$ is the variance of *a priori* input of the decoder. The average transfer functions for variable node decoder (VND) and check node decoder (CND) are computed as

$$I_{VND,e}\left(I_A\right) = \sum_{i=1}^{D_v} \lambda_i I_{VND,e}\left(I_A, d_v^i\right), \tag{5.58}$$

$$I_{CND,e}\left(I_A\right) = \sum_{i=1}^{D_c} \rho_i I_{CND,e}\left(I_A, d_c^i\right) \tag{5.59}$$

where D_v and D_c are the number of different variable and check node degrees, and λ_i and ρ_i are the fraction of edges connected to the variable and check nodes with degrees d_v^i and d_c^i, respectively. If we define the number of inner iterations within the decoder as Q_D, the transfer function of DEC after Q_D iterations is

$$I_{dec,e} = J\left(\sqrt{d_v} J^{-1}\left(I_{CND,e}^{(Q_D)}\right)\right), \tag{5.60}$$

where $I_{dec,e}$ is the mutual information between the extrinsic LLR and the corresponding information bit. One single global iteration is completed after the extrinsic information from the detector is processed by the decoder. The information flow is continued by feeding back $I_{dec,e}$ to the detector to be processed as $I_{\mathrm{det},a}$. We denote the total number of global iterations as Q_G. In Fig. 5.4, we plot the EXIT chart for the asynchronous system having perfect source relay channel and employing BPSK modulation. The necessary condition for the system to converge is the existence of an open tunnel between DET and DEC transfer function curves. The smallest SNR value for which this tunnel exists is the convergence threshold.

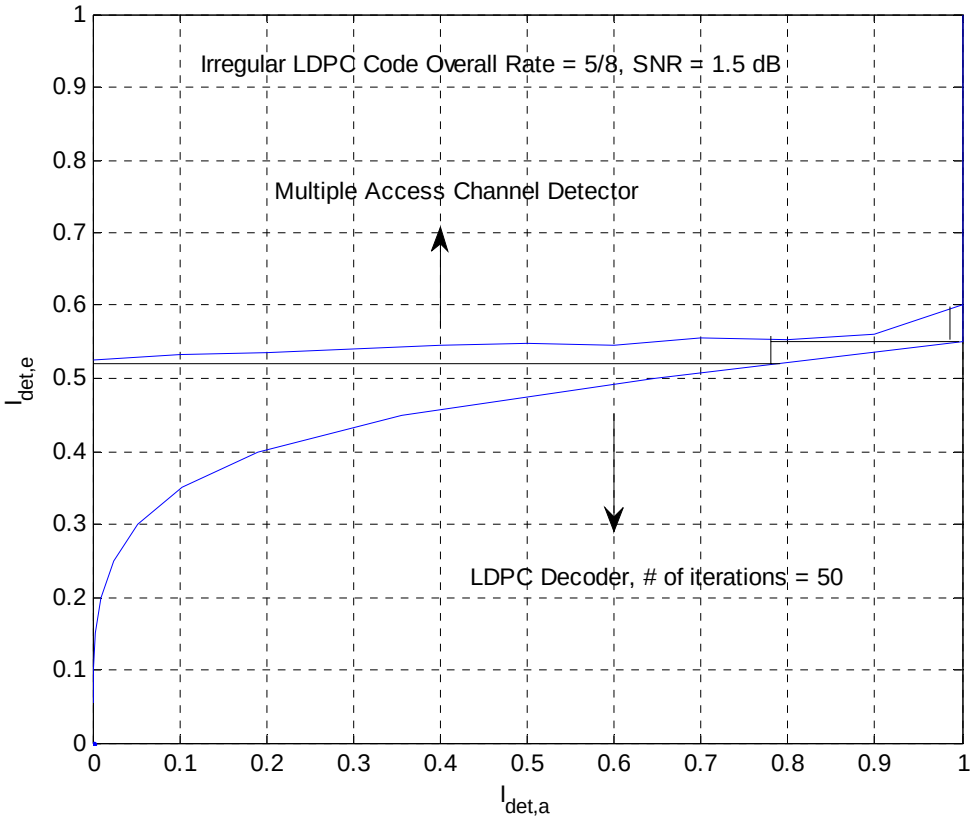

Figure 5.4 EXIT chart of LDPC coded relay system.

For the general case, i.e. for imperfect source-relay channel condition, we track the iterative trajectory of mutual information between the information bits and the soft outputs to predict the convergence threshold. The necessary condition for the system to converge is

$$I_{\text{det},a}^{s} \to 1 \text{ and } I_{\text{det},a}^{r} \to 1 \text{ when } Q_G \to \infty .$$

In order to investigate the effects of asynchronism on overall system performance, Monte Carlo simulations have been performed. We apply two ensembles of irregular systematic LDPC codes under two different scenarios. In the first case (case 1), we employ LDPC code (code 1) with rate $R_c^1 = 1/3$ and obtain an overall rate R_c = 4/9 by using α = 2/3. For the second case (case 2), a mother code with rate $R_c^1 = 1/2$ (code 2) ensures an overall rate of $R_c = 5/8$ with α= 3/4. The code parameters are given in Table 5.1. The block size of the codes are 64800 and Q_D is 50 for the LDPC decoder. For both two cases, the gains are assumed as K_1 = 12 dB and K_2 = 3 dB.

Table 5.1 Code Parameters

	$\lambda(x) = \sum_i \lambda_i x^{d_v^i}$	$\rho(x) = \sum_i \rho_i x^{d_c^i}$
Code 1	$0.667x^2 + 0.222x^3 + 0.111x^{12}$	x^5
Code 2	$0.5x^2 + 0.3x^3 + 0.2x^8$	$0.25x^5 + 0.75x^7$

We compare the performance of asynchronous transmission scheme applying rectangular pulse shaping filter with synchronous counterpart. We use BPSK type of modulation for all simulations. We consider both AWGN and Rayleigh fast fading channel, i.e. the channel coefficients are independent of each other. The relative delay between the source and relay transmission is assumed to be uniform on the intervals [0, T/4] or [0, T/2] where T is the symbol period. Also the phase offset is uniform on [0,2π) for the asynchronous case. Both the delay and phase

offset information are assumed to be known at the destination. Additionally, perfect channel side information is assumed at respective receiver nodes. In Fig. 5.5, we compared the performances of synchronous and asynchronous systems over AWGN channel. Global iteration, Q_G, is set to 2 (i.e. the extrinsic information was fed back to the channel detector/s only once).

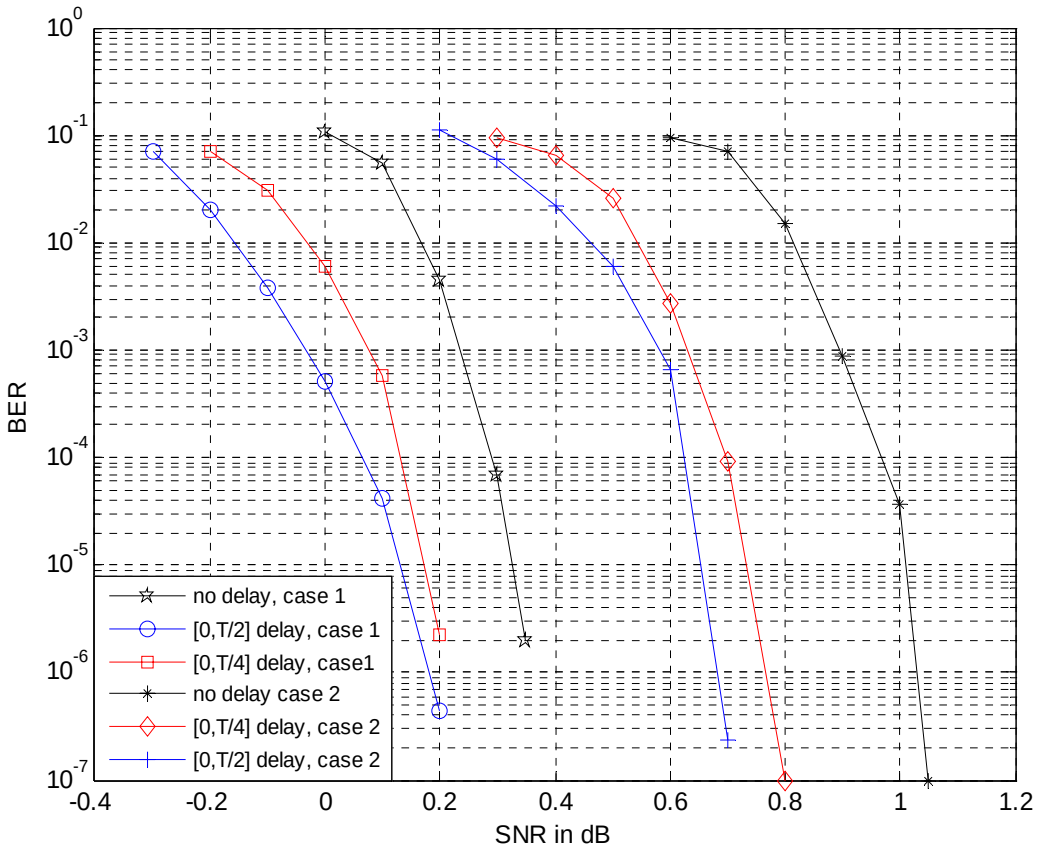

Figure 5.5 Performance evaluations over AWGN channel.

A remarkable observation is that asynchronous system outperforms synchronous case, such that an SNR improvement of approximately 0.2 and 0.35dB is observed for case1 and case 2, respectively, at a bit error rate (BER) value of 10^{-4} for the [0, T/4) delay interval. It can also be stated that this gain increases with the time delay. The reason of this gain can be explained as follows. Since the asynchronism decreases energy for the interfering signal, it can provide benefit to the whole system by incorporating the full knowledge of system

parameters. For Rayleigh fading channel, we present the convergence thresholds obtained by tracking the iterative trajectory of mutual information in Table 5.2.

Table 5.2 Iterative Trajectory of Mutual Information

Case 1					Case 2				
SNR	$I^{s}_{\mathrm{det},e}$	$I^{r}_{\mathrm{det},e}$	$I^{s}_{\mathrm{det},a}$	$I^{r}_{\mathrm{det},a}$	SNR	$I^{s}_{\mathrm{det},e}$	$I^{r}_{\mathrm{det},e}$	$I^{s}_{\mathrm{det},a}$	$I^{r}_{\mathrm{det},a}$
0.1 dB	/	/	0	0	1.4 dB	/	/	0	0
	0.2926	0.4648	0.5274	0.5274		0.4376	0.6129	0.7326	0.7326
	0.3152	0.4860	0.8517	0.8517		0.46	0.6358	0.9536	0.9536
	0.3166	0.4867	1	1		0.47	0.65	1	1
SNR	$I^{s}_{\mathrm{det},e}$	$I^{r}_{\mathrm{det},e}$	$I^{s}_{\mathrm{det},a}$	$I^{r}_{\mathrm{det},a}$	SNR	$I^{s}_{\mathrm{det},e}$	$I^{r}_{\mathrm{det},e}$	$I^{s}_{\mathrm{det},a}$	$I^{r}_{\mathrm{det},a}$
0 dB	/	/	0	0	1.3 dB	/	/	0	0
	0.2935	0.4543	0.4884	0.4884		0.42	0.60	0.6821	0.6821
	0.3036	0.4686	0.5987	0.5987		0.4438	0.6244	0.8264	0.8264
	0.3046	0.4754	0.6321	0.6321		0.4492	0.6304	0.877	0.877
	0.3052	0.4774	0.6622	0.6622		0.4541	0.6311	0.8863	0.8863
	0.3052	0.4690	0.5933	0.5933		0.4540	0.6306	0.8847	0.8847

We deduce that convergence thresholds for case 1 and case 2 are 0.1dB and 1.4dB, respectively. We also present the simulation results in Fig. 5.6 and Fig. 5.7. In order to observe the steady state performance Q_G is increased up to 3 for both cases and it is observed that no additional significant gain can be achieved by increasing Q_G beyond this value. For case 1, it is observed that the asynchronous system can achieve the performance of synchronous case for the [0, T/4) delay interval. Meanwhile, a slight degradation of about 0.2 dB is observed for [0,T/2) delay interval.

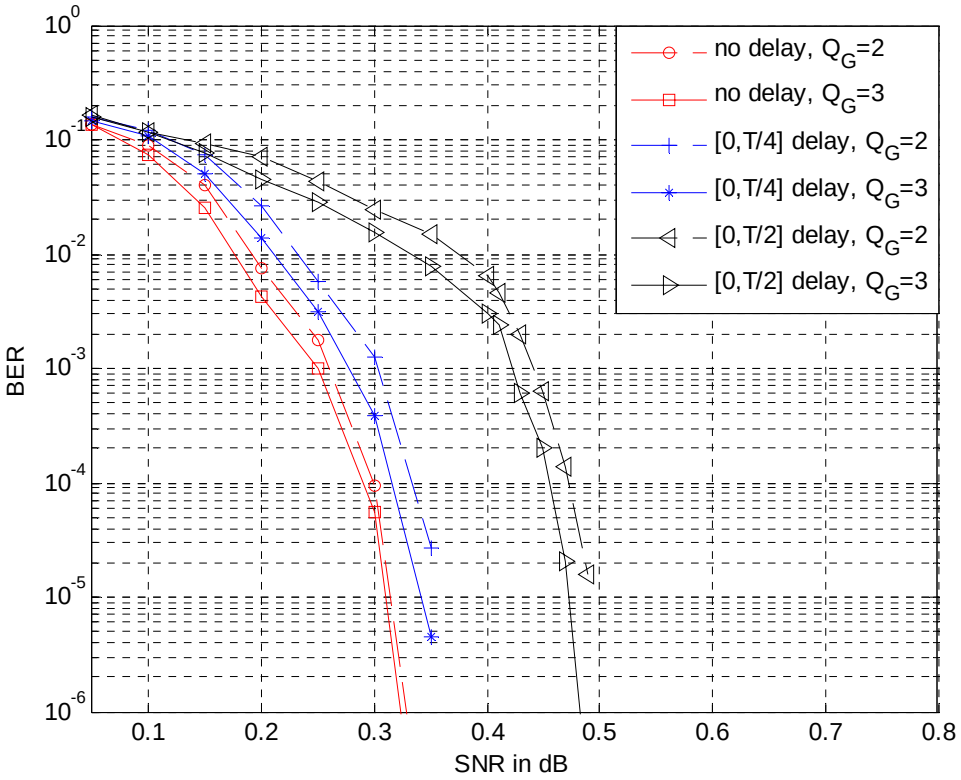

Figure 5.6 Performance evaluations over Rayleigh fast fading channel (case 1).

Similar results are also obtained for case 2 where the loss for [0, *T*/2) delay interval increases to approximately 0.3 dB, which is still reasonable. For Rayleigh fading, the phase information is incorporated into channel coefficients. Hence, we can state that the effects of the phase offset disappears since we assume perfect phase offset and channel coefficient information at the receiver.

The simulation results for full duplex case considering both SIC and asymmetric information combining (AIC) configurations are illustrated in Fig. 5.8. In AIC scheme, we apply a mother code with rate $R_c / 2$ at the source and puncture half of the coded bits. The first partition is sent by the source and the second partition is sent by the relay at the next block after proper decoding and re-encoding. The overall code rate we applied is 1/2 for both cases in the simulations. We observe that the AIC scheme outperforms the SIC scheme for both synchronous and asynchronous cases. Also similar to half duplex case, a small performance loss appears with asynchronism.

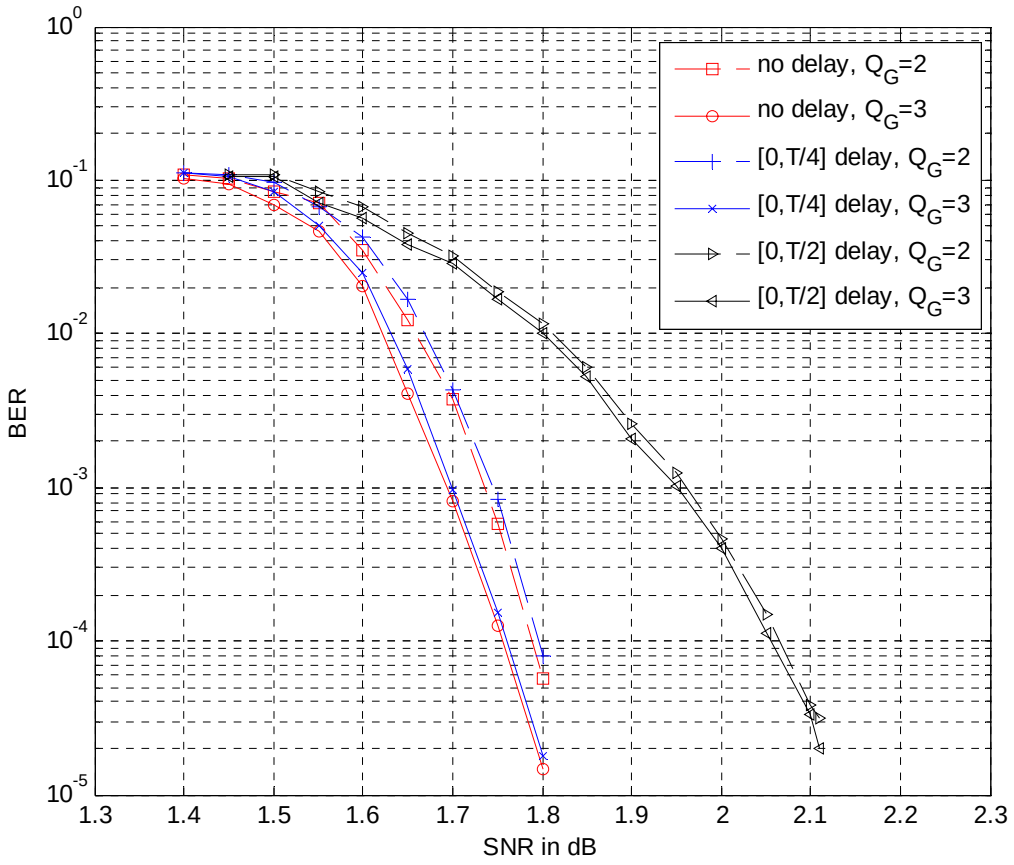

Figure 5.7 Performance evaluations for Rayleigh fast fading channel (case 2).

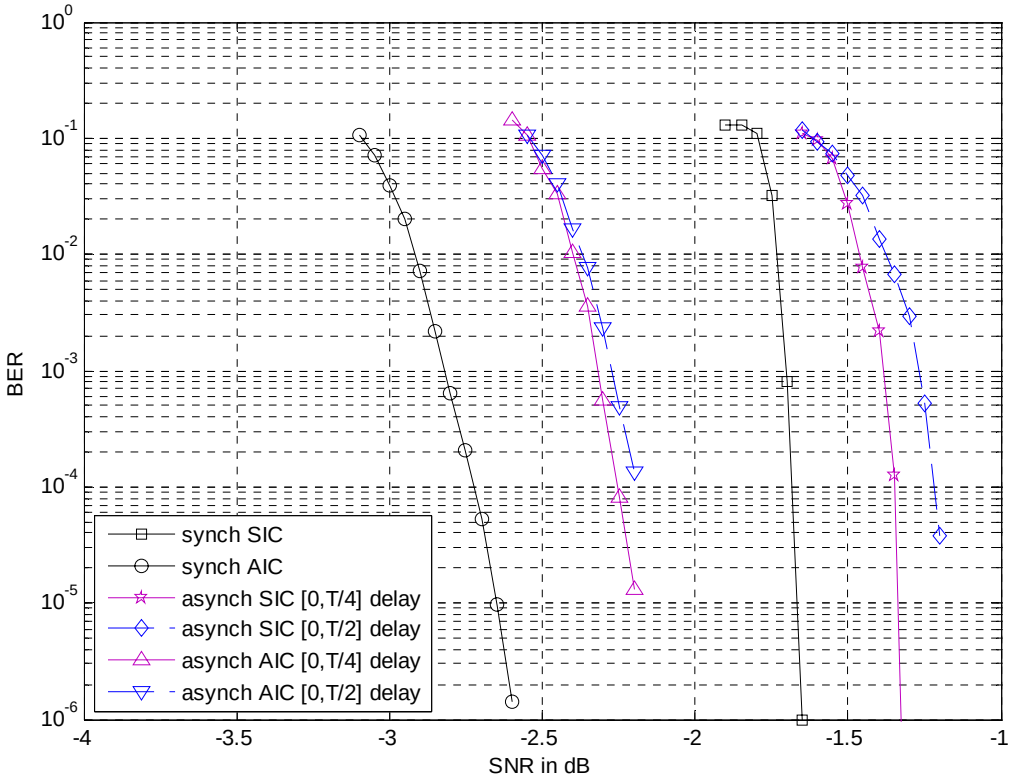

Figure 5.8. Performance evaluations for full duplex case.

The performances of proposed MAP and LMMSE type detectors for relay assisted asynchronous transmission scheme applying both rectangular and SQRC type of pulse shaping filters are evaluated via simulations. The MMSE filter parameters are $L = 1$ and $W = 2$. SQRC pulse whose impulse response length is truncated as $[-4T,4T]$ is applied in the system for both detectors and β is chosen as 0.5. The results are presented in Fig. 5.9. The 0.3 dB loss for MAP detector in the delay interval $[0, T/2]$ is again observed for SQRC pulse at a BER level of 10^{-4} when compared with synchronous case. This performace loss increases to 0.5 dB for the proposed LMMSE detector for the same delay interval

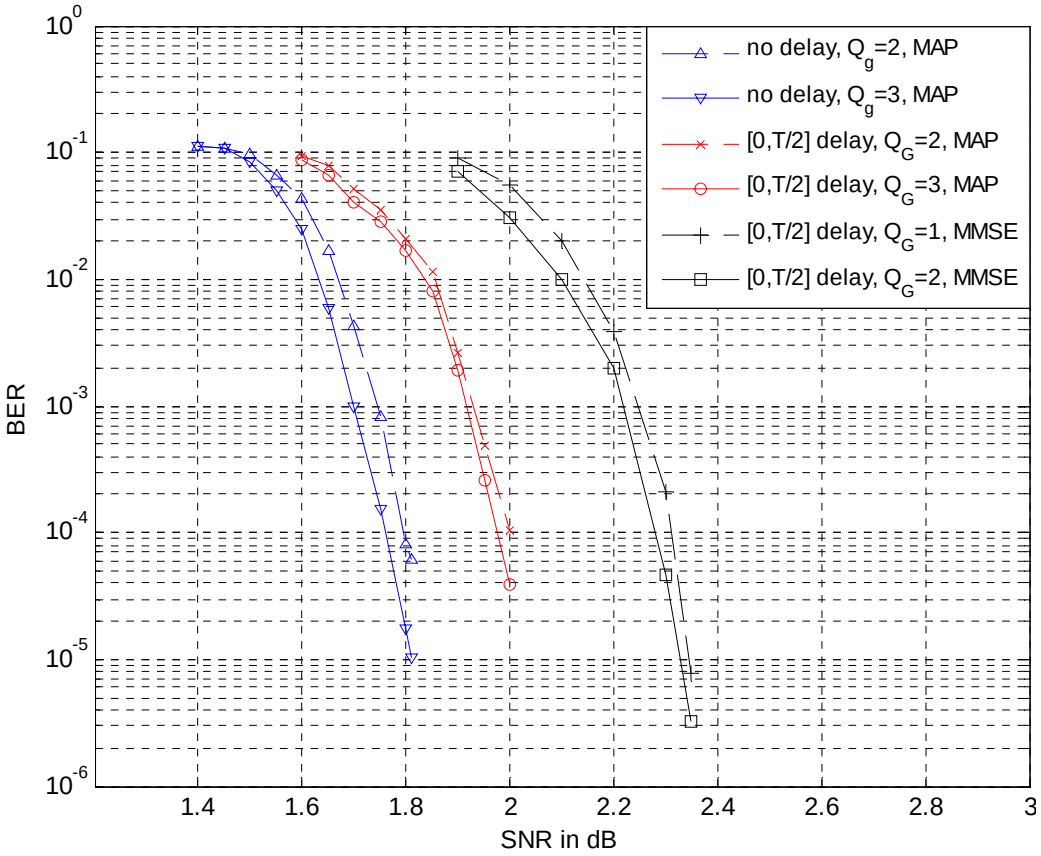

Figure 5.9 Performance evaluations of MAP and MMSE detectors over ergodic fading channel.

but is still desirable when the complexity issue is also considered. We also remark that the LMMSE detector requires only two global iterations to reach the steady state while it is 3 for the MAP detector.

We present the simulation results for quasi-static Rayleigh fading case for both types of detectors in Fig. 5.10. The global iteration number is 2 for both types of detectors and no additional gain is observed for higher iterations. We remark that the LMMSE detector performs almost the same as MAP detector for this type of channel. The synchronous case outperforms asynchronous case but only about 0.5dB at a BER level of 10^{-2}.

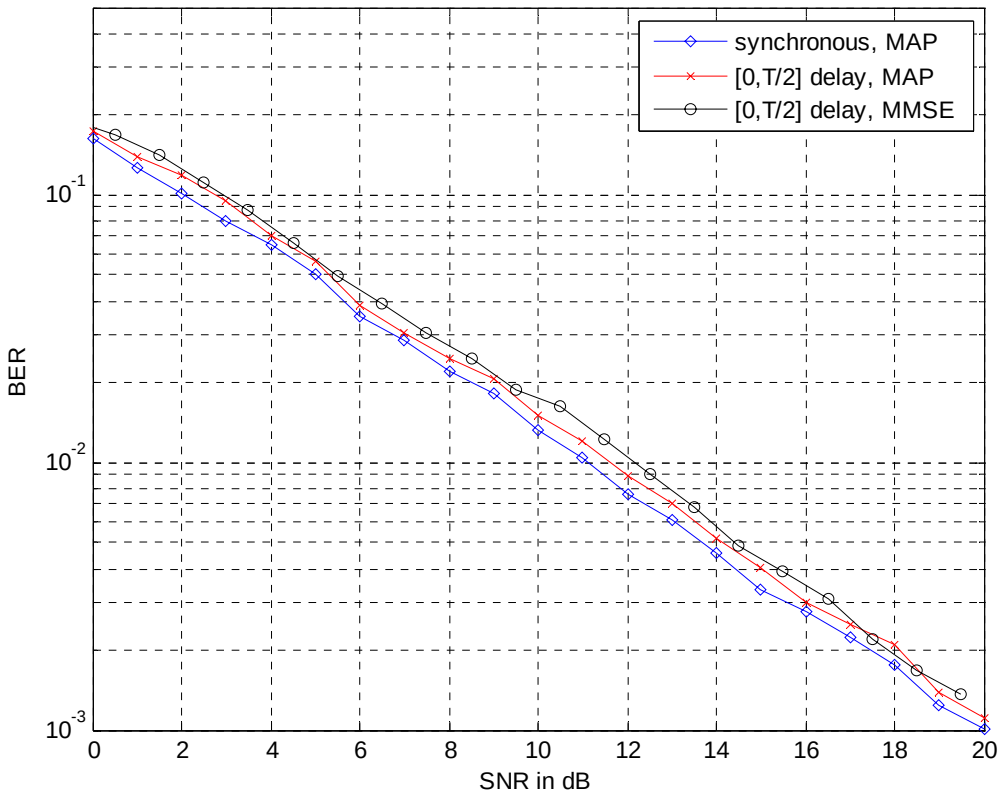

Figure 5.10 Performance evaluations of MAP and MMSE detectors over quasi-static Rayleigh fading channel.

5.5 Chapter Summary

In this chapter, we have examined the asynchronism between the source and relay transmissions over wireless relay channel and proposed MAP and LMMSE detectors considering the optimality and complexity criteria. The ISI, appearing as a result of non-ideal sampling, causes a reduction in the interfering signal energy, which directly results in an increase in the signal-to-interference-plus-noise ratio

(SINR). This increase in SINR is shown to be beneficial in the overall system performance for AWGN channel and asynchronism is shown to improve the system performance. The simulation results for fading channel have shown that, provided that perfect time delay and phase offset information exist at the destination, the performance of asynchronous case is approximately the same with that of its synchronous conterpart when the delay values are relatively small compared to symbol period. On the other hand, a small performance degradation arises when time delay increases up to half of the symbol period. The suboptimal MMSE criteria based detector exhibits some performance degradation when compared with MAP detector for ergodic Rayleigh fading case but provides reduced complexity. The work in this chapter is published in (Yılmaz & Yılmaz, 2009).

CHAPTER SIX
CONCLUSIONS

In this thesis, we have focused on analysis and design of both synchronous and asynchronous cooperative communication techniques. Initially, we have considered user cooperative communication and specifically, we have applied turbo codes distributively, in a two user scenario, for both fast and quasi-static fading channels. As a result of increased diversity, the DTCC scheme has shown a performance gain over non-cooperative scheme for quasi-static fading channel. For equal uplink SNR's, the users do not benefit much from cooperation for fast fading case. Also, the effect of erroneous inter-user transmission appears as error floor on overall system BER for both types of fading channels. We have also presented a BER analysis that calculates the union upper bound for DTCC scheme. The analysis includes the effect of inter-user BER on overall system BER as well. The calculated union upper bound of BER is supported with simulation results.

In the context of user cooperation, we have also exploited multilevel codes under cooperative framework. We have developed a multilevel coded cooperative scheme for two user cooperation which includes orthogonal signaling in order to increase the bandwidth efficiency. Both users' information is embedded in a single symbol via orthogonal signaling. We have proposed a two-level code with convolutional encoders as component codes. The levels are constituted with codewords of two users individually. In order to obtain additional protection, we have also applied turbo codes as an alternative to convolutional codes. Diversity gain is achieved by cooperation in two consecutive frames. We have determined the theoretical union upper bound of BER for cooperative scheme. As a benchmark for cooperative scheme, we have also simulated a multilevel coded non-cooperative scheme in which a single user transmits from two antennas over orthogonal channels. The multilevel coded cooperative scheme have attained the performance of non-cooperative multilevel coded scheme with two transmit antennas for perfect inter-user channel. In addition, the MCC scheme employing turbo codes performed better than the MCC with convolutional codes. The error

floor that was observed for MCC scheme with convolutional codes has vanished with turbo codes.

As a second research direction, we have worked on relay channels and investigated both the information theoretical analysis and overall performances of synchronous and asynchronous schemes. For synchronous case, we revisited the classical three node relay channel and set up LDPC coded cooperative scheme in which source and relay nodes transmit over the same channel in order to increase the capacity. We have considered both half and full duplex modes in which relay implements one of the three forwarding modes, namely DF, DetF or AF. For both quasi-static fading and fast fading type of channels we have investigated the protocol that achieves the best performance. We have shown by simulation results that DF protocol outperforms the other two for fast fading case. On the other hand, DetF protocol has been shown to achieve the best performance for quasi static fading channel. The DF protocol is the most sensitive to inter-user transmission errors and deteriorates overall system performance when the relay is not able to decode the source codeword without error.

In the last part, we have focused on impact of asynchronism on relay channels. We have shown that the existence of time delay and phase offset between the received source and relay signals causes ISI at destination. We have determined unconstrained ergodic capacity bound of asynchronous communication over wireless relay channel using max-flow min-cut theorem. When compared with the synchronous case, we have observed a small reduction at the capacity for asynchronous transmission if the source-relay path has a positive relative gain over the source-destination path. The reduction has been shown to vanish when the source-relay path has no relative gain. We have also proposed a receiver employing MAP type detector that can cope with the negative effects of asynchronism. Since a continuous time analysis is performed, the type of pulse shaping filter should also be taken into account for the case of asynchronism. Hence, we have applied both rectangular and SQRC type of filters in the system design. We also have used EXIT chart tool to predict the convergence threshold and hence evaluate the system performance. Through simulations, we have shown

that asynchronism can even provide increase in performance for AWGN channel. For fading channels, asynchronism has resulted with a performance loss which is insignificant for small values of relative time delay. Additionally, the simulation results confirmed the predicted convergence thresholds calculated via EXIT charts. We have also devised a reduced complexity LMMSE type of detector as an alternative to MAP type of detector which has increasing complexity with the length of ISI and modulation level. The proposed MMSE type of soft output detector has performed worse than MAP detector but considering the complexity issue, it is more reasonable to employ the former.

There exist several future research directions to be considered. First the use of multiple relays has the potential to increase the channel capacity. Hence, the extension of LDPC coded cooperative scheme with multiple relays and corresponding practical schemes need to be exploited. Additionally, forwarding techniques that we did not consider like compress-and-forward and estimate-and-forward could be applied as well. We assumed equal power constraint on source and relay nodes individually, but assuming a total power constraint and optimizing allocated powers have the potential to further increase the performance.

There are remaining complicated scenarios for asynchronous cooperative communication over relay channels as well. Employing higher level of modulation techniques other than BPSK and considering multiple relays have the priority among these scenarios. Finally, the impact of asynchronism on channels other than flat fading like frequency selective needs to be worked on. The ISI, arising with asynchronism, is dependent on signal energy. Therefore, optimization of allocated powers of source and relay nodes with a total power constraint would be interesting.

REFERENCES

Alamouti, S.M., (1998). A simple transmit diversity technique for wireless communications. *IEEE J. on Selected Areas in Comm.*, 16 (8),1451-1458.

Bahl, L. R., Cocke, J., Jelink, F. & Raviv, J., (1974). Optimal decoding of linear codes for minimizing symbol error rate. *IEEE Trans. Inform. Theory*, 20, 284–287.

Barak, O., & Feder, D. B. M., (2004). Bounds on achievable rates of LDPC codes used over the binary erasure channel. *IEEE Trans. Inform. Theory*, 50, 2483–2492.

Benedetto, S., Garello, R., & Montorsi, G., (1998). A search for good convolutional codes to be used in the construction of turbo codes. *IEEE Trans. Commun.*, 46, 1101–1105.

Benjillali M., & Szczecinski, L., (2009). A simple detect-and-forward scheme in fading channels. *IEEE Commun. Letters,* 13, 309-311.

Bo, D., Lin, X., Peiliang, Q., & Qinru, Q., (2006). Low density parity check coded distributed space-time cooperative system. *Vehicular Technology Conference*, 2383-2387.

Berrou, C. , Glavieux, A. & Thitimajshima, P., (1993). Near coding and decoding: Turbo codes. *Proceedings of the 2003 IEEE International Conference on Communications,* Geneva, Switzerland, 1064–1070.

Bölcskei, H., Nabar, R. U., Oyman, O., & Paulraj, A. J., (2006). Capacity scaling laws in MIMO relay Networks. *IEEE Trans. Wireless Commun*., 5, 1433–1444.

Chakrabarti, A., De Baynast, A., Sabharwal A., & Aazhang, B., (2007). Low density parity check codes for the relay channel. *IEEE J. on Selected Areas in Comm.*, 25, 280-291.

Cheng, R. S., & Verdu, S., (1992). The effect of asynchronism on the total capacity of Gaussian multiple-access channels. *IEEE Trans. Inform. Theory*, 38, 2-13.

Chung, S-Y., Forney, D., Richardson, T., & Urbanke R., (2001). On the design of low-density parity-check codes within 0.0045 dB of the Shannon limit. *IEEE Comm. Letters*, 5, 58-60.

Cover T. M., & El Gamal, A., (1979). Capacity theorems for the relay channel. *IEEE Trans. Inform. Theory*, 25, 572–584.

Cover, T. M., McEliece, R. J., & Posner, E. C., (1981). Asynchronous multiple-access channel capacity. *IEEE Trans. Inform. Theory*, 27, 409-413.

De Baynast, A., Chakrabarti, A., Sabharwal, A., & Aazhang, B., (2006). A systematic construction of LDPC codes for relay channel in time-division mode. *Asilomar Conference on Signals, Systems and Computers.*

Divsalar, D., Dolinar, S., McEliece, R. J., & Pollara, F., (1995). Transfer function bounds on the performance of turbo codes. *Jet Propulsion Lab., Pasadena, CA, TDA Progress Report 42-122*, 44–55.

Divsalar, D., Dolinar, S., & Pollara, F., (2001). Iterative turbo decoder analysis based on density evolution. *IEEE Journal on Selected Areas in Communications*, 19, 891-907.

Dohler, M., Rassool, B., & Aghvami, H., (2003). Performance evaluation of STTCs for virtual antenna arrays. *Proc. IEEE Vehicular Tech. Conf*., Jeju, Korea, 57–60.

Duman, T. M. & Salehi, M., (1998). "New performance bounds for turbo codes," *IEEE Trans. Commun.*, 46, 717–723.

Duman, T. M., (2002). Interleavers for serial and parallel concatenated (turbo) codes. J. G. Proakis, (Ed.) *Wiley Encyclopedia of Telecommunications*.

Gallager, R. G. , (1963). Low-density parity-check codes. *The MIT Pres.*

Guo, X., & Xia, X.G., (2008). A distributed space-time coding in asynchronous wireless relay networks. *IEEE Trans. Wireless Commun*., 7, 1812-1816.

Host-Madsen, A. & Zhang, J., (2005). Capacity bounds and power allocation for wireless relay channels. *IEEE Trans. Inform. Theory*, 51, 2020–2040.

Hou, J., Siegel, P. H., & Milstein, L. B., (2001). Performance analysis and code optimization of low density parity-check codes on Rayleigh fading channels. *IEEE J. Select. Areas Commun*., 19, 924–934.

Hu, J. & Duman, T., (2007). "Low density parity check codes over wireless relay channels," *IEEE Trans. Wireless Commun*., 6, 3384-3394.

Imai H. & Hirakawa, S., (1977). "A new multilevel coding method using error correcting codes", *IEEE Trans. Inform. Theory*, 23, 371-377.

Ishii, K., Ishibashi, K., & Ochiai, H., (2008). Multilevel coded cooperation: concepts and design criteria. *Proceedings of the 2008 International Symposium on Information Theory and its Applications,* Auckland, New Zealand,

Ishii, K., Ishibashi, K., & Ochiai, H., (2009). A novel cooperative diversity based on multilevel coded modulation. *Proceedings of the 2009 IEEE International Conference on Communications*.

Janani, M., Hedayat, A., Hunter, T. E., & Nosratinia, A., (2004). Coded cooperation in wireless communications: Space-time transmission and iterative decoding. *IEEE Trans. Signal Processing*, 52, 362–371.

Kavcic, A., Ma, X., & Mitzenmacher, M., (2003). Binary intersymbol interference channels: Gallager codes, density evolution, and code performance bounds. *IEEE Trans. Inform. Theory*, 49, 1636–1652.

Kofman Y. , Zehavi, E., & Shamai, S., (1992). A Multilevel Coded Modulation Scheme for Fading Channels**.** *AEU*, 46, 420-427.

Kramer, G., Gastpar, M., & Gupta, P., (2005). Cooperative strategies and capacity theorems for relay Networks. *IEEE Trans. Inform. Theory*, 51, 3037–3063.

Laneman, J. N., Tse, D. N. C., & Wornell, G. W., (2004). Cooperative diversity in wireless networks: Efficient protocols and outage bahavior. *IEEE Trans. Inform. Theory*, 50, 3062–3080.

Laneman, J. N., & Wornell, G. W., (2003). Distributed space-time coded protocols for exploiting cooperative diversity in wireless networks. *IEEE Transactions on Information Theory*, 49, 2415-2425.

Li, C., Yue, G., Khojastepour, M.A., Wang, X., & Madihian, M., (2008). LDPC coded cooperative relay systems: performance analysis and code design. *IEEE Transactions on Communications*, 56, 485-496.

Li, X., (2004). Space time coded multi transmission among distributed transmitters without perfect synchronization. *IEEE Signal Processing Letters*, 11, 948-951.

Li, X., Wong, T. F., & Shea, J. M., (2008). Performance analysis for collaborative decoding with least-reliable-bit exchange on AWGN channels. *IEEE Trans. Commun.*, 56, 58-69.

Li, Y., & Xia, X.G., (2007). A family of distributed space-time trellis codes with asynchronous cooperative diversity. *IEEE Trans. Commun.*, 55, 790–800.

Li, Y., Vucetic, B., Wong, T. F., & Dohler, M., (2006). Distributed turbo coding with soft information relaying in multihop relay networks. *IEEE Journal on Selected Areas in Communications*, 24, 2040–2050.

Luby, M. G., Mitzenmacher, M., Shokrollahi, M. A., & Spielman, D. A., (2001). Improved low-density parity-check codes using irregular graphs. *IEEE Trans. Inform. Theory*, 47, 585–598.

Mackay, D. J. C., (1999). Good error correcting codes based on very sparse matrices. *IEEE Trans. Inform. Theory*, 45, 399–431.

Mahinthan, V., & Mark, J. W., (2005). A simple cooperative diversity scheme based on orthogonal signaling. *IEEE Wireless Communications and Networking Conference*, 2, 1012-1017.

Mantravadi, A., & Veeravalli, V. V., (2001). Chip-matched filtering and discrete sufficient statistics for asynchronous band-limited CDMA systems. *IEEE Trans. Commun.*, 49, 1457-1467.

Nabar, R. U., Bölcskei, H., & Kneubühler, F.W., (2004). Fading relay channels: Performance limits and space-time signal design. *IEEE J. Select. Areas Commun*., 22, 1099–1109.

Razaghi, P., & Yu, W., (2007). Bilayer low-density parity-check codes for decode-and-forward in relay channels. *IEEE Transactions on Information Theory*, 53, 3723-3739.

Reznik, A., Kulkarni, S. R., & Verdu, S., (2004). Degraded Gaussian multi-relay channel: Capacity and optimal power allocation. *IEEE Trans. Inform. Theory,* 50, 3037–3046.

Richardson, T. J., Shokrollahi, M. A., & Urbanke, R. L., (2001). Design of capacity approaching irregular low-density parity-check codes. *IEEE Trans. Inform. Theory*, 47, 619–637.

Richardson T.J., & Urbanke, R., (2001). Efficient encoding of low-density parity-check codes. *IEEE Trans. Inform. Theory*, 47, 638–656.

Richardson, T. J., & Urbanke, R. L., (2001). The capacity of low-density parity-check codes under message-passing decoding. *IEEE Trans. Inform. Theory*, 47, 599–618.

Roy, S., & Duman, T. M., (2006). Performance bounds for turbo coded half duplex relay systems. *IEEE Int. Conf. on Communications*, 1586-1591.

Sendonaris, A., Erkip, E., & Aazhang, B., (2003). User cooperation diversity: Part I & Part II. *IEEE Trans. Commun.*, 51, 1927–1948.

Seshadri, N., & Sundberg, C.W., (1993). Multilevel trellis coded modulations for the Rayleigh fading channel. *IEEE Trans. on Commun*., 41, 1300-1310.

Shannon, C. E., (1948). A mathematical theory of communication. *Bell Sys. Tech. Journal*, 27, 379–423 & 623–656.

Souryal, M. R., & Vojcic, B. R., (2004). Cooperative turbo coding with time-varying Rayleigh fading channels. *Proc. IEEE Intl. Conf. on Commun.*, 356–360.

Stefanov, A., & Erkip, E., (2004). Cooperative coding for wireless networks. *IEEE Trans. Commun*.,52, 1470–1476.

Tanner, R. M., (1981). A recursive approach to low complexity codes. *IEEE Trans. Inform. Theory*, 27, 533–547.

Tarokh, V., Seshadri, N., & Calderbank, A.R., (1998). Space-time codes for high data rate wireless communications: Performance criterion and code construction. *IEEE Trans. Inform. Theory*, 44, 744-765.

Ten Brink, S., (2001). Convergence behavior of iteratively decoded parallel concatenated codes. *IEEE Trans. Commun.*, 49, 1727–1737.

Ten Brink, S., Kramer, G. & Ashikhmin, A., (2004). Design of low-density parity-check codes for modulation and detection. *IEEE Trans. Commun.*, 52, 670–678.

Tuchler, M., Singer, A. C., & Koetter, R., (2002). Minimum mean squared error equalization using a-priori information. *IEEE Trans. Sig. Processing*, 50, 673–683.

Tuchler, M., Koetter, R., & Singer, A. C., (2002). Turbo equalization: Principles and new results. *IEEE Trans. Commun.*, 50, 754–767.

Ungerboeck, G., (1982). Channel coding with multilevel/phase signals. *IEEE Trans. Inform. Theory*, 28, 55-67.

Van der Meulen, E. C., (1971). Three-terminal communication channels. *Advanced Appl. Prob.*, 3, 120–154.

Wachsmann, U., (1995). Power and bandwidth efficient digital communication using turbo codes in multilevel codes. *European Trans. on Telecom.,* 6, 557-567.

Wang, B., Zhang, J., & Host-Madsen, A., (2005). On the capacity of MIMO relay channels. *IEEE Trans. Inform. Theory*, 51, 29–43.

Wei, S., Goeckel, D., & Valenti, M., (2006). Asynchronous cooperative diversity. *IEEE Trans. Wireless Commun.*, 5, 1547-1557.

Yılmaz, M., & Yılmaz, R., (2008). A novel cooperative communication scheme based on multilevel codes. *J. of Electrical&Electronics Eng.,* 8 (2), 683-692

Yılmaz, M., & Yılmaz, R., (2008). Multilevel coded cooperation for wireless vehicular Networks. *IEEE Int. Symp. on Wireless Vehicular Comm*.

Yılmaz, M., & Yılmaz, R., (2009). Impact of asynchronism on wireless relay channels. *Frequenz*, 63(11-12), 258-264.

Yılmaz, M., & Yılmaz, R., (2009). Capacity bounds for asynchronous transmission over relay channel. *IEICE Trans. on Comm.*, submitted.

Zhao, B., & Valenti, M. C., (2003). Distributed turbo coded diversity for relay channel. *Electronic Letters*, 39, 786–787.

Zhang L. & Vucetic, B., (1995). Multilevel block codes for Rayleigh fading channels. *IEEE Trans. Commun.*, 43, 24-31.

Zhang, Z., & Duman, T. M., (2005). "Capacity approaching turbo coding and iterative decoding for relay channels," *IEEE Trans. Commun.*, 53, 1895–1905.

Zhang, Z., & Duman, T. M., (2007). Capacity approaching turbo coding for half-duplex relaying. *IEEE Trans. Commun.*, 55, 1895–1906.

APPENDICES

LIST OF FIGURES

LIST OF TABLES

LIST OF ACRONYMS

AF	Amplify and forward
APP	A posteriori probability
ASIC	Asymmetric information combining
AWGN	Additive white Gaussian noise
BPSK	Binary phase shift keying
BCJR	Bahl-Cocke-Jelinek-Raviv
BEC	Binary erasure channel
BER	Bit error rate
BSC	Binary symmetric channel
CDMA	Code division multiple access
CF	Compress and forward
CND	Check node decoder
CRC	Control redundancy check
DF	Decode and forward
DetF	Detect and forward
DTC	Distributed turbo coding
DTCC	Distributed turbo coded cooperative
EF	Estimate and forward

EXIT	Extrinsic information transfer
FEC	Forward error correction
ISI	Inter-symbol interference
LDPC	Low density parity check
LLR	Log likelihood ratio
LMMSE	linear minimum mean square error
MAP	Maximum a posteriori probability
MC	Multilevel coded
MCC	Multilevel coded cooperative
MRC	Maximum ratio combining
MGF	Moment generating functions
MIMO	Multiple-input multiple-output
MMSE	Minimum mean square error
MSE	Mean square error
OFDM	Orthogonal frequency division multiplexing
PEP	Pairwise error probability
PIC	Perfect inter-user channel
PSK	Phase shift keying
QAM	Quadrature amplitude modulation
QPSK	Quadrature phase shift keying
RCPCC	Rate compatible punctured convolutional code
RSC	Recursive systematic convolutional
SIC	Symmetric information combining
SISO	Soft input soft output
SINR	Signal-to-interference-plus-noise ratio
SNR	Signal to noise ratio
SQRC	Square root raised cosine
TCM	Trellis coded modulation
VND	Variable node decoder